Evaluation of the Performance of Sailing Vessels Based on Towing Tank and Sailforce Data

by

Demetrios Alexis Mantzaris

M.Eng. (Elec. Eng.), Imperial College, University of London (1990)

Submitted to the Department of Ocean Engineering
in partial fulfillment of the requirements for the degree of

Master of Science in Naval Architecture and Marine Engineering

at the

MASSACHUSETTS INSTITUTE OF TECHNOLOGY

June 1992

Author .....
Department of Ocean Engineering
May 1, 1992

Certified by .....
Jerome H. Milgram
Professor of Ocean Engineering
Thesis Supervisor

Accepted by .. ..
A. Douglas Carmichael
Chairman, Departmental Committee on Graduate Students

Evaluation of the Performance of Sailing Vessels Based on Towing Tank and Sailforce Data

by

Demetrios Alexis Mantzaris

Submitted to the Department of Ocean Engineering
on May 1, 1992, in partial fulfillment of the
requirements for the degree of
Master of Science in Naval Architecture and Marine Engineering

Abstract

This thesis is concerned with several aspects and techniques of converting data obtained from sailforce models and from towing tank tests into an evaluation of the performance of sailing yachts.

Froude's assumption that the resistance of a body moving through water may be treated as the independent sum of its residuary resistance and its frictional resistance, is the base of towing tank testing theory. Hughes refined Froude's method by introducing a *form factor* to account for the 3-dimensional nature of the hull, and Prohaska suggested an accurate method of determining this form factor.

The actual speed of a sailing vessel at a given sailing angle and wind speed is estimated by a Velocity Prediction Program (VPP), which balances static, hydrodynamic and aerodynamic forces and moments for equilibrium. Hydrodynamic data are usually obtained from towing tank testing, while aerodynamic data are given by a sailforce model, which consists of a table of lift and drag coefficients for a range of angles of attack of the rig.

The areas on which research was done for this thesis are summarized below, along with some conclusions.

For sailing vessels, it is best to calculate the form factor of the hull excluding appendages such as fin-keels, bulbs and rudders. The relation between form factor and heel angle is weak, and a sensitivity analysis showed that it is not worth calculating a new form factor at each heel angle.

The resistance due to heel and yaw may be assumed to be a parametric function of the speed-length ratio, the sideforce and the heel angle of the vessel. The parameters of the above function are found by a weighted least-square-error fit of the towing tank data. There is no easy way of determining the weight of each run for the above process. Fortunately, however, the VPP prediction is not very sensitive to reasonable weighting schemes. Another way of modeling the resistance due to heel and yaw, based on the interpolation between data points, was examined. This method was not successful and was abandoned until a way of overcoming its problems is found.

It is best to consider the frictional drag of the appendages separately, perform-

ing the data analysis on the bare hull, although the tests must be done with the appendages on the model. Some experimental work was done for determining the model scale appendage drag, and it was concluded that the errors in appendage frictional drag prediction were small, but the velocity prediction was quite sensitive to them.

After experimentally examining the errors in turbulence stimulator drag, it was found that the final results were relatively insensitive to them, especially when relative performance prediction is of primary concern.

Several sources of bad data repeatability were examined and it was concluded that sideforce measurement errors were associated in part with carriage vibrations and had a great effect on repeatability. Water temperature was not believed to affect the results, although the model age was found to have some effect. The importance of testing under identical conditions and within a short time span was recognized.

From all the above analysis, it was evident that it can be quite misleading to merely compare resistances in the tank in order to evaluate performance. Relative performance estimates require use of a VPP that uses model test data for its hydrodynamic force modeling.

Thesis Supervisor: Jerome H. Milgram
Title: Professor of Ocean Engineering

Evaluation of the Performance of Sailing Vessels Based on Towing Tank and Sailforce Data

by

Demetrios Alexis Mantzaris

Submitted to the Department of Ocean Engineering
on May 1, 1992, in partial fulfillment of the
requirements for the degree of
Master of Science in Naval Architecture and Marine Engineering

Abstract

This thesis is concerned with several aspects and techniques of converting data obtained from sailforce models and from towing tank tests into an evaluation of the performance of sailing yachts.

Froude's assumption that the resistance of a body moving through water may be treated as the independent sum of its residuary resistance and its frictional resistance, is the base of towing tank testing theory. Hughes refined Froude's method by introducing a *form factor* to account for the 3-dimensional nature of the hull, and Prohaska suggested an accurate method of determining this form factor.

The actual speed of a sailing vessel at a given sailing angle and wind speed is estimated by a Velocity Prediction Program (VPP), which balances static, hydrodynamic and aerodynamic forces and moments for equilibrium. Hydrodynamic data are usually obtained from towing tank testing, while aerodynamic data are given by a sailforce model, which consists of a table of lift and drag coefficients for a range of angles of attack of the rig.

The areas on which research was done for this thesis are summarized below, along with some conclusions.

For sailing vessels, it is best to calculate the form factor of the hull excluding appendages such as fin-keels, bulbs and rudders. The relation between form factor and heel angle is weak, and a sensitivity analysis showed that it is not worth calculating a new form factor at each heel angle.

The resistance due to heel and yaw may be assumed to be a parametric function of the speed-length ratio, the sideforce and the heel angle of the vessel. The parameters of the above function are found by a weighted least-square-error fit of the towing tank data. There is no easy way of determining the weight of each run for the above process. Fortunately, however, the VPP prediction is not very sensitive to reasonable weighting schemes. Another way of modeling the resistance due to heel and yaw, based on the interpolation between data points, was examined. This method was not successful and was abandoned until a way of overcoming its problems is found.

It is best to consider the frictional drag of the appendages separately, perform-

ing the data analysis on the bare hull, although the tests must be done with the appendages on the model. Some experimental work was done for determining the model scale appendage drag, and it was concluded that the errors in appendage frictional drag prediction were small, but the velocity prediction was quite sensitive to them.

After experimentally examining the errors in turbulence stimulator drag, it was found that the final results were relatively insensitive to them, especially when relative performance prediction is of primary concern.

Several sources of bad data repeatability were examined and it was concluded that sideforce measurement errors were associated in part with carriage vibrations and had a great effect on repeatability. Water temperature was not believed to affect the results, although the model age was found to have some effect. The importance of testing under identical conditions and within a short time span was recognized.

From all the above analysis, it was evident that it can be quite misleading to merely compare resistances in the tank in order to evaluate performance. Relative performance estimates require use of a VPP that uses model test data for its hydrodynamic force modeling.

Thesis Supervisor: Jerome H. Milgram
Title: Professor of Ocean Engineering

Acknowledgments

I have always dreamed of being professionally involved in sailing and yacht design. My acceptance, despite my EE background, at the department of Ocean Engineering at MIT, helped me come close to this goal.

I would like to thank my advisor, Jerry Milgram, for understanding my ambitions and for giving me unique opportunities to learn the principles of Naval Architecture.

I would also like to thank my friends Daniel LaMere and John Mass, for always being happy to provide me with whatever information I needed regarding the towing tank data, Noah Eckhouse for coming to the rescue whenever I had any computer problems, Don Peters for willingly undertaking the design and assembly of "Thor", and Rob Scala for all the successful data analysis software he produced.

Many results used in this thesis are from the 1991 tank testing program of the *America*^{3} Foundation.

This thesis was sponsored by the *America*^{3} Foundation
for the defense of the 1992 America's Cup.

Contents

List of Figures

List of Tables

Chapter 1

INTRODUCTION

In this chapter, the background theory for estimating the performance of sailing vessels from towing tank data is presented. Froude's assumption, Hughes' form factor concept and Prohaska's method for experimentally calculating the form factor are part of this background information. The principles of operation of a Velocity Prediction Program (VPP), which takes towing tank and sail-force data and calculates the speed of a sailing yacht over a range of sailing angles and wind speeds are also explained.

In chapter 2, the form factor is further examined, by including a study on its variation with heel angle and on the sensitivity of the full scale resistance prediction to form factor variations.

Chapter 3 looks at methods of dealing with the resistance due to heel and yaw angles and tries to examine the effect of various design parameters on these components of drag.

In chapter 4, the drag of the keel and rudder is examined. It is explained why it is advantageous to consider appendage friction drag separately, how it is calculated and how sensitive the final result is to appendage drag errors.

Chapter 5 deals with turbulence stimulation of the flow past the tank models. The accuracy of the nominal turbulence stimulator drag is examined by looking at tests of the same model with a different number of stimulators. The sensitivity of the velocity prediction to the estimate of the stimulator drag is also examined.

Chapter 6 deals with various sources of bad data repeatability, such as sideforce

measurement errors, carriage vibrations, water temperature variation and model deterioration.

Finally, in chapter 7, some concluding comments and recommendations are presented.

1.1 Prediction of the Full Scale Resistance from Towing Tank Data

1.1.1 Froude's assumption

In 1872, William Froude made a bold assumption which has proved to be of the utmost practical importance, but of somewhat inadequate theoretical justification. Faced with the dilemma that the frictional resistance of a body moving through a viscous fluid is a function of the dimensionless Reynolds number, $Rn_L = \frac{UL}{\nu}$, and that the wave-making and form resistances of a body at the free surface is a function of the Froude number, $Fn = \frac{U}{\sqrt{gL}}$, Froude assumed that the total resistance can be treated as the independent sum of these two components. This assumption is made necessary in ship model testing by the impossibility of operating a ship and a ship model at both the same Froude number and the same Reynolds number simultaneously. [5]

Assuming both the ship and model to be operating in the same fluid at the same Froude number, it is evident that model speed, U_m, must equal the ship speed, U_s divided by the square root of the scale factor, λ.

$$U_m = \sqrt{gL_m}\frac{U_s}{\sqrt{gL_s}} = \frac{U_s}{\sqrt{\lambda}} \tag{1.1}$$

For the ship and model to operate at equal Reynolds numbers, the model speed must equal the ship speed multiplied by the scale factor.

$$U_m = \frac{\nu}{L_m}\frac{U_s L_s}{\nu} = U_s\lambda \tag{1.2}$$

It is obviously impossible to satisfy both of these conditions in water, yet it is essential

that naval architects use model tests, and the laws of similitude, to obtain predictions of the resistance of the full size ship. Froude's assumption solves this problem, as ship models may be tested at Froude numbers corresponding to those of the full scale ship, estimating the frictional resistance to be that of a flat plate at the appropriate Reynolds number.

Briefly, the model test procedure, as suggested by Froude, is as follows :

- The model is tested at speeds corresponding to the full scale Froude numbers in order to determine the total model resistance coefficient, C_{tm}, as a function of Froude number.

- The model frictional resistance coefficient, C_{fm}, at the appropriate Reynolds number, is found from tabulated results of flat plate friction experiments and calculations.

- The wave-making and form drag of the model is the difference of the total drag and the friction drag. The coefficient of this drag is known as the residual resistance coefficient, C_{rm}.

$$C_{rm} = C_{tm} - C_{fm} \tag{1.3}$$

- The residual resistance coefficient is assumed to be a function of the Froude number only. Since model and ship operate at the same Froude number, the ship's residual resistance coefficient is the same as the model's.

$$C_{rs} = C_{rm} \tag{1.4}$$

- The ship's frictional resistance coefficient, C_{fs}, is found from the tabulated data for plates operating at the full scale Reynolds number.

- The ship's total resistance coefficient is the sum of the frictional and residual resistance coefficients, plus corrections for bottom roughness, appendage drag,

etc :

$$C_{ts} = C_{fs} + C_{rm} + \{CORRECTIONS\} \tag{1.5}$$

and the total resistance, D_{ts}, of a ship traveling at speed, U_s and having wetted surface, S_s, is given by :

$$D_{ts} = C_{ts}\frac{1}{2}\rho S_s U_s^2 \tag{1.6}$$

1.1.2 Hughes' form factor method

As mentioned above, Froude's method assumes that the wave-making and form drag (residuary resistance) coefficient depends only on the Froude number. It is known, however, that the form drag is viscous in nature and is caused by the pressure gradients present when a 3-dimensional hull moves through a fluid. Hughes therefore assumed that the model residual resistance coefficient is comprised of the sum of the wavemaking resistance coefficient, C_{wm}, plus the form drag coefficient, C_{frm}, but with C_{frm} equal to some fraction, κ, of the flat plate resistance coefficient.

$$C_{rm} = C_{wm} + C_{frm} = C_{wm} + \kappa C_{fm} \tag{1.7}$$

The factor κ accounts for the three-dimensional form, and is appropriately termed the form factor. [5]

The form factor is assumed to be invariant with Reynolds number and the quantity $(1+\kappa)C_{fm}$ is subtracted from the total model resistance in order to find the ship's wavemaking resistance. Given the total model resistance coefficient (equation 1.8), the ship's total resistance coefficient may therefore be predicted as shown in equation 1.9.

$$C_{tm} = C_{fm} + C_{wm} + \kappa C_{fm} \tag{1.8}$$

$$C_{ts} = C_{fs} + C_{wm} + \kappa C_{fs} \Longrightarrow C_{ts} = C_{tm} + (1+\kappa)(C_{fs} - C_{fm}) \tag{1.9}$$

where C_{fm} and C_{fs} are found from tabulated data at the appropriate Reynolds numbers.

1.1.3 Prohaska's experimental method of calculating the form factor

A method for experimentally evaluating the form factor was proposed by C. W. Prohaska in 1966. [4] His method is based on the supposition that the wave-making resistance component, C_{wm}, for Froude numbers between 0.1 and 0.2 is approximately proportional to the fourth power of the Froude number. Assuming that equation 1.8 is valid, the following relation is obtained by substitution.

$$\frac{C_{tm}}{C_{fm}} = \frac{Fn^4}{C_{fm}} A + (1 + \kappa) \tag{1.10}$$

where A is a constant.

Thus, the curve of C_{tm}/C_{fm} versus Fn^4/C_{fm} will be a straight line in the low Fn region, which if extended would intersect the ordinate (Fn=0) at $(1 + \kappa)$. This enables the form factor to be determined with good accuracy. [1]

1.2 The Velocity Prediction Program

The Velocity Prediction Program (VPP) provides a means of estimating the speeds of ocean racing yachts over a range of sailing angles and wind speeds. In this section, the basic principles on which the VPP is based are explained. [3]

The basic task of the VPP is to balance static, hydrodynamic and aerodynamic forces and moments so that the equilibrium boat speed may be found.

1.2.1 The sail-force data

The sail-force data consists of a table of lift and drag coefficients for a range of angles of attack of the rig. Therefore, for a given apparent wind angle, there are data for the following aerodynamic force coefficients:

1. *A maximum lift coefficient, C_{LM}.* This is the value of lift coefficient used only when the sails are *not* flattened.

2. *An induced drag coefficient,* C_I, which is proportional to the square of the lift coefficient. While this is predominantly associated with the aspect ratio of the sail plan, it also contains that portion of the viscous drag which varies as the square of the lift coefficient.

3. *A parasitic drag coefficient,* C_{DP}, attributed to viscous forces and/or flow separation on the sails which is independent of the lift coefficient.

A parasitic drag coefficient, C_{DPO}, due to the mast, rigging and hull is calculated from the particular yacht characteristics and is added to the aerodynamic coefficients listed above.

To get the actual aerodynamic forces from the above coefficients, it is necessary to multiply the coefficients by $\frac{1}{2}\rho_a r^2 S_a V_{AW}^2$, where ρ_a is the density of air, r is the reefing ratio, S_a is the nominal sail area and V_{AW} is the apparent wind velocity.

1.2.2 The hull resistance coefficients

The hull resistance as a function of boat speed is found either from towing tank data, or is estimated by empirical formulae as a function of standard measurable characteristics of the hull of the yacht.

In any case, however, the total resistance is assumed to consist of the hull upright resistance plus a resistance increase due to heel and yaw (sideforce). When towing tank data is available, the full scale total upright resistance as a function of speed is found using the methods described in section 1.1.

The residuary resistance increase due to heel and yaw is found by fitting a polynomial function of the heel angle, sideforce and speed to the towing tank data. This method of calculating resistance due to heel and sideforce is presented more analytically in section 3.1.

Similarly, a fit of the hull hydrodynamic righting moment is also found and is used by the VPP when balancing heeling moments. As with the resistance coefficients, when towing tank data are not available, an experimental formula is used to calculate this righting moment.

1.2.3 The VPP calculation procedure

The VPP follows the following procedure in order to evaluate the performance of a boat :

1. A boat speed is chosen which represents a first guess to the final velocity prediction.

2. The apparent wind velocity is calculated and hence all aerodynamic forces are found.

3. The hydrodynamic sideforce produced by the hull is equated to the aerodynamic sideforce.

4. A heel angle is found so that the hydrodynamic and aerodynamic heeling moment is equal to the hull static and dynamic righting moment plus the crew righting moment.

5. The net aerodynamic driving force is compared to the total hull resistance for the above speed, sideforce and heel.

6. Steps 2 through 4 above are repeated while adjusting boat speed so that the two quantities compared in step 5 converge to be equal within a desired accuracy range.

This procedure is repeated in order to optimize boat speed for various amounts of sail reefing and flattening.

Chapter 2

THE FORM FACTOR

In this chapter, the form factor concept will be further examined. The effect of form factor variation with heel angle will be discussed and the total resistance sensitivity to form factor errors will be examined. Towing tank results will be used as examples in many cases.

2.1 Prohaska Plots for Sailing Yachts

It has been explained (section 1.1.3) that C. W. Prohaska came up with an experimental method for calculating the form factor. The difficulty in accurately measuring resistance at low speeds and the failure of turbulence stimulators at very low Reynolds numbers, made it necessary for Prohaska's method to go further than assuming that all the resistance at very low speeds is residuary.

Hence, he proposed a method of extrapolating the low-Froude number total model resistance from data in the range $0.1 < Fn < 0.2$ by assuming that the wave-making resistance coefficient at $Fn < 0.2$ is proportional to the fourth power of the Froude number. [4], [1]

For sailing vessels which have appendages such as fin-keels, bulbs and deep rudders, it is best to estimate the form factor of only the canoe-body (i.e. the hull excluding the appendages). This is done because most work on form factor theory has been done for conventional ship forms, which have no such appendages. Thus,

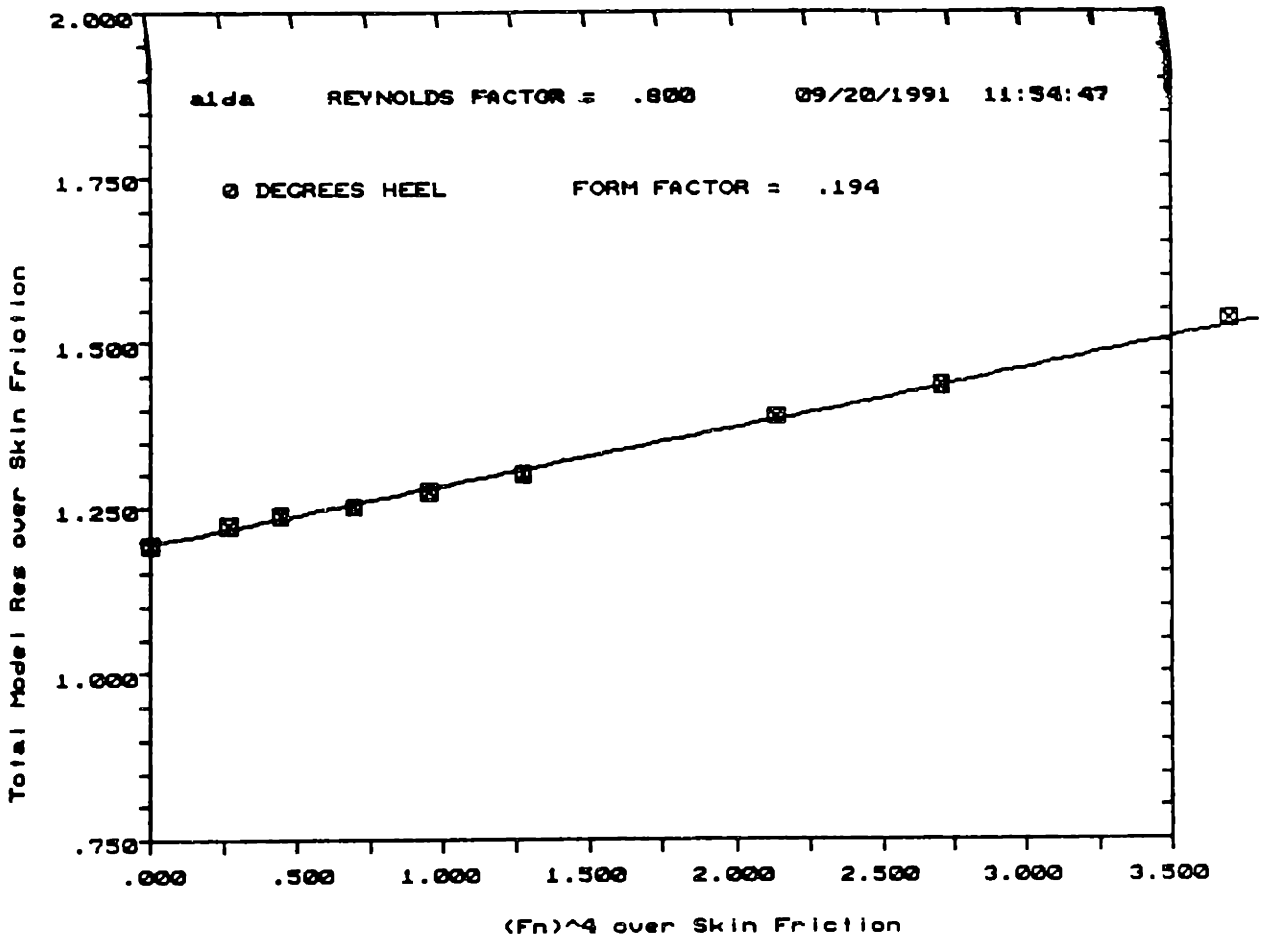

Figure 2-1: Example of a Prohaska plot

the complicated form of a complete underbody of a sailboat with appendages presents potential problems of not being in accordance with Prohaska's experiments. However, the shapes of keels, bulbs and rudders are such that their no-yaw drag may be predicted with reasonable accuracy and subtracted from the total model resistance, hence safely obtaining the canoe-body form factor by Prohaska's method.

An example of the form factor determination by Prohaska's method is given in figure 2-1. Note that in this figure, there is actually no data point at zero Froude number, but it is estimated from the straight line fit of the other data points. The data needed to produce this graph was obtained from a towing tank test of an America's Cup class boat.

2.2 Form Factor Variation with Heel Angle

A fundamental difference between performing towing tank tests for ships and for sailing vessels is that the later normally sail at heel angles up to 30 degrees whereas the former are tested assuming they are to be operated upright. Thus, sailboats are tested at a range of heel angles, making it possible that when heeled, their changed underwater shape results in a different form factor at that heel angle.

It is also possible that the wetted surface of these boats changes with heel. This may be a problem because the extra frictional resistance which occurs due to the wetted surface increase is incorrectly attributed to wave-making drag due to heel. It must be noted, however, that if this change of wetted surface is incorporated into the change of form factor with heel, then the above situation is automatically accounted for, as shown below.

If the wetted surface of the vessel is increased from the nominal value, $S_{m(nom)}$, by $S_{m(extra)}$, then the actual frictional drag coefficient normalized by $S_{m(nom)}$ will be given by equation 2.1.

$$C_{fm(real)} = \frac{R_{fm(real)}}{\frac{1}{2}\rho U_m^2 S_{m(nom)}} = \frac{R_{fm(nom)} + R_{fm(extra)}}{\frac{1}{2}\rho U_m^2 S_{m(nom)}} \tag{2.1}$$

where $R_{fm(real)}$ is the actual frictional resistance, and $R_{fm(extra)}$ is the extra frictional resistance due to the wetted surface increase.

Making use of the fact that the frictional resistance is proportional to the wetted surface area at a specific Reynolds number, the following relation holds.

$$C_{fm(nom)} = C_{fm} = \frac{R_{fm(nom)}}{0.5\rho U_m^2 S_{m(nom)}} = \frac{R_{fm(extra)}}{0.5\rho U_m^2 S_{m(extra)}} \tag{2.2}$$

Substituting into equation 2.1, the final result is :

$$C_{fm(real)} = C_{fm}(1 + \frac{S_{m(extra)}}{S_{m(nom)}}) \tag{2.3}$$

Thus, it has been proved that the change in wetted surface due to heel acts like a change in form factor, and hence it is not necessary to account for both of those

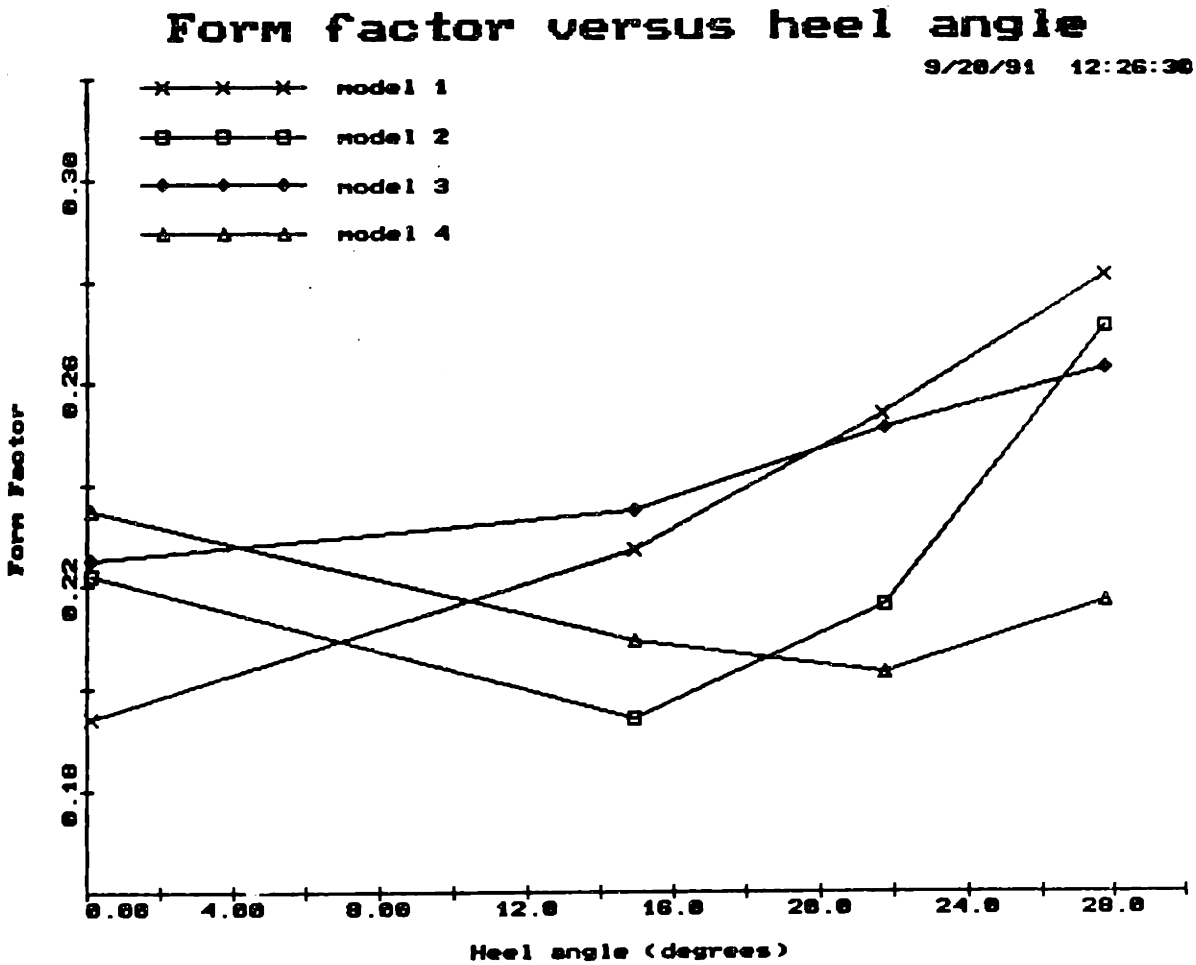

Figure 2-2: Form factor versus heel angle

effects of heel separately.

In order to investigate how the form factor (including the effect of wetted surface change) behaves with heel angle, towing tank results for several America's Cup class boats were examined. The form factor was obtained as a function of heel by making a Prohaska plot for each angle tested. Figure 2-2 summarizes this experimental investigation by plotting form factor versus heel angle for several boats. It is interesting to note that the form factor does not always monotonically increase, but for some hull forms it decreases to a minimum and then starts to increase again.

As it can be seen, the effect of heel on κ is not very large. It is therefore questionable whether the determination of the heel–form factor relationship is worth the expense of making so many low speed runs with heel and no yaw, since these condi-

tions never occur when the yacht is actually sailing. A sensitivity analysis is needed to answer this question.

2.3 Sensitivity Analysis

In the previous section, it was indicated that it may not be worth making the low speed upright runs required in order to determine the form factor at several heel angles. In other words, it may be possible to obtain more accurate results by assuming a constant form factor and making more runs closer to the sailing conditions of the vessel. The error from assuming a constant form factor may thus be offset by more accurately obtaining the wavemaking resistance and sideforce of the boat for heel and yaw combinations that actually occur when under sail.

A sensitivity analysis is therefore needed to examine the effect that small errors in the form factor determination have on the prediction of the full scale resistance of the yacht.

Equation 2.4 gives the total upright resistance coefficient of the full scale boat.

$$C_{ts} = C_r + (1+\kappa)C_{fs} = C_{tm} + (1+\kappa)(C_{fs} - C_{fm}) \tag{2.4}$$

Defining the sensitivity of the total resistance prediction to form factor to be the inverse of the total resistance multiplied by the partial derivative of total resistance w.r.t. form factor, equation 2.5 is obtained.

$$\frac{1}{R_{ts}}\frac{\partial R_{ts}}{\partial \kappa} = \frac{1}{C_{ts}}\frac{\partial C_{ts}}{\partial \kappa} = \frac{C_{fs} - C_{fm}}{C_{tm} + (1+\kappa)(C_{fs} - C_{fm})} = \frac{\frac{C_{fs}}{C_{fm}} - 1}{\frac{C_{tm}}{C_{fm}} + (1+\kappa)(\frac{C_{fs}}{C_{fm}} - 1)} \tag{2.5}$$

From equation 2.5, it can be seen that the effect of form factor errors is small when :

1. the model frictional resistance coefficient approaches that of the full scale vessel. This happens only when model and ship are moving at similar Reynolds num-

bers. But when their Froude numbers are identical, their Reynolds numbers can be similar only when model and ship approach the same size. Therefore, as the scale factor, λ, increases, the full scale resistance prediction becomes insensitive to form factor.

2. the total model resistance becomes large compared to the frictional resistance. This means that the wave-making component of resistance is high. Therefore, errors in form factor become less significant at high speeds when a large part of the total resistance is due to wave-making.

Actual values for the form factor sensitivity were obtained for a specific America's Cup model tested at the towing tank. The scale factor for this model was $\lambda = 0.31$, and its form factor was $\kappa = 0.235$. Figure 2-3 shows the total resistance sensitivity to form factor of this model at several speeds and was obtained by calculating the frictional resistance from the I.T.T.C. line, measuring the total model resistance from the towing tank test and then substituting them into the above formula for sensitivity.

For this example, it can be seen that the change in predicted total resistance per unit error in form factor is $\leq 26.7\%$. But referring to figure 2-2, the error from assuming a constant form factor is less than 0.07 in the worst condition (model 1). Thus, for the America's Cup class models tested, the worst case error in predicted resistance when assuming a heel-invariant form factor is less than 1.6%.

Although this 1.6% may not seem much, it is translated to 2–3 minutes around the course. Of course, this is a worst case estimate because it assumes that the boat is sailing at the heel angle whose form factor differs most from the upright form factor; but still, it illustrates that ignoring the heel dependence of the form factor is a potential problem.

Fortunately, the full VPP model, which accounts for wavemaking drag due to heel and yaw, is not as sensitive to form factor variations with heel as one would fear from the above example. So when a constant form factor is assumed and the boat is heeled, the change in viscous drag due to the different form factor is accounted for by a change in the wavemaking drag. The error produced in this case is only

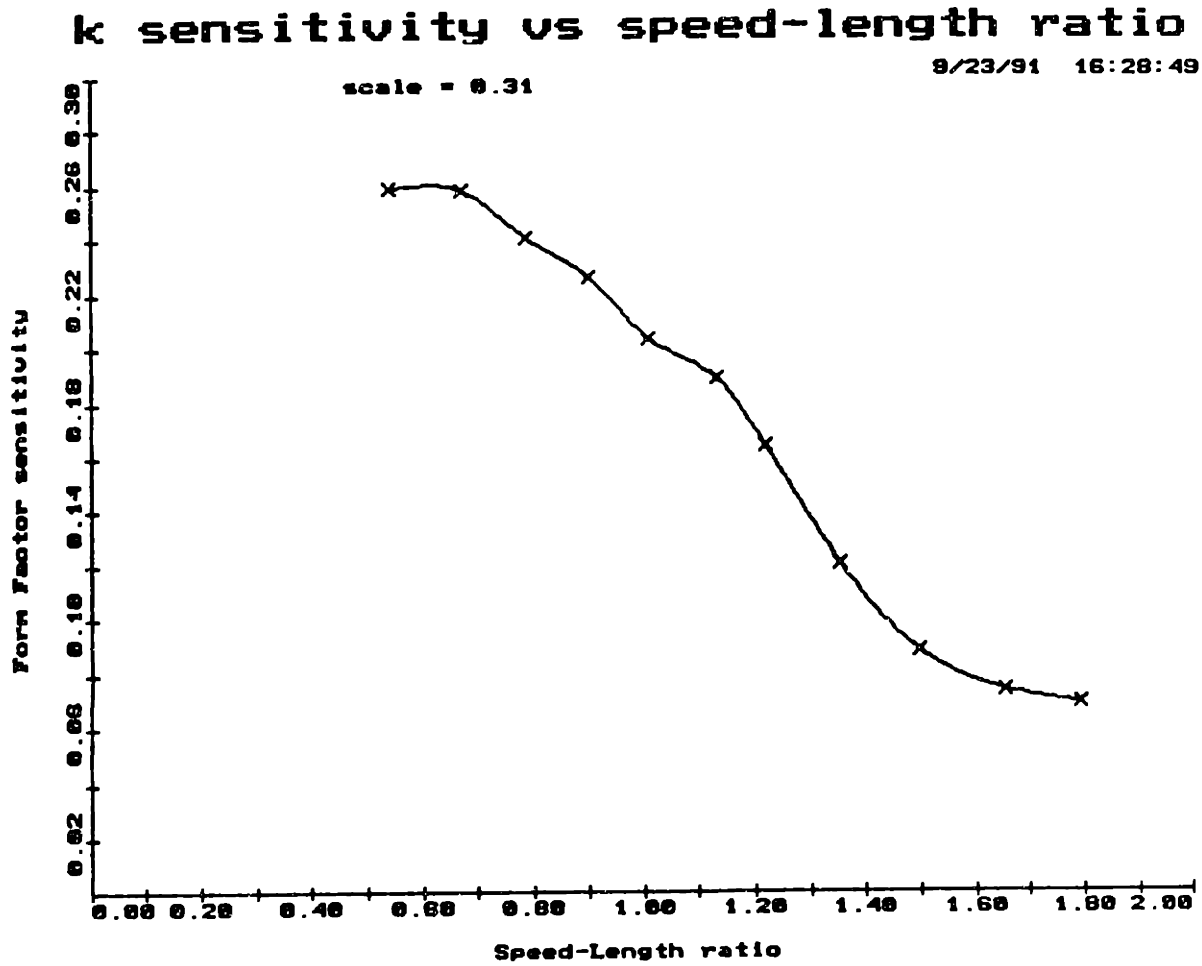

Figure 2-3: Form factor sensitivity versus speed-length ratio

America's Cup Course Race Times (Minutes)

Wind Speed (kts)	Windward	Leeward	135 Reach	100 Reach	TOTAL
7.00	99.23	69.98	29.94	15.35	214.50
8.00	91.11	62.06	26.56	14.67	194.40
9.00	86.11	55.91	23.84	14.14	180.00
10.00	83.02	51.18	22.13	13.71	170.03
11.00	80.84	47.53	20.84	13.31	162.52
12.00	79.24	44.62	19.84	12.94	156.64
13.00	78.02	42.34	18.98	12.60	151.94
14.00	76.97	40.51	18.20	12.29	147.97
16.00	75.33	37.53	16.81	11.73	141.39
18.00	74.03	34.70	15.43	11.24	135.40

Table 2.1: VPP Output assuming constant form factor

due to the difference in the way the wavemaking and viscous forces are translated to full scale (see section 1.1). Specifically, with the assumption of constant form factor, the Reynolds number dependent change in total resistance coefficient, which occurs due to the heel dependent form factor, is incorrectly included in the wavemaking resistance coefficient due to heel and yaw which is only Froude number dependent.

For model 1, the design with the most form factor variation out of those shown in figure 2-2, the VPP was run assuming both constant and heel dependent form factor. The output is shown in tables 2.1 and 2.2 respectively. The difference between the two cases is of the order of 0.03%, or 4 seconds around the course, which is quite acceptable. Note how all of this difference occurs in the windward legs of the course where the boat is heeled and yawed the most.

Thus it can be concluded that modeling the form factor to be dependent on heel angle is not worth the extra runs needed to obtain the form factor at several heel angles. For a prescribed number of tank data runs, with fewer "form factor" runs, more can be done at speeds and heel–yaw combinations that correspond to actual sailing conditions in order to obtain better data accuracy within the sailing range.

In order to examine the resistance sensitivity to form factor versus scale factor, equation 2.5 was used in conjunction with actual towing tank data. Different scale ratios were obtained by assuming various lengths of the full scale boat, calculating

America's Cup Course Race Times (Minutes)

Wind Speed (kts)	Windward	Leeward	135 Reach	100 Reach	TOTAL
7.00	99.16	69.98	29.94	15.35	214.43
8.00	91.03	62.06	26.55	14.67	194.32
9.00	86.03	55.90	23.84	14.14	179.92
10.00	82.94	51.18	22.13	13.70	169.96
11.00	80.77	47.53	20.84	13.30	162.44
12.00	79.18	44.62	19.84	12.93	156.57
13.00	77.96	42.34	18.98	12.59	151.87
14.00	76.91	40.51	18.20	12.29	147.91
16.00	75.26	37.53	16.81	11.73	141.33
18.00	73.98	34.70	15.43	11.23	135.34

Table 2.2: VPP Output assuming heel dependent form factor

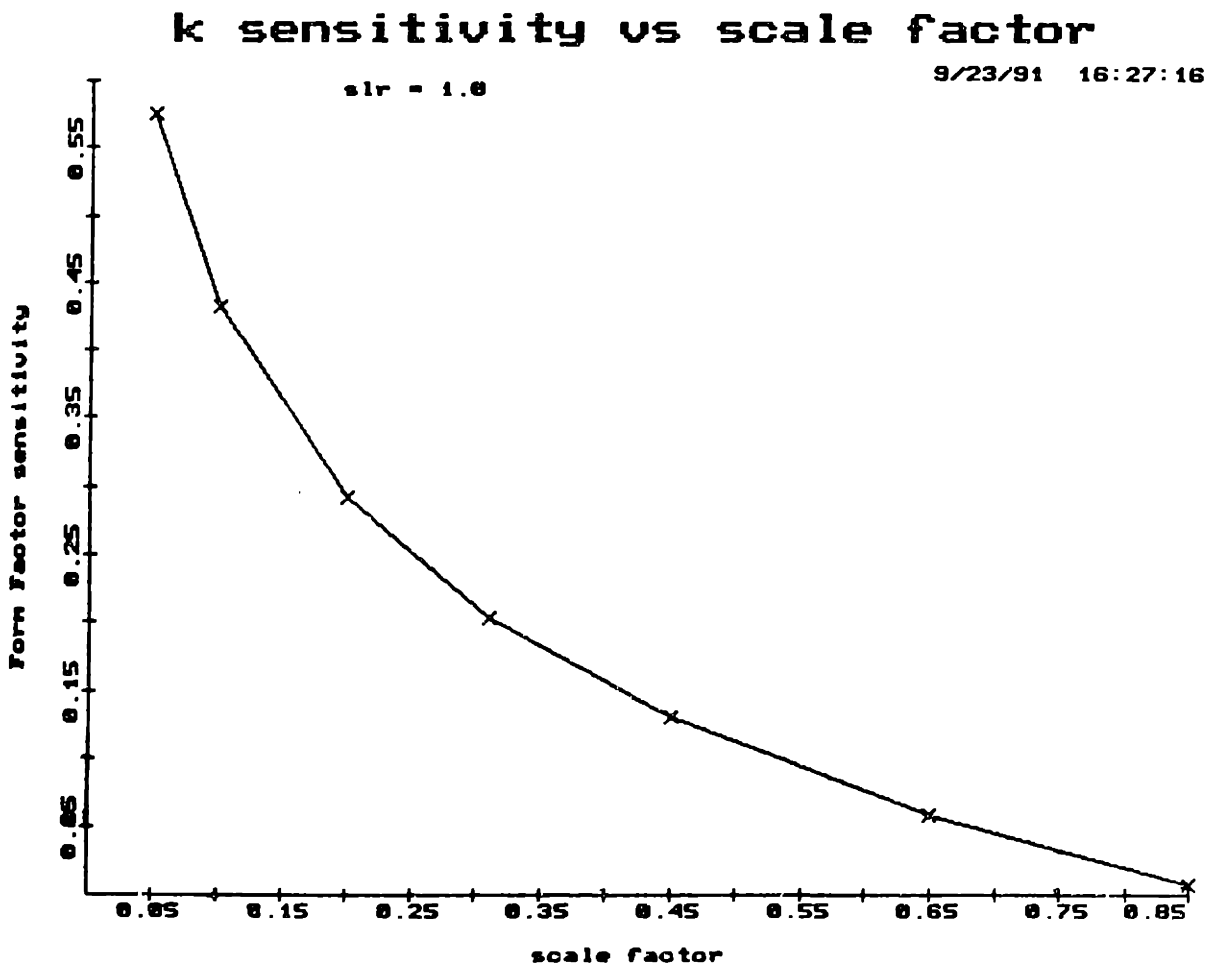

Figure 2-4: Form factor sensitivity versus scale factor

the full scale frictional resistance coefficients, and hence obtaining the form factor sensitivities.

A similar plot to figure 2-3 was made, only this time with a constant speed-length ratio at a range of scale factors. This plot is shown in figure 2-4. As expected, the sensitivity of the full scale resistance prediction to form factor decreases rapidly with the scale factor.

Chapter 3

THE EFFECT OF HEEL AND YAW ON RESISTANCE

In this chapter, the modeling of residuary resistance due to heel and yaw will be examined. Two methods were implemented in the VPP and their relative merits will be discussed.

3.1 The VPP Fit of the Resistance due to Heel and Yaw

When a sailboat moves through the water under heel and yaw, it presents more resistance than when it is upright and moving with no leeway. The VPP tries to model this fact by assuming that the coefficient of resistance due to heel and yaw, C_{hay}, is given by :

$$C_{hay} = C_1 \, C_h^2 + C_2(\frac{\phi}{30})^2 + \{error \ fit\} \tag{3.1}$$

where C_h is the heel force coefficient, ϕ is the heel angle and C_1 and C_2 are coefficients to be determined.

The first term of the above equation is due to the theoretical result that the induced drag on a lifting surface is proportional to its lift squared, while the second term is empirically justified. The "error fit" term is a polynomial fit of the difference

between the first two terms and the actual data obtained from the towing tank, as a function of the speed-length ratio, the heel-force coefficient and the heel angle.

$$\{error fit\} = \sum_{i,j,k} X_{i,j,k} (\frac{V}{\sqrt{L}})^{(i-1)} C_h^{(2j-2)} \phi^{(k-1)} \tag{3.2}$$

where the indices i,j and k range from 1 to a value depending on the number of data points available. The values of the coefficients, $X_{i,j,k}$, are found by performing a least-square-error calculation using the tank data.

Obviously, as the number of coefficients increases, the agreement between this VPP model and the data improves. However, if too many coefficients are used, the fit is not smooth enough and hence produces large errors in regions between data points. The exact number of coefficients to be used for a given towing tank run sequence is found by observing the total resistance as predicted by this VPP model. A way of doing this is to look at curves of C_{t_s} versus speed-length ratio, to see if they look smooth enough and if they are in fair agreement with the data points.

The exact range of the indices i,j and k is also found empirically. For example, it was found that for the 105 run sequence which was used for the testing of America's Cup boats, the optimum range of indices was *i=1..3, j=1..2, k=1..3.*

With the indices taking the above values, the polynomial fit usually had a low root-mean-square error at the data points while still being well behaved between them. So this 18 coefficient fit was adopted for the testing program. An example of this fit on the 105 run sequence is shown if figure 3-1.

3.1.1 Weighting of the Data Points

Towing tank data is taken for a wide range of model speeds and several heel and yaw angles, including speeds at which the boat is never expected to sail and heel/yaw combinations which are impossible to occur in reality.

There are several reasons for this apparent waste of runs. First of all, since the VPP model separates resistance due to heel and yaw from upright resistance, it is necessary to calculate the upright residuary resistance as accurately as possible. This

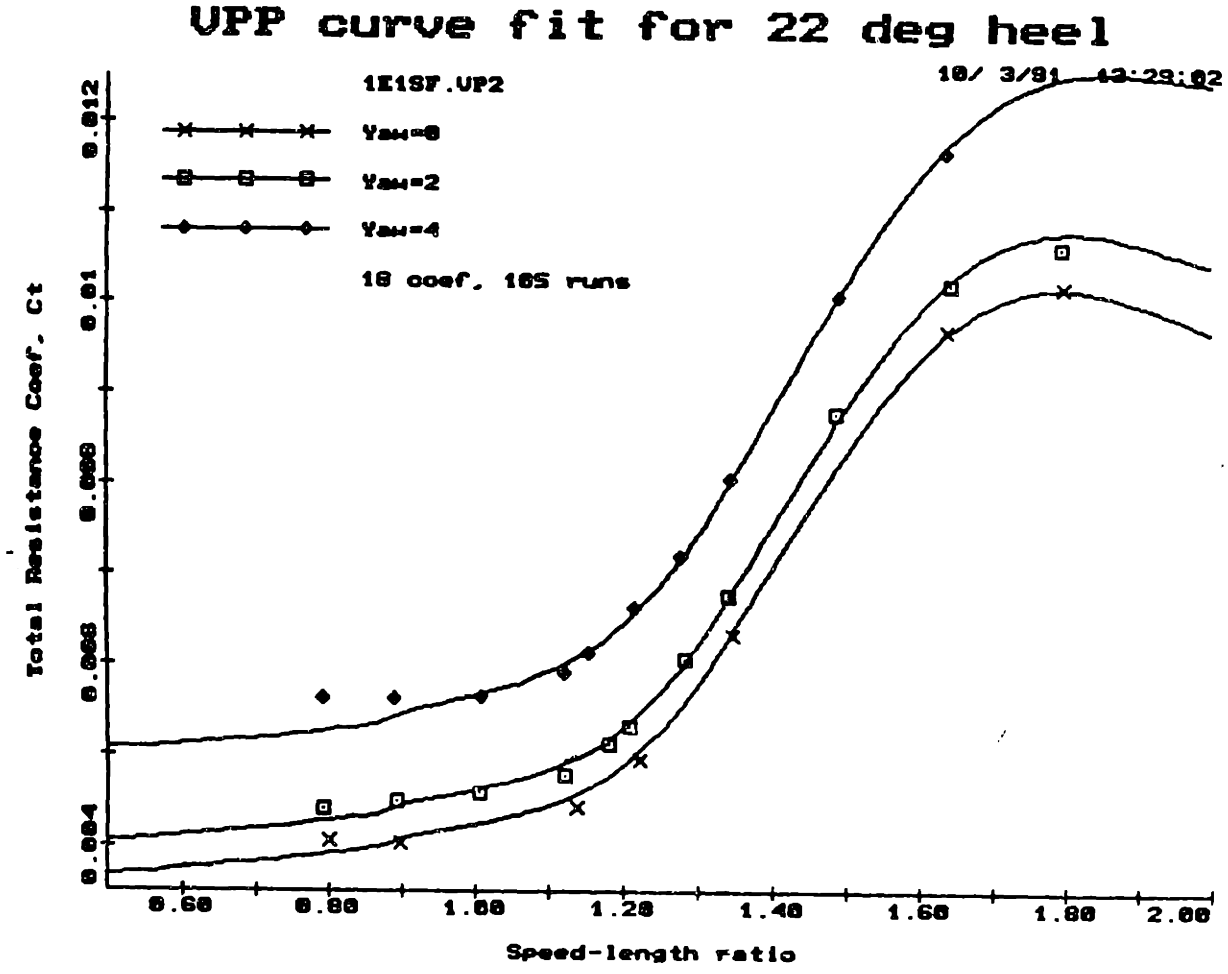

Figure 3-1: VPP fit for 105 runs with 18 polynomial coefficients

means making quite a few runs at no heel and no yaw which is not a likely situation for a sailboat under sail. Also, in order for the VPP to reach convergence when iteratively determining the vessel's speed, it is necessary to have a wide range of conditions for which reasonable values of resistance are produced. Finally, it is very cumbersome to have to estimate the expected sideforce/righting moment combinations, convert them to yaw/heel combinations at each speed and then adjust the heel and/or yaw setting on the carriage before each run.

Thus, only a few heel angles (perhaps four) are tested at a few standard yaw angles (perhaps three) each.

In order to have the most accurate results possible, it is therefore desirable to have the VPP fit match the data as closely as possible at conditions which are expected to occur when the vessel is sailing. On the other hand, the accuracy of the fit is not as important at unlikely combinations of heel, yaw and velocity. Therefore, a weighting scheme was devised which tries to weight each run when the $X_{i,j,k}$ coefficients of the error fit are determined.

This scheme gives a run double weight when the heel force and the heel angle are in accordance. When the boat is sailing, the aerodynamic heel force coupled with the equal and opposite hydrodynamic heel force, are balanced by the hull's righting moment. Hence, in order to determine whether a run is close to the above condition, the heel angle is compared to the heel force multiplied by the vertical distance between the sail and hull centers of sideforce and divided by an average static righting moment per degree. If these two values are within a specified range, then the run is given a double weight.

The above method is somewhat arbitrary in that there is no theoretical indication why the weight of some runs should be exactly twice that others, and no specification exists on how close the runs need to be in order to be weighted double. These values were determined empirically, and thus the errors introduced by taking an *average* hull righting moment and by ignoring the dynamic righting moment. In other words, the offset in the heel–sideforce balance due to the errors, is compensated by the empirical choice of the range of heel angles for double weight.

For a particular testing program, the criterion for giving a run double weight might be :

$$0.6\frac{F_H\ h}{RM_{av}} \leq \phi \leq 1.5\frac{F_H\ h}{RM_{av}}$$

where h is the distance between sail and hull centers of effort (about 12 meters full scale), RM_{av} is the average righting moment per degree and F_H is the heel force.

In addition, if the above criterion is satisfied, a run may be given quadruple weight if it is within a specified velocity range. This is done in order to make the VPP fit of the data as accurate as possible within the expected sailing speeds of the actual boat. For the above example, runs at speed-length ratios between 1.0 and 1.2 satisfying the heel–sideforce condition may be given quadruple weight.

3.1.2 Sensitivity to Weighting

The arbitrariness of the weighting of each run, as illustrated above, made necessary an examination of the sensitivity of the VPP output to the weighting scheme used.

It is not obvious what kind of weighting produces the most accurate results. As one extreme take the case where all runs have the same weight. Then, the fit in the sailing region of the data will be affected by mismatches between the VPP model and the data outside this region. On the other hand, if only runs in the sailing region are considered, there is not enough data to have an accurate fit.

In order to further investigate the sensitivity of the performance prediction to weighting, the weighting functions shown below were used in analyzing the data for a specific boat.

- A parametric weighting function such that if $0.6\frac{F_H\ h}{RM_{av}} \leq \phi \leq 1.5\frac{F_H\ h}{RM_{av}}$, then $weight = 2a$. If in addition the speed-length-ratio is between 1.0 and 1.2 then $weight = 4a$. Otherwise, $weight = 1.0$. Here a is the parameter to be varied. A "standard weighting" that seemed appropriate is the above weighting function with $a = 1$. Cases for a=0 (all runs equal weight), a=0.5, a=2, and a=10 were also examined.

- The standard weighting scheme but with no extra weighting for runs in the

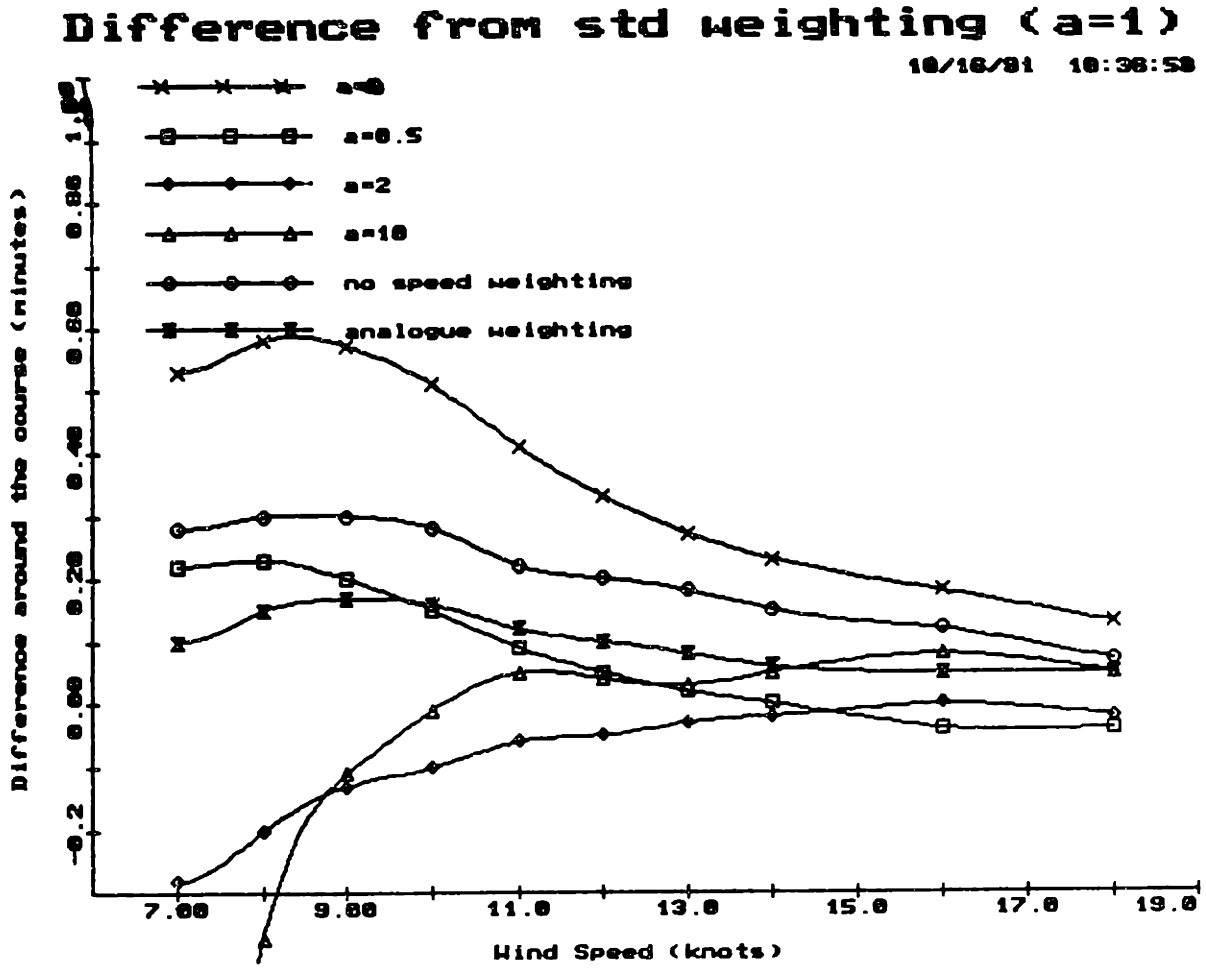

Figure 3-2: Differences in performance prediction due to different weighting schemes

speed range $1.0 \leq \frac{V}{\sqrt{L}} \leq 1.2$.

- An analogue weighting function such that :

$$weight = (1 + \frac{1}{cosh(2.5\frac{\phi RM_{sv}}{F_H h} - 1.05)})(1 + \frac{1}{cosh(11\frac{V}{\sqrt{L}} - 1.1)})$$

this function attempts to approximate the standard weighting, which seems intuitively correct, with a continuous function.

The VPP was run for all the above run weightings and the results are summarized in figure 3-2. It can be seen that the weighting scheme that gives too little weight on the data outside the sailing range (i.e. $a = 10$), is inaccurate at low speeds. It is also suspected that the prediction with all runs having equal weighting is biased

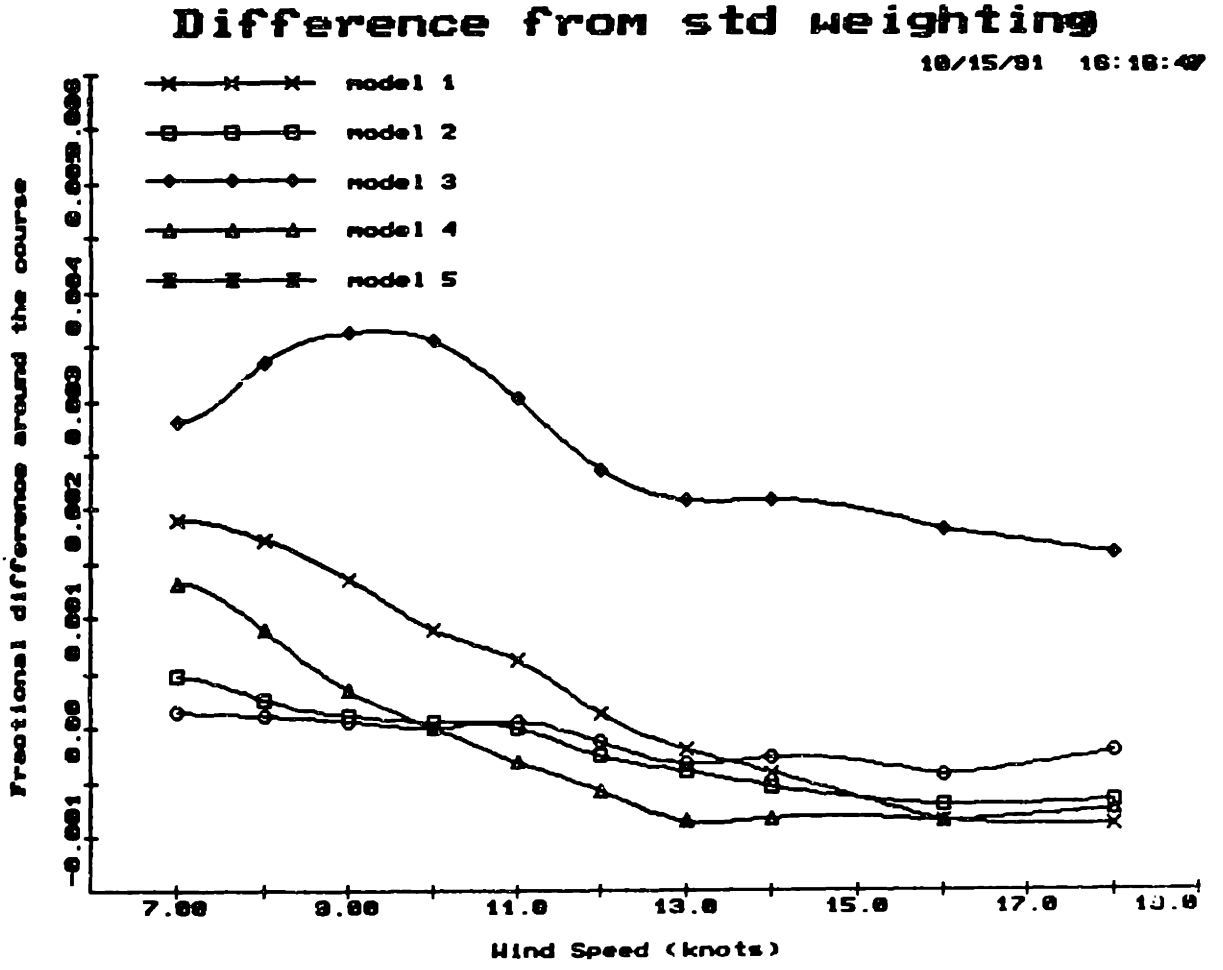

Figure 3-3: Fractional differences in time around the course between standard and no weighting cases

from data outside the sailing region, and hence must also be inaccurate.

Excluding the above two extreme cases, the sensitivity to the rest of the weighting schemes is not very high. For the particular model examined, the VPP outputs for the rest of the cases, agree within half a minute around the course at low wind speeds and within 10 seconds at high wind speeds. Although this is not especially good accuracy for purposes such as America's Cup class boat velocity prediction, there is not much that can be done about it, except to investigate the sensitivity to weighting of other models.

Figure 3-3 shows, for several models, the fractional difference between the predicted time around the course for the standard weighting (a=1) and for no weighting (a=0). Model 3 in this figure corresponds to the model investigated for the various

weightings (figure 3-2). As it can be seen, this model is actually the most sensitive to weighting, with quite a large difference from the rest of the models examined. Most models should therefore be considerably less sensitive to weighting than indicated in figure 3-2.

Intuitively, one would expect a weighting with $0.5 \leq a \leq 2.0$ to produce the most accurate results. However, there is no easy way of finding the optimum weighting scheme. Fortunately however, the VPP prediction is not very sensitive to reasonable weighting schemes.

3.2 An Alternative Approach to the VPP Fit

As seen in the previous section, the VPP error fit was somewhat arbitrary and the results were affected by the weighting of each run for determining this fit. An alternative method of determining the resistance due to heel and yaw, which does not rely on such an arbitrary polynomial fit, was therefore investigated. The outline and results of this investigation are given below.

Instead of trying to fit the data with a specific 3-dimensional function, it was thought possible to *interpolate* between data points, keeping in mind the dominant effect of the square of the heel and the square of the sideforce on the resistance due to heel and yaw.

Tank testing of sailboats usually involves making runs at a few nominal values of heel and yaw, at a range of model speeds. However, the heel seldomly takes its nominal value, due mostly to the speed dependent roll moment produced by yaw, coupled with deflections in the heel restraint system. Similarly, runs at nominally constant yaw, produce sideforce coefficients which are speed and heel dependent.

One way to interpolate between data points could be to select the nearest data points to the required speed, heel and sideforce and then take some sort of average in order to find the resistance due to heel and yaw at that point. This method would be highly inaccurate, mostly because at speed-length ratios relatively far from data points, the resistance would not be accurately represented.

Another more accurate way of interpolating would make use of the structure of the data, in order to obtain the resistance at any speed for all nominal combinations of heel and yaw. This is considerably more complicated, because all data points must first be interpolated to their nominal values of heel and sideforce.

The correction to nominal heel is quite simple, because of the relatively small effect of heel variations on resistance. Thus, the partial derivative of C_{hay} with respect to ϕ^2 is assumed to be constant and equal to the average ratio of C_{hay}/ϕ^2 at zero sideforce. The resulting value for the heel corrected residual resistance is given by equation 3.3.

$$C_{hay,1} = C_{hay} - [\frac{C_{hay}}{\phi^2}]_{(ave),(C_h=0)} \Delta\phi^2 \tag{3.3}$$

where $C_{hay,1}$ is the resistance due to heel and yaw, at nominal heel and $\Delta\phi^2$ is the difference between the actual and nominal values of heel squared.

The correction for sideforce variations requires more care, because small differences in sideforce account for relatively large differences in induced drag. Hence, $\frac{\partial C_{hay,1}}{\partial C_h^2}$ is assumed to be roughly the average $C_{hay,1}/C_h^2$ over all speeds for that particular heel/yaw combination. The resistance corrected to nominal sideforce coefficient, $C_{hay,2}$, is therefore given below.

$$C_{hay,2} = C_{hay,1} - [\frac{C_{hay,1}}{C_h^2}]_{(ave),(\substack{\phi=nominal \\ yaw=const})} \Delta C_h^2 \tag{3.4}$$

where ΔC_h^2 is the difference between the actual and nominal values of sideforce coefficient squared.

After the above corrections, fitting a curve to $C_{hay,2}$, made possible the accurate estimation of resistance at any nominal combination of heel and yaw. Usually, enough runs are made at each heel/yaw combination so that a cubic spline is expected to accurately define the resistance at any speed.

In order to obtain a value of resistance for *any* value of heel and sideforce, it is necessary to interpolate between the curves of nominal heel and yaw, obtained by the above method. From theoretical considerations and experimental verifications, it is expected that resistance due to heel and yaw depends on the square of the sideforce

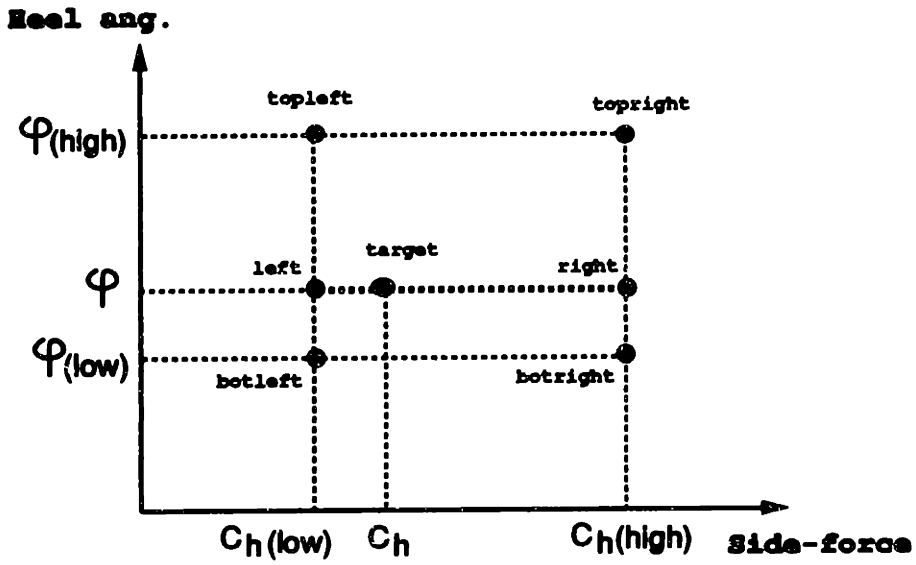

Figure 3-4: Interpolation between curves of nominal heel/yaw

and the square of the heel angle. Thus, the interpolating scheme should incorporate this dependence. Figure 3-4 graphically shows how the resistance due to heel and yaw at arbitrary ϕ and C_h may be determined by the four closest nominal heel/yaw combinations.

The resistance at the top-left point of figure 3-4 is therefore assumed to be given by equation 3.5.

$$C_{hay(topleft)} = \alpha_2 \phi^2_{high} + \alpha_1 \tag{3.5}$$

where α_1 and α_2 are constants to be determined.

Similarly, the resistance due to heel and yaw at the bottom-left point is given by equation 3.6.

$$C_{hay(botleft)} = \alpha_2 \phi^2_{low} + \alpha_1 \tag{3.6}$$

Combining the two above equations, the resistance at any point with the same sideforce coefficient and speed as the top-left and bottom-left points of figure 3-4 but

with heel angle ϕ, may be found as shown in equation 3.7.

$$C_{hay_{(left)}} = \frac{(C_{hay_{(topleft)}} - C_{hay_{(botleft)}})\phi^2 + C_{hay_{(botleft)}}\phi^2_{high} - C_{hay_{(topleft)}}\phi^2_{low}}{(\phi^2_{high} - \phi^2_{low})} \quad (3.7)$$

Similarly, for the side of high sideforce (right), the resistance is interpolated according to equation 3.8

$$C_{hay_{(right)}} = \frac{(C_{hay_{(topright)}} - C_{hay_{(botright)}})\phi^2 + C_{hay_{(botright)}}\phi^2_{high} - C_{hay_{(topright)}}\phi^2_{low}}{(\phi^2_{high} - \phi^2_{low})} \quad (3.8)$$

Finally, an interpolation between the points with high and low sideforce, at the target heel angle, gives the following formula for the resistance at C_h and ϕ.

$$C_{hay_{(target)}} = \frac{(C_{hay_{(right)}} - C_{hay_{(left)}})C_h^2 + C_{hay_{(left)}}C^2_{h,high} - C_{hay_{(right)}}C^2_{h,low}}{(C^2_{h,high} - C^2_{h,low})} \quad (3.9)$$

where $C_{hay_{(right)}}$ and $C_{hay_{(left)}}$ are given by equations 3.8 and 3.7 respectively.

Figures 3-5 to 3-7 show the calculated C_{hay} curves for nominal heel and sideforce for a typical towing tank test. As it can be seen, these curves fluctuate considerably over the speed range, even with a least-square-error cubic spline fit through the data points. This is undesirable because it causes convergence problems to the VPP. Also, the fact that C_{hay} does not behave exactly according to the square of the sideforce and heel, makes the makes $\frac{\partial C_{hay}}{\partial \phi}$ and $\frac{\partial C_{hay}}{\partial C_h}$, discontinuous, thus creating more convergence problems. For example, if at a particular sideforce, the resistance at a higher heel angle is actually less than that at a data point with less heel, the interpolated C_{hay} versus heel curve will have an unwanted sharp maximum.

Another disadvantage of this method was the fact that the interpolation was made not between actual data points, but between *estimates* of data points at the "nominal" values of heel and sideforce. These estimates are based on the assumption of quadratic dependence of C_{hay} on ϕ and C_h, which is not entirely accurate. Hence

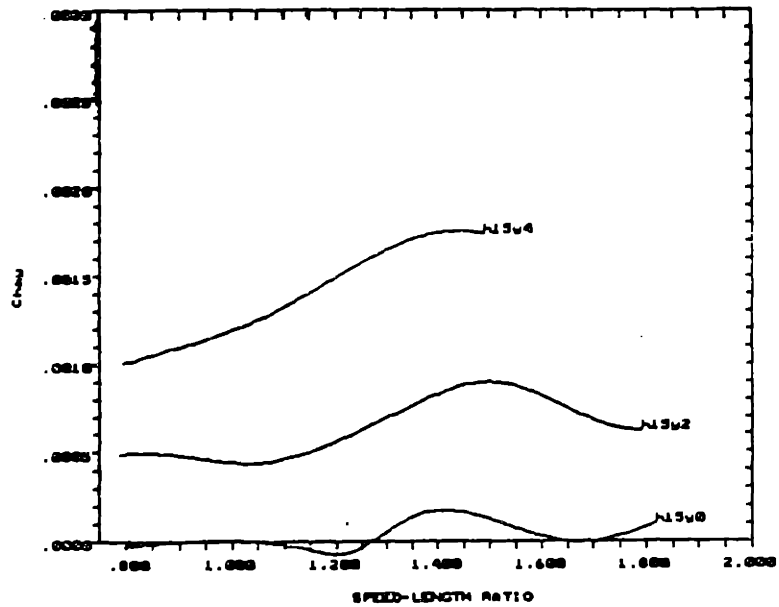

Figure 3-5: Curves of Resistance due to heel and yaw (nominal values of heel & sideforce, heel=15 deg)

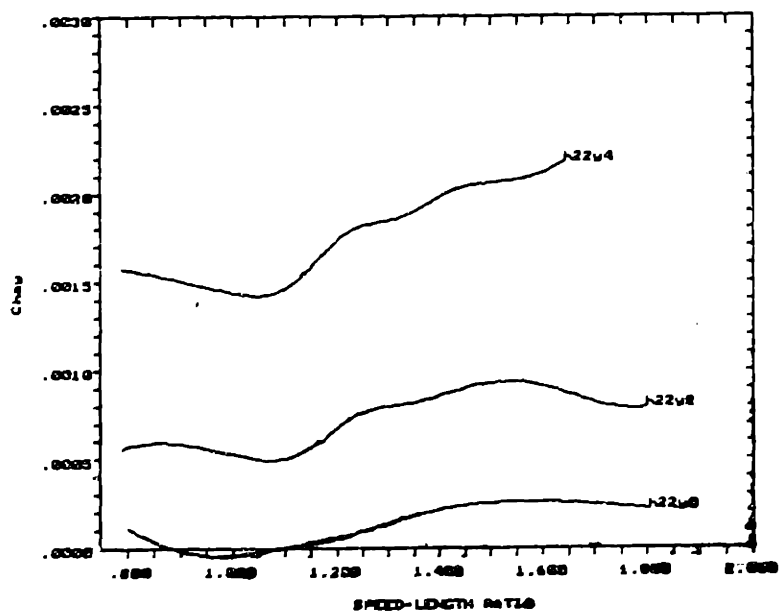

Figure 3-6: Curves of Resistance due to heel and yaw (nominal values of heel & sideforce, heel=22 deg)

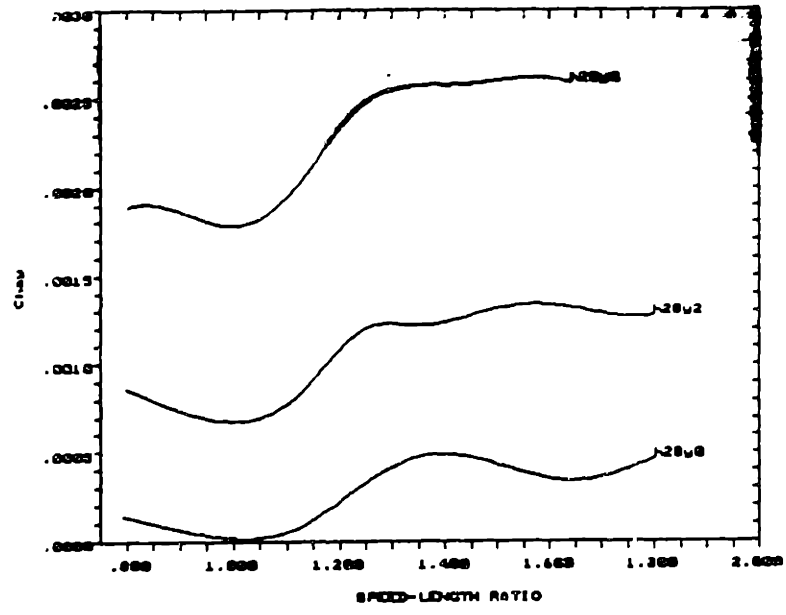

Figure 3-7: Curves of Resistance due to heel and yaw (nominal values of heel & sideforce, heel=28 deg)

if the actual data points are considerably different than the nominal values (which is often the case for sideforce), interpolation is done between erroneous values.

The VPP results for the above method of modeling the resistance due to heel and yaw were not satisfactory. The VPP did not always converge to a solution, and when it did, the results were generally not within the desired accuracy range (0.2 minutes around the course) from the polynomial fit method.

Thus, the interpolation of curves method for C_{hay} determination was abandoned until a way is found to overcome the problems stated above.

Chapter 4

APPENDAGE DRAG CONSIDERATIONS

This chapter deals with the drag of sailboat appendages. The reason why such appendages should be considered separately in a tank test will be explained. A calculation of the drag of the model keel and rudder was performed experimentally and will be compared to the prediction assuming fully turbulent flow. Finaily, a sensitivity study will be performed, so that the effect of the errors in calculating the model appendage drag can be examined.

4.1 Introduction

As it has been mentioned in section 2.1, it is best to consider the frictional drag of the appendages separately, and hence perform the data analysis on the hull (canoe-body) without this component. The logic behind this argument is that the local Reynolds numbers of the appendages are quite different from that of the hull, and therefore extrapolate to hull scale somewhat difficultly.

Separation of the appendage drag allows a more reasonable Reynolds factor selection for the hull. The frictional resistance coefficient of a vessel is assumed to be a function of the Reynolds number, $Rn = \frac{UL}{\nu}$. For a flat rectangular plate with motion parallel to two of its sides, the selection of the length to use for the Reynolds number

is the length of the plate in the direction of motion. For other shapes, however, the choice of length is not so obvious. In order to use the experimental data collected for flat plates to estimate the frictional resistance of a complex shape, a length equal to the length of a flat plate of equal resistance at the same speed must be chosen. It has been suggested that this length should be the mean "contact length" of a water particle with the body. The ratio of the length of the body to the length to be used for calculating the Reynolds number is called the Reynolds factor.

For conventional hull-forms, it has been found that a Reynolds factor in the range of 0.7 to 1.0, produces satisfactory results. Specifically, hulls such as the canoe-body of modern sailing yachts require a Reynolds factor of 0.7 to 0.8. If, however, the appendages are considered together with the bare hull, then there exists no empirical value for the Reynolds factor, mainly because the shape and size of the keel and rudder vary considerably from boat to boat. It is thus much easier to deal with the appendages separately.

4.2 Calculation of Model Appendage Drag

The only component of appendage drag which is best calculated separately is the frictional drag. The residuary resistance of the appendages is then included in the residuary resistance of the entire boat.

The easiest way to calculate the frictional drag of the appendages is to assume that they are in agreement with the International Towing Tank Conference (ITTC) friction line. For an appendage moving at Reynolds number, Rn, the frictional resistance coefficient as suggested by the ITTC is estimated as follows.

$$C_f = \frac{0.075}{(log(Rn) - 2)^2} \tag{4.1}$$

Here, the Reynolds number is based on an average length of the appendage in the direction of motion.

This method, when corrected for form drag, gives satisfactory results for the full

scale appendages. It is not as accurate, however, for the model scale appendages tested in the towing tank. The actual frictional drag of a model appendage may vary from the ITTC prediction due to some (unknown) degree of laminar flow on the appendage.

For a more accurate approach, a set of upright (no heel, no yaw) runs could be made with the appendage removed, and compared to the upright runs with the appendage in place. The difference in low speed drag between the two tests should be equal to the appendage drag, and could be used to model appendage frictional drag for all the runs of the test sequence.

Such an experiment was performed in order to investigate the drag of the keel and rudder of the 0.31 scale models used.

A particular model was tested, first with all appendages in place, then with the rudder removed, and finally with both rudder and keel removed. By subtracting the total drag of the second test from that of the first test, the drag of the rudder was found. This drag was normalized by $\frac{1}{2}\rho U^2 S_{rud}$, where S_{rud} is the wetted surface of the rudder, in order to obtain the actual resistance coefficient of this appendage.

Figure 4-1 shows the total drag coefficients of the hull and keel with and without the rudder, based on the wetted surface of the model with all appendages. The difference between these two curves, when multiplied by the ratio $\frac{S_{rud}}{S_m}$, gives the actual drag coefficient of the rudder (here, S_m is the wetted surface of the model with all appendages). This drag coefficient is shown in figure 4-2, along with the ITTC friction line, as a function of the model speed-length ratio. As it can be seen, the two estimations of rudder drag coefficient are not in compete agreement. Specifically, the experimental estimation of the rudder drag is somewhat lower than the ITTC prediction. The fluctuations of the experimental curve at high speed-length ratios are due to the wavemaking resistance of the rudder.

It can be argued that a rudder drag prediction of $C_d = 0.0033$ is closer to reality than the ITTC friction line, because for model speed-length ratios less than 1.15 the measured drag fluctuates around the above value. For greater speed-length ratios, the difference of behavior between ITTC and experimental rudder frictional drag

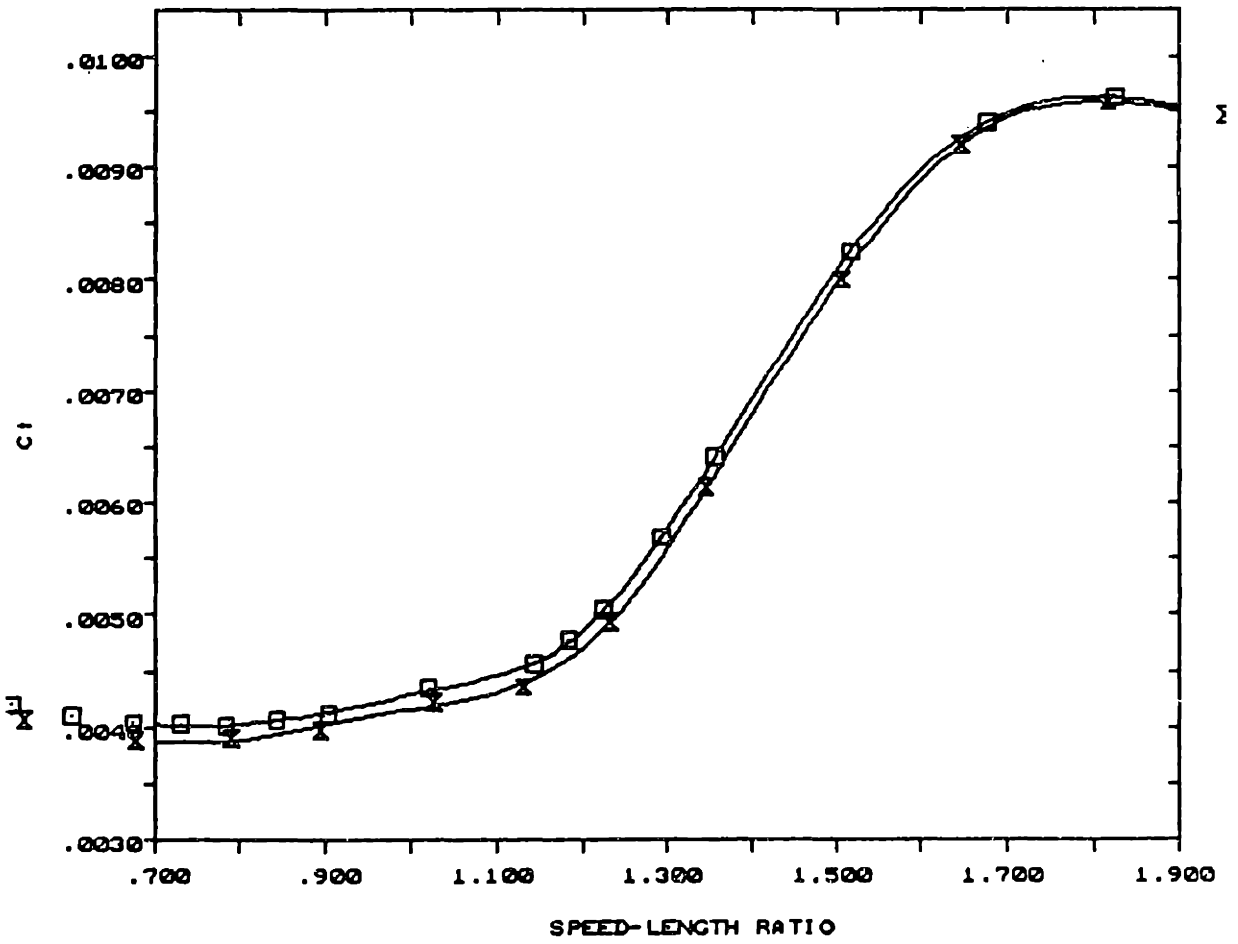

Figure 4-1: Total drag coefficients of the hull and keel, with and without the rudder, based on the wetted surface with all appendages

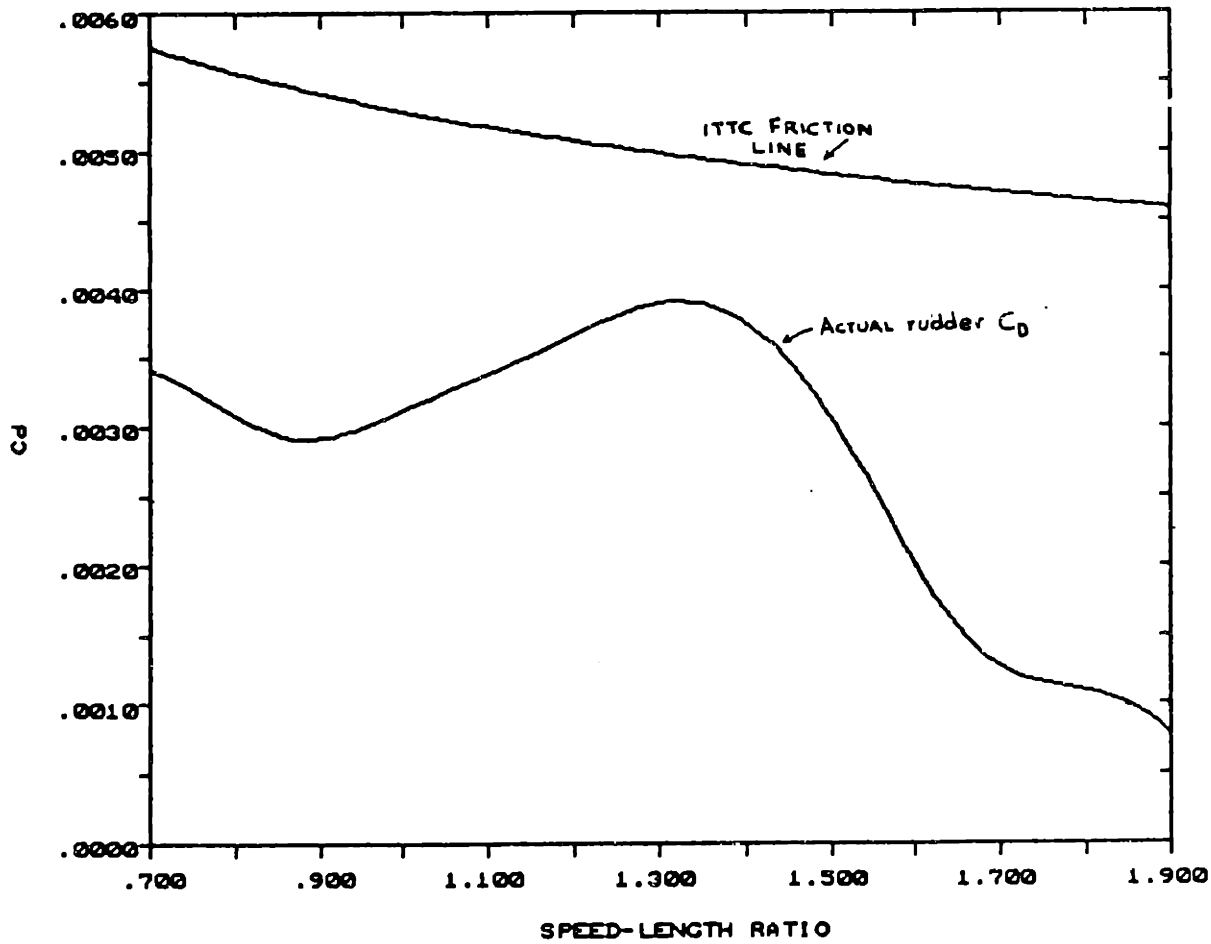

Figure 4-2: Actual and ITTC Rudder drag coefficients

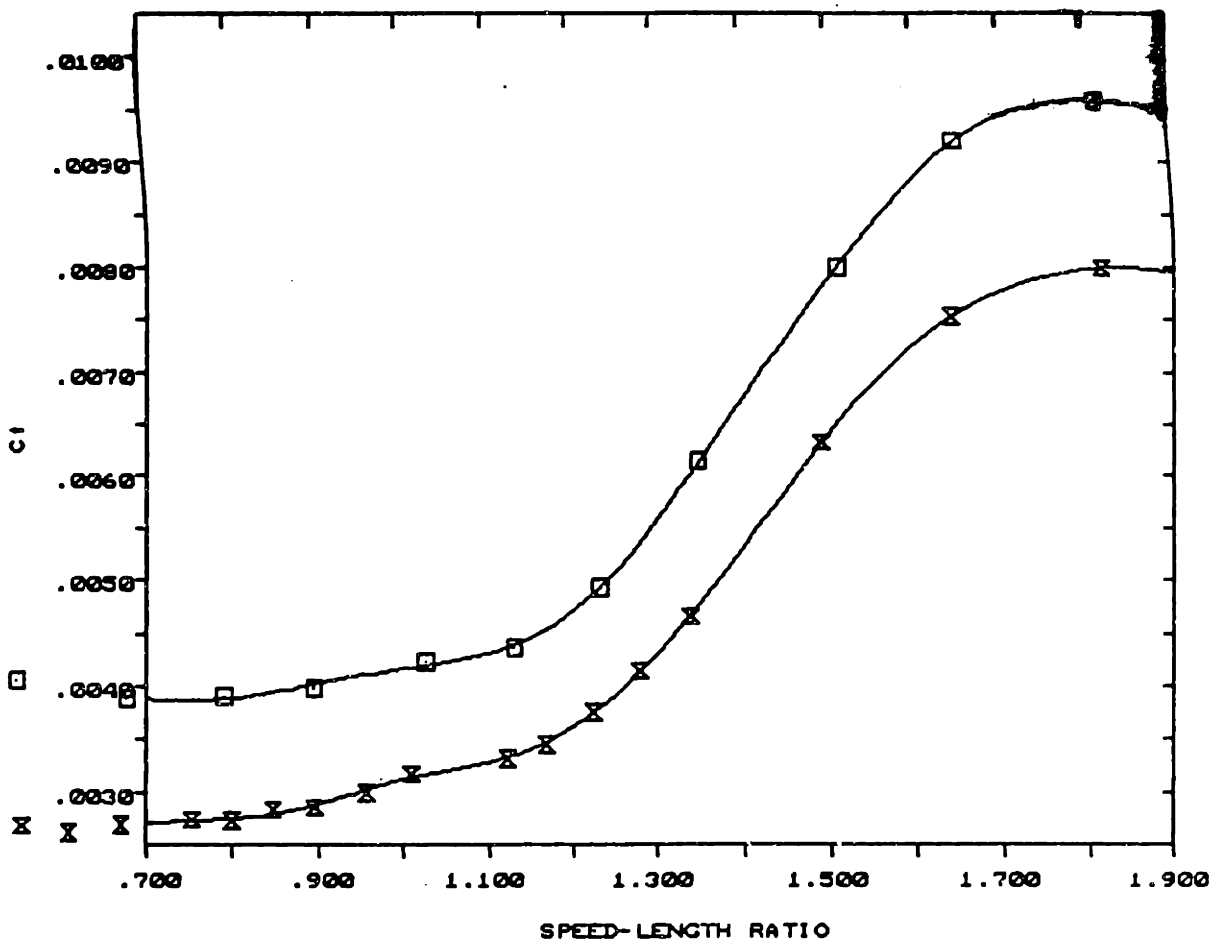

Figure 4-3: Total drag coefficients of the hull, with and without the keel, based on the wetted surface with all appendages

coefficients is due to the wave-making resistance of this appendage. Therefore, the high speed portion of figure 4-2 is not suitable for determining the frictional resistance of the rudder.

A similar experiment was performed for the drag of the keel fin and bulb. Figure 4-3 shows the model (with the rudder removed) total drag coefficients, with and without the keel, based on the wetted surface of the model with all the appendages in place. Similarly to the rudder test, the difference between the two curves, multiplied by $\frac{S_{keel}}{S_m}$ gives the drag coefficient of the keel. This keel drag coefficient as a function of model speed-length ratio is shown in figure 4-4.

The drag of the keel seems to agree with the ITTC line until a model speed-length ratio of 1.15. After this, it increases rapidly due to the wave-making of the keel. Thus,

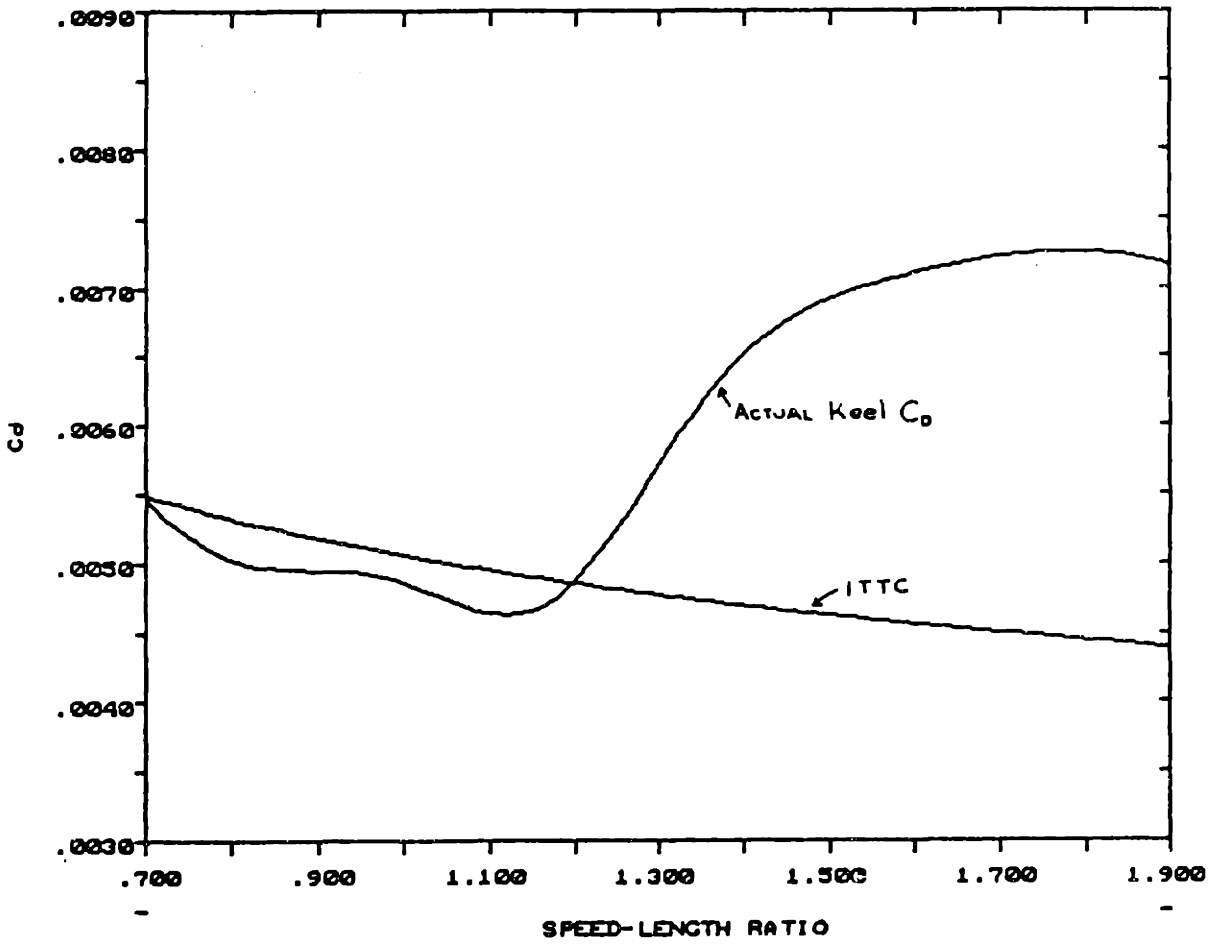

Figure 4-4: Actual and ITTC Keel drag coefficients

it was concluded that the ITTC friction line was a good approximation to the model keel frictional drag.

4.3 Sensitivity to Appendage Drag Prediction

With the above experimental method, the drag of the appendages is obtained relatively accurately for the upright runs. It is not known, however, if for the runs with heel and yaw the appendage resistance remains unchanged. For example, reduction of the keel–rudder interaction may change the the flow from turbulent to partially laminar on the rudder when the model is yawed. It is also not known if slightly different appendages that may be tested would have exactly the same behavior as those examined in the above experiments, or if the same appendages would behave in exactly the same way when mounted to (and hence interacting with) a different hull. Hence, a sensitivity study was performed, to examine the effect of model appendage drag estimation errors on the predicted resistance of the full scale ship.

The total resistance of the full scale boat is found by adding the full scale viscous drag (hull frictional and form drag plus appendage drag, R_{aps}) to the estimated wave-making resistance (Total model resistance minus hull viscous drag, minus appendage drag, R_{apm}).

$$R_{ts} = (1+\kappa)R_{fs} + R_{aps} + \frac{1}{\lambda^3}\{R_{tm} - (1+\kappa)R_{fm} - R_{apm}\} \tag{4.2}$$

Therefore, the fractional change in total resistance per unit error in appendage drag is given by the following expression :

$$\frac{1}{R_{ts}}\frac{\partial R_{ts}}{\partial R_{apm}} = \frac{-1}{\lambda^3 R_{ts}} \tag{4.3}$$

From figure 4-4 it can be seen that the error between the ITTC line and the experimental keel drag coefficient is within 0.0003 at low speeds.

For a speed-length ratio of 0.8, a typical resistance of the full scale boat is of the order of 350 lbs. At this speed, for a 0.31 scale keel with a wetted surface of 17.5 ft^2,

this error in C_d is translated to approximately 0.19 lbs (assuming model length of 20 ft).

Using equation 4.3, the above error in model keel drag prediction error gives a total resistance prediction error of 0.6%, which is of the order of a minute around an America's Cup course. This is a potential problem, because this is often the difference between the performances of designs being compared in the tank. If, however, all the boats to be compared have similar appendages, it can be assumed that the total resistance prediction error is the same for all vessels and their performances may still be accurately evaluated on a relative basis.

When different appendages are attempted to be tested in the towing tank, however, the assumption that the appendage drag error is the same for all tests may not be true. Hence, the maximum error in estimating appendage drag may be at different speeds and of different magnitudes. Thus, it could be dangerous to compare boats which are fitted with different appendages in the towing tank, as their relative performances may not be accurately predicted.

Therefore, from the above sensitivity analysis, it was concluded that towing tank tests could give misleading results when comparing models with different appendages. This is not surprising, considering that the difference in Reynolds number between the model and full scale boats, and the complexity of the flow past the appendages as compared to that past the hull, could well result in a lack of flow similarity over the appendages.

Hence, if it is desired to investigate the performance of various appendages, this might be best done in a wind tunnel rather than in a towing tank. Ideally, both towing tank and wind tunnel tests would be done so Reynolds and Froude number effects could be assesed.

If various hull forms are tested in the towing tank and various appendages in the wind tunnel, it is then possible to estimate the performance of any combination of hull and appendages using the VPP, appropriately modified to incorporate towing tank and wind tunnel data. This is based on the assumption that the interaction between hull and appendages is similar enough for all combinations. Hence, the optimum

appendages, as determined in the tunnel, combined with the optimum canoe-body, as determined from the tank, is assumed to produce the best vessel.

Chapter 5

TURBULENCE STIMULATION

This chapter deals with turbulence stimulation of the flow past the tank models. The accuracy of the nominal turbulence stimulator drag will be examined by looking at tests of the same model with a different number of stimulators. The sensitivity of the velocity prediction to the exact determination of the stimulator drag will also be examined.

5.1 Introduction

The Froude assumption requires that the frictional resistance of the model be known well enough so that it can be accurately subtracted from the total resistance in order to determine the residuary resistance (section 1.1).

Theoretically, therefore, the full scale resistance could be predicted even with laminar flow persisting over areas of the model, provided that those areas are known. In practice, however, it is much simpler to ensure that the flow over the model is fully turbulent, and then use the ITTC friction line to estimate the frictional resistance of the model.

Experiments with ship models have shown that without special devices to stimulate turbulence, laminar flow often persists over considerable areas. The persistence of laminar flow has been found to depend to a great extent on the pressure gradient along the entrance and on the factors which affect this, such as the shape of stem

profile, half-angle of entrance on the load waterline and the shape of the of the entrance area curve. When these features combine to give a negative pressure gradient just abaft the bow, with consequent increasing velocity, the flow is stable and laminar flow tends to persist over large areas, until the pressure gradient becomes constant or positive.

Without turbulence stimulation, therefore, even comparative model tests may be misleading. Two similar models with different sections forward could give results apparently showing one model to have less resistance, whereas some or all of this difference could be due to a greater area of laminar flow on the other model which could not occur at full scale. [2], [5].

The practical answer to the problem is to deliberately "trip" the laminar flow by some kind of roughness near the bow. The same principle is used for appendages, if necessary. The device used for this turbulence stimulation often consists of a number of cylindrical studs, fixed to the surface of the model.

In order to obtain the drag of the model, the stimulator drag is subtracted from the total measured drag. For this reason, a drag coefficient, C_{stud}, is given for each stud. However, the uncertainty of the stream turbulence level, the interaction between studs and between the hull and the studs, the speed dependence of the stud drag coefficient, the possibility of over-stimulation, all contribute to the given value of C_{stud} being very approximate.

Although similar boats with the same number of stimulators may still be accurately compared using an incorrect value of C_{stud}, this is a possible source of error, especially if the absolute performance of a vessel is of concern, or when comparing models with a different number of stimulators.

5.2 Stimulator Drag Calculation

It is difficult to accurately calculate the actual stimulator drag coefficient. The most straightforward method, which is presented below, consists of measuring the total model drag for two tests with a different number of studs, and then subtracting the

two values of total drag in order to find the drag of the extra stimulators.

This method has the disadvantage of estimating a small number by subtracting two large ones, and hence is very prone to experimental error. Nevertheless, a reasonable estimate of the stud drag can be found by averaging over the entire run matrix, and over several tests.

For a particular set of tests, the value of the drag coefficient of each cylindrical stud, non-dimensionalized by its frontal area (height $\times$ diameter $= 8.68 \times 10^{-5}\ ft^2$) was $C_{d_{stud}} = 1.0$. Hence, normalized by a 78.4 ft^2 model wetted surface, $C_{stud} = 1.11 \times 10^{-6}$. Thus, this value was multiplied by the total number of stimulators under water in order to obtain a drag coefficient due to the stimulators, C_{turb}, which was in turn subtracted from the total model resistance coefficient so that the drag exclusively due to the bare model could be found.

Two tests of the same model with a different number of stimulators were used to check the accuracy of the above value. The first test had a total number of 261 studs attached to the hull and appendages, while the second one had the "standard" for the particular testing program, of 134 studs.

Figure 5-1 shows the upright total model resistance coefficients as a function of speed-length ratio, for the two above tests. As it can be seen, the test with the extra stimulators has more resistance.

By subtracting the two curves and dividing by the number of extra stimulators (127), an estimate of C_{stud} as a function of speed-length ratio may be found. Here C_{stud} is, as mentioned above, the stimulator drag coefficient, made non-dimensional by dividing by the model wetted surface. This curve, along with the line of nominal C_{stud}, is shown in figure 5-2. Examining this result, it can be concluded that the actual stimulator drag is on average slightly less than the nominal value.

The large effect of experimental error on this method of C_{stim} calculation may be detected by the "wavy" nature of the curve of figure 5-2. In other words, the expected smooth behavior of the stimulator drag with speed is distorted by tank measurement errors. It is clear, however, especially after calculating C_{stim} from runs with heel and/or yaw (see appendix C), that the nominal value of the stud drag coefficient was

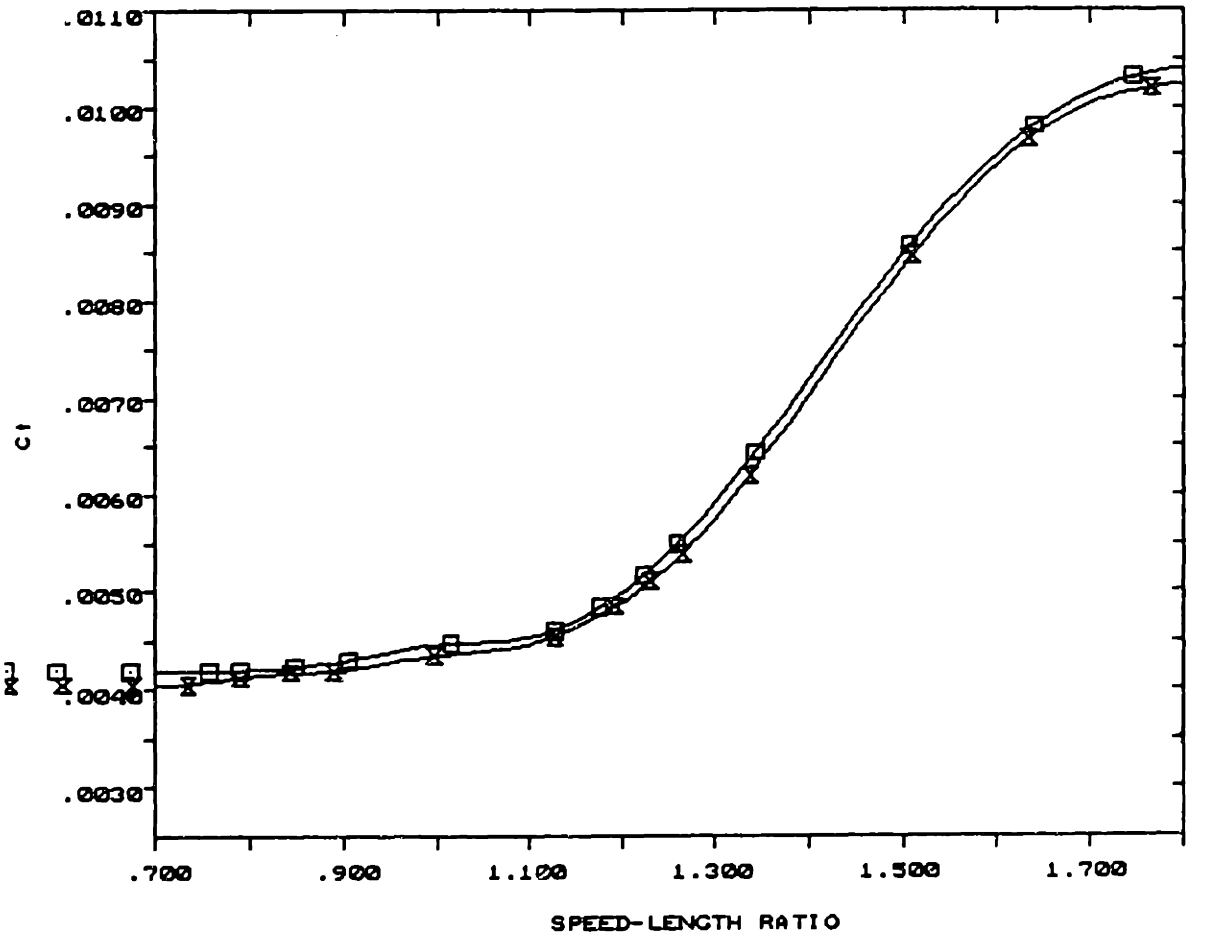

Figure 5-1: Total upright model resistance (including stimulator drag) for two tests of the same model with a different number of studs

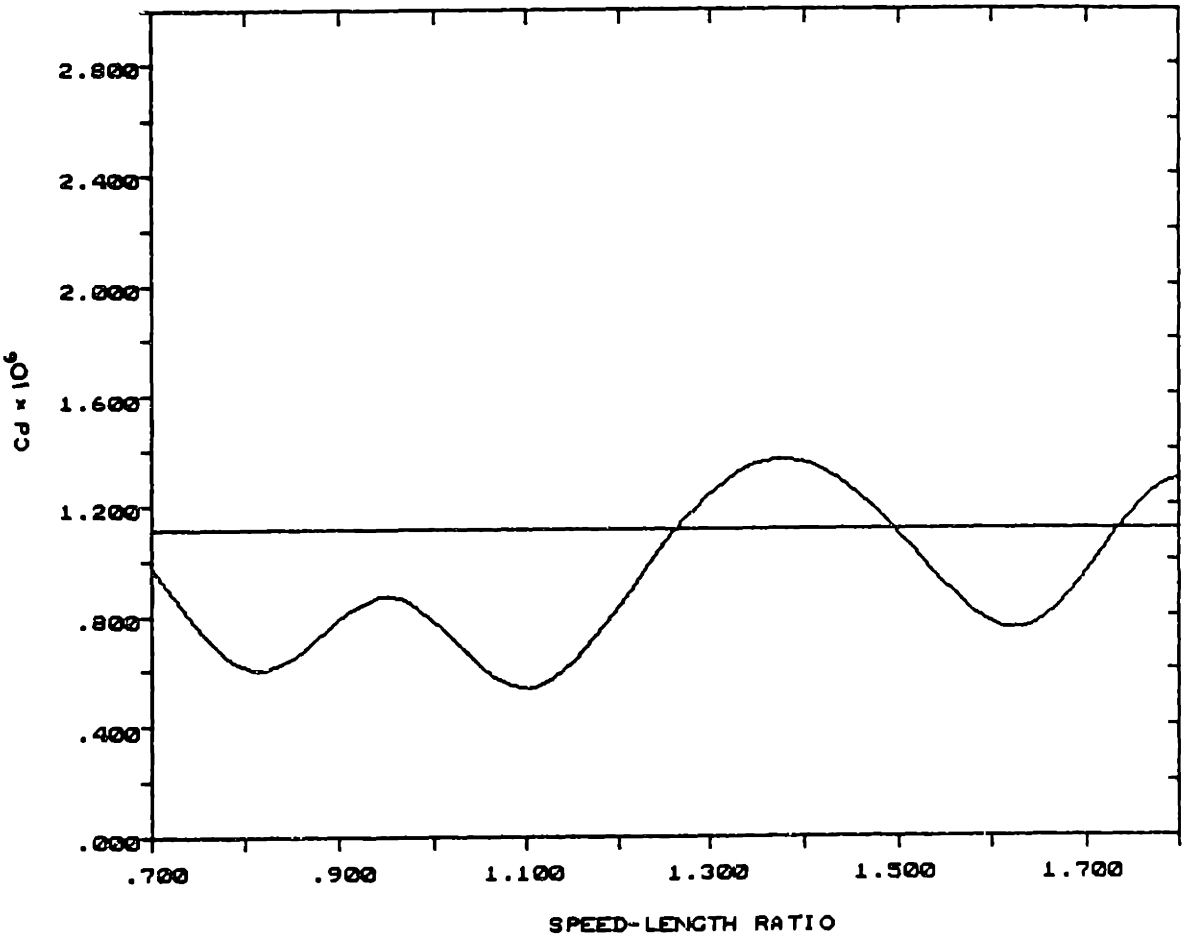

Figure 5-2: Stimulator drag coefficient (per stimulator) as estimated from the upright runs of two tests performed with a different number of studs. Shown also is the nominal value of 1.11×10^{-6}.

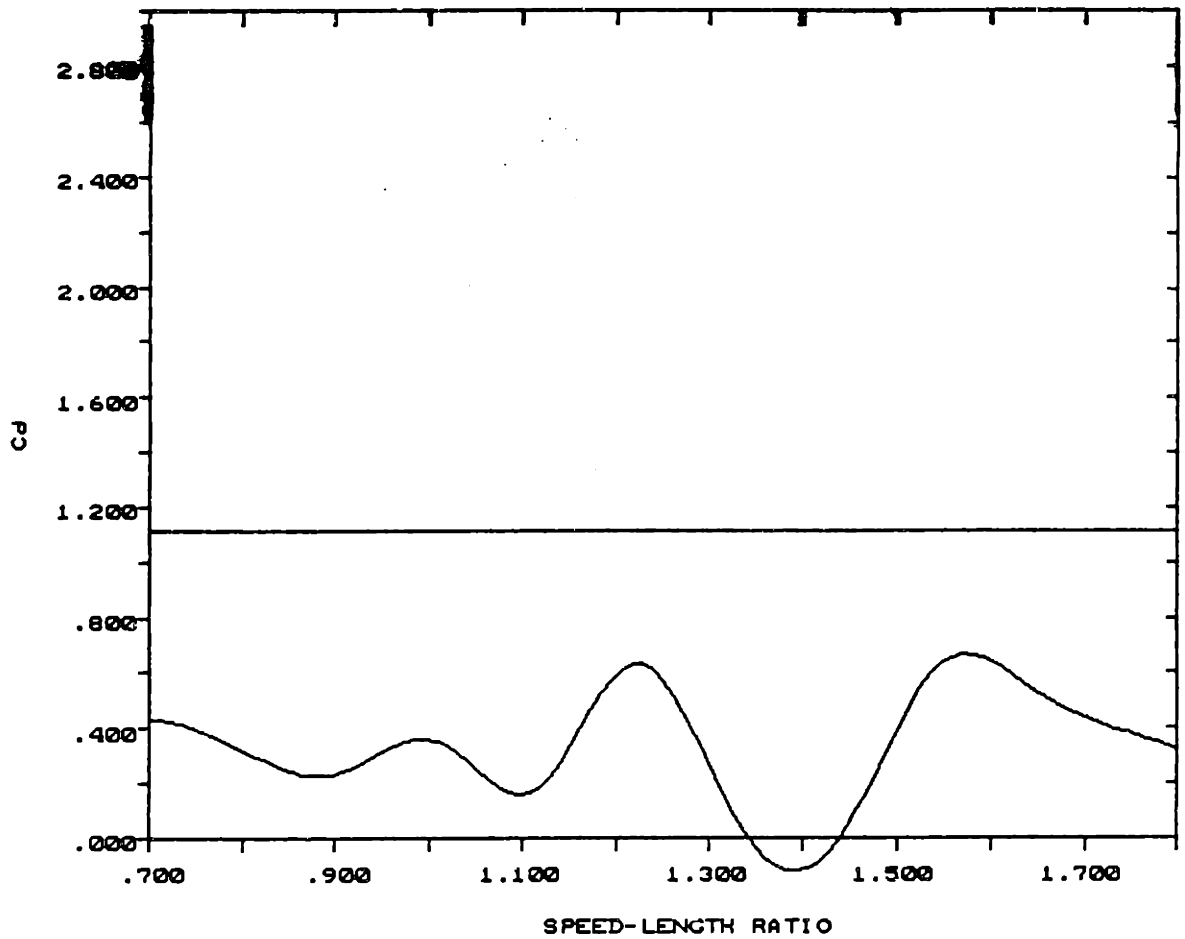

Figure 5-3: Stimulator drag coefficient (per stimulator) as estimated from the upright runs of another pair of tests performed with a different number of studs. Shown also is the nominal value of 1.11×10^{-6}.

too high for this test.

A pair of tests of another model also suggested that the nominal value of $C_{stud} = 1.11 \times 10^{-6}$ was too high. Figure 5-3 shows that the experimental value of the stimulator drag coefficient for this model is even lower than that of figure 5-2. It was suspected, however, that some sort of experimental error was associated with this pair of tests, because the value of the stimulator drag turned out too low to be credible (in some cases of runs with heel and yaw, it actually was negative over part of the speed range!).

Two conclusions may be drawn from the above analysis. First of all, it is difficult to accurately calculate stimulator drag. Secondly, it seems that the nominal value

for the stimulator drag for this particular testing program was higher than its actual value. A rough guess is that it could be wrong by as much as 50%. In order to examine the effect of errors in the nominal value of the stud drag, a sensitivity analysis was performed.

5.3 Sensitivity Analysis

In order to investigate the effect of errors in stimulator drag prediction on the performance evaluation of the full scale boat, a sensitivity analysis was performed.

Equation 1.8 gives the total model resistance coefficient as a function of the wavemaking and frictional resistance coefficients. Adding the drag effect of the turbulence stimulators, equation 5.1 is obtained.

$$C_{tm} = C_{wm} + (1+\kappa)C_{fm} + C_{turb} \tag{5.1}$$

Thus, by analogy to equation 1.9, the total full scale resistance coefficient, taking the stud drag into consideration, is given below.

$$C_{ts} = C_{tm} + (1+\kappa)(C_{fs} - C_{fm}) - C_{turb} \tag{5.2}$$

Defining the sensitivity of the total resistance prediction to stimulator drag to be the inverse of the total resistance multiplied by the partial derivative of total resistance w.r.t. stimulator drag, equation 5.3 is obtained for sensitivity.

$$\frac{1}{C_{ts}}\frac{\partial C_{ts}}{\partial C_{turb}} = \frac{-1}{C_{tm} - (1+\kappa)(C_{fm} - C_{fs}) + C_{turb}} \tag{5.3}$$

Some typical values were substituted into the above equation, in order to determine the effect of a typical stud drag error. For a 19.4 ft model made at a scale ratio of 0.31, towed at a speed-length ratio of 1.00, a typical value for the total upright resistance coefficient is $C_{tm} = 0.00423$. For 135 exposed studs, the nominal value of C_{turb} is 0.00015. Using the above values and a Reynolds factor (see section 4.1) of 0.8, the sensitivity obtained from equation 5.3 is -308.

As seen in the previous section, a stud drag uncertainty of up to 50% was observed. This means that C_{turb} was correct within ± 0.000075. By multiplying this value by the sensitivity, it was found that there was a 2.31% uncertainty of the drag prediction due to stimulator drag errors.

As previously mentioned, this error is not important when comparing the performance of similar models with the same number of stimulators. For comparison of designs, it is important to use the same number of stimulators in similar arrangements.

Given that C_{fm} is greater[1] than C_{fs}, it can be concluded that the sensitivity of the results to stimulator drag decreases as the size of the model increases.

The sensitivity also decreases when the difference between C_{tm} and C_{fm} increases. This happens at high speed-length ratios, where most of the resistance of the model is due to wave-making.

Finally, as C_{turb} increases, the sensitivity decreases but the difference between actual and nominal stud drag, ΔC_{turb}, also increases. Hence, the percentage error in velocity prediction increases if it is assumed that the error associated with the stimulator drag is a constant percentage of the actual stimulator drag.[2] It is therefore important not to use more stimulators than necessary (over-stimulation), so that the error associated with them is minimized.

[1] For a model and ship operating in water at the same Froude number ($Fn = U/\sqrt{g\,L}$), the Reynolds number ($Rn = U\,L/\nu$) of the model is lower than that of the ship. Since the ITTC friction line monotonically decreases with Reynolds number, the model always has a higher coefficient of frictional resistance than the ship.

[2] For the case investigated, where the error was assumed to be 50% of C_{turb}, the percentage error of the resistance prediction is given by the function:

$$error(\%) = \frac{50\,C_{turb}}{C_{tm} - (1+\kappa)(C_{fm} - C_{fs}) + C_{turb}}$$

which monotonically increases with positive C_{turb}.

Chapter 6

DATA REPEATABILITY

One of the most serious problems of tank testing is the difficulty in achieving data repeatability. This is especially true for the evaluation of the performance of ocean racing yachts, where the difference between a "good" and a "bad" boat may be of the order of a tenth of a knot.

It is not uncommon, however, to have retests of the same boat give speed predictions as far apart as a few hundredths of a knot. Obviously this is a problem and some reasons for this data inconsistency were searched.

6.1 Errors in Sideforce Measurement

Errors in model resistance measurement are universally recognized to be of great importance and hence care is taken to minimize them. On the other hand, one would not think that errors in sideforce measurement affect performance evaluation as much.

It was observed, however, that it was quite common to have sideforce variations between retests of the same model. This may be a clue about the origin of bad data repeatability, hence a study on sideforce sensitivity was performed.

For example, figure 6-1 shows the sideforce coefficients for two tests of the same model, at 15 degrees heel. As it can be seen, these two tests have different sideforces by 3–9%. In order to make sure that this sideforce change is not due to a different rudder or tab setting on the model for each test, the drag must also be examined.

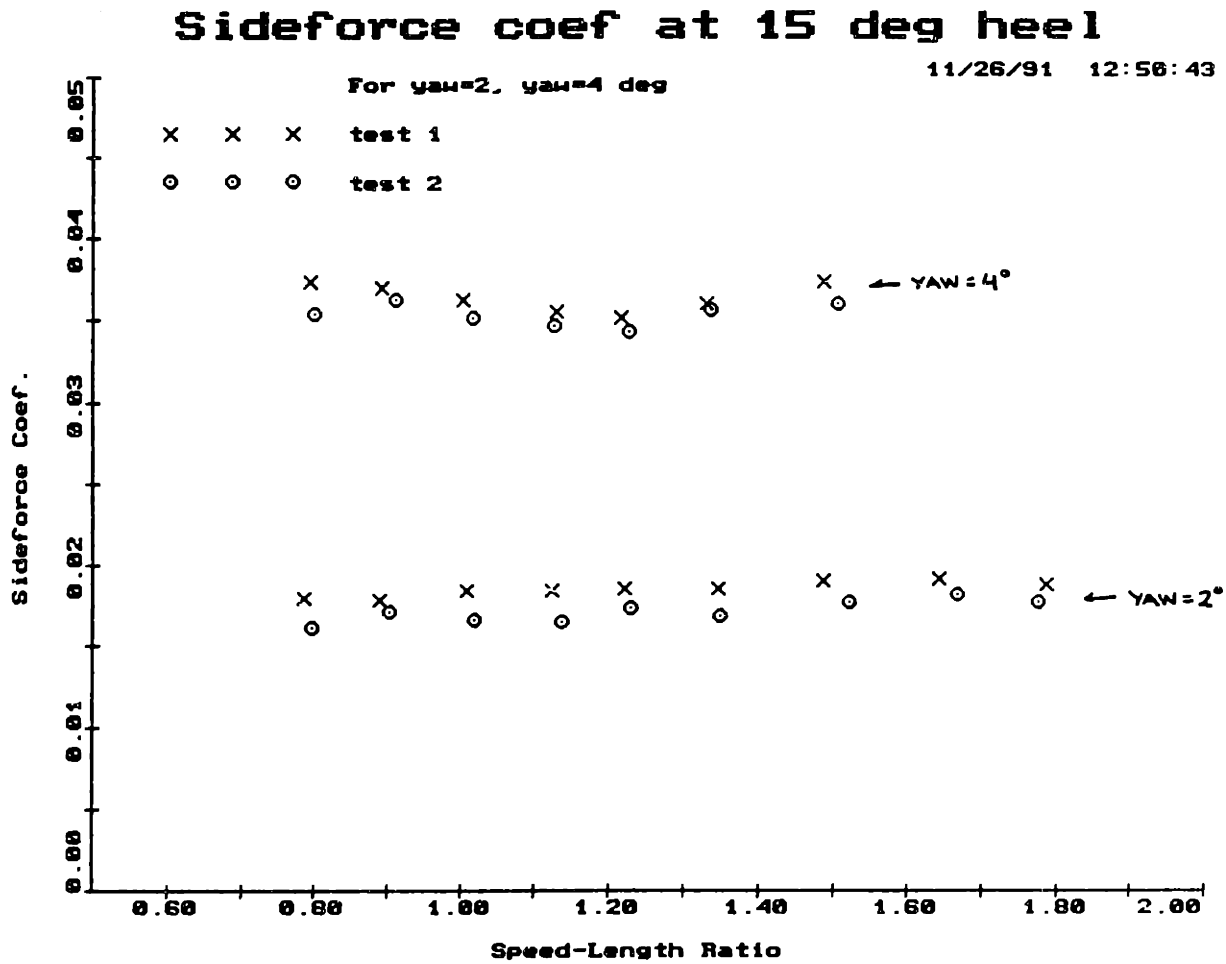

Figure 6-1: Sideforce Coefficients at 15 degrees heel, for two tests of the same model

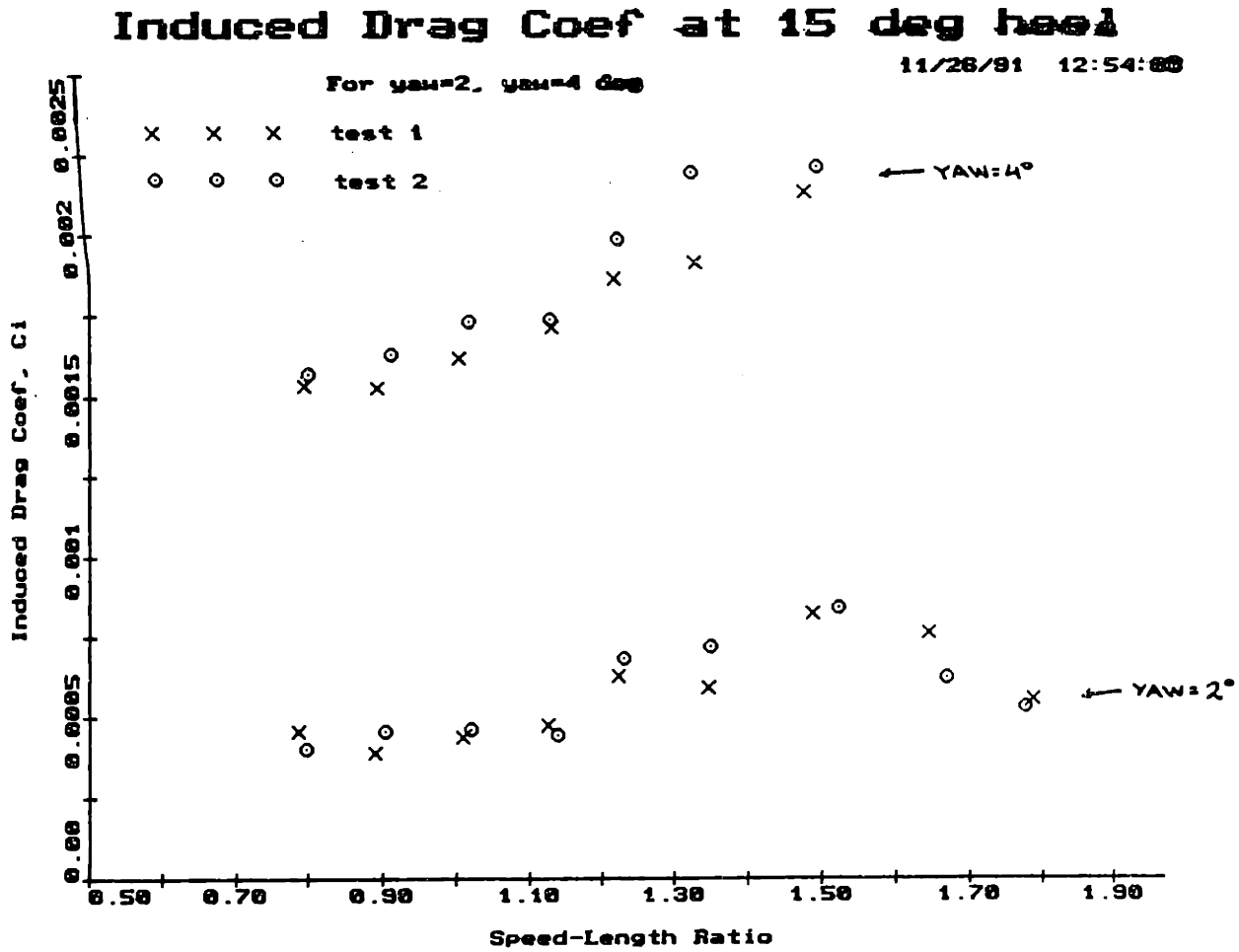

Figure 6-2: Induced Drag Coefficients at 15 degrees heel, for two tests of the same model

Theoretically, the induced drag at a given speed is proportional to the square of the sideforce. Hence, for the above example, if the induced drag of the test with the high sideforce were greater by 6–19%, then a rudder or tab offset would be probable, and the performance prediction for the two tests would be very close.

Figure 6-2 shows the induced drag coefficients for the two tests. Induced drag was calculated by fitting a cubic spline through the model resistance at the nominal heel angle (15 degrees in this example), then correcting it to account for measurement at the actual heel angle, and finally subtracting it from the model resistance at heel and yaw. Correction is done by means of the C_2 coefficient according to equation 3.1.

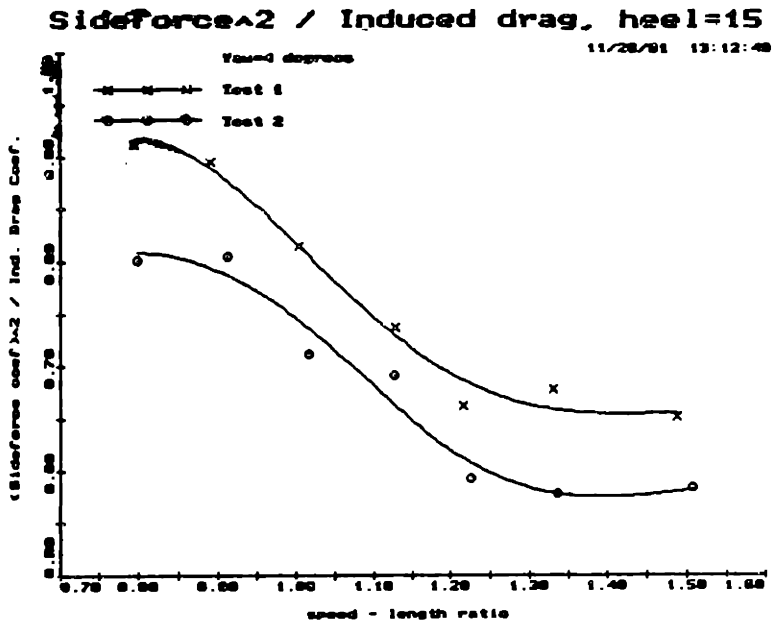

Figure 6-3: Sideforce squared over Induced Drag at 15 degrees heel, 2 degrees yaw, for two tests of the same model

Thus, the induced drag coefficient is given below.

$$C_{ind}(\phi, C_h) = C_t(\phi, C_h) - C_t(\phi_{nominal}, 0) - C_2 \frac{\phi^2 - \phi^2_{nominal}}{30^2} \tag{6.1}$$

where $C_{ind}(\phi, C_h)$ is the induced drag at a certain speed, heel angle ϕ and sideforce coefficient C_h, $C_t(\phi, C_h)$ is the total model resistance as measured at the above conditions, and $\phi_{nominal}$ is the nominal heel angle at which the no-yaw runs were taken.

As it can be seen from figure 6-2, the induced drag coefficients of the two tests are not sufficiently different to justify the sideforce difference. This may be confirmed by looking at the ratio of sideforce squared to induced drag for the two tests (see figures 6-3 and 6-4). For the 15 degree heel runs, the one test seems to have a consistently higher ratio, thus improving its performance prediction over the other test and hence implying tank measurement errors. Note that the drag differences between these two tests, over all the data taken, were negligible. However, VPP analysis predicted the boat performance to be considerably higher for one test than the other.

In order to further investigate this effect of sideforce measurement errors, a complete set of tank data points was taken and the sideforce on all of them was multiplied by a specified factor. Then the whole data analysis was carried out with the modified

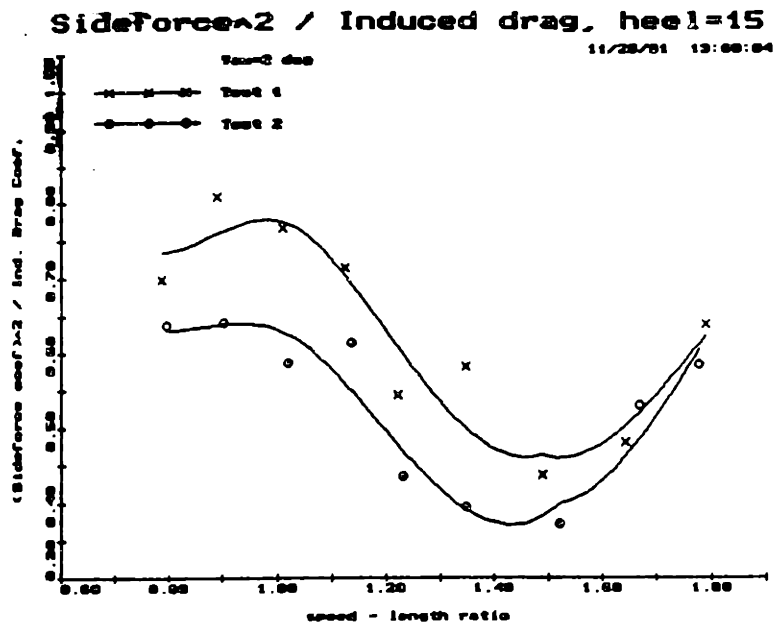

Figure 6-4: Sideforce squared over Induced Drag at 15 degrees heel, 4 degrees yaw, for two tests of the same model

data, and the velocity prediction was compared to the original case.

Figure 6-5 shows the change in performance prediction versus wind-speed, for various amounts of sideforce increase. The performance is measured by minutes around an America's Cup course. A typical performance prediction of the VPP for America's Cup yachts is roughly 210 minutes at a 7 knot wind speed and 135 minutes at an 18 knot breeze. As it can be seen, sideforce errors affect performance considerably. A 1% increase in sideforce improved the overall performance of the boat by almost 10 seconds, a 2.5% sideforce increase made the boat approximately 20 seconds faster, a 5% increase made it 40 seconds faster and a 10% sideforce increase resulted in an 80 second performance increase. From the above, it can be concluded that the effect of a fixed percentage error in sideforce measurement, produces a roughly constant velocity prediction error with wind speed. Furthermore, this velocity error is proportional to the percentage error of sideforce measurement. Therefore, on a percentage basis, the performance prediction at high wind speeds is more strongly affected by sideforce measurement accuracy than that at low wind speeds.

In towing tank tests, it is quite common to have 2–5% difference in sideforce measurement between retests of the same model, while differences of the order of

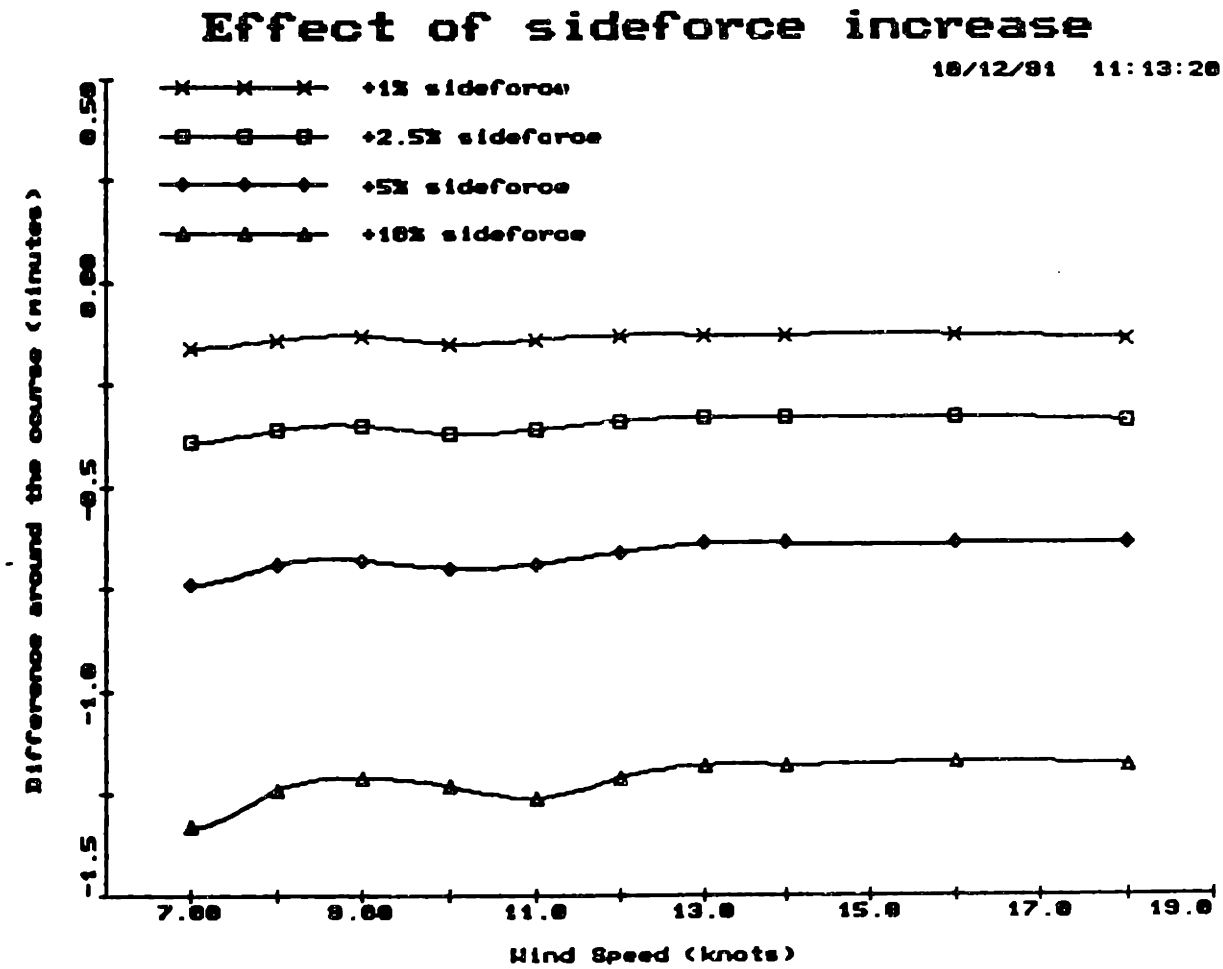

Figure 6-5: Change in Velocity Prediction versus Wind Speed, for constant Sideforce Measurement Errors.

10% have been known to occur (Figure 6-1, for example). This means that sideforce measurement errors are a potential problem, and care must be taken to minimize them.

In the particular tank used, the model was supported in the water by means of its own buoyancy and hence was free to perform heaving motions. This was accomplished using two vertical heave posts, on which the model frame slid in order to allow vertical motion of the model. It was thought possible that the sideforce inconsistency from test to retest was due to some amount of friction in the heave posts. An attempt was made to investigate this further by means of an experiment, as described in section 6.2.1.

6.2 Errors due to Carriage Vibrations

Another source of error which may contribute to bad data repeatability is the fact the towing tank carriage motions may distort the measurements.

6.2.1 The "shaker" experiment

For the towing tank used, some "flat spots" in the carriage tires caused vibrations as the model was towed down the tank. It was therefore desired to determine the extent of the added resistance and/or the error due to non-linearity of the sensors caused by such vibrations.

An experiment was therefore designed, the basis of which was to subject a model to additional vibrations, of the order of magnitude of those imposed by the carriage, and then to compare the results with and without the extra vibrations. In this manner, it was hoped to determine the effect of carriage motions on the force measurements.

A possible additional effect of this experiment was thought to be the elimination of some or all of the "go-no go" motion in the vertical heave posts. This was hoped to be observed from the sideforce measurements.

A means of producing vibrations of the order of magnitude of those due to the carriage, was to install a "shaker" in the model. This shaker consisted of an electric

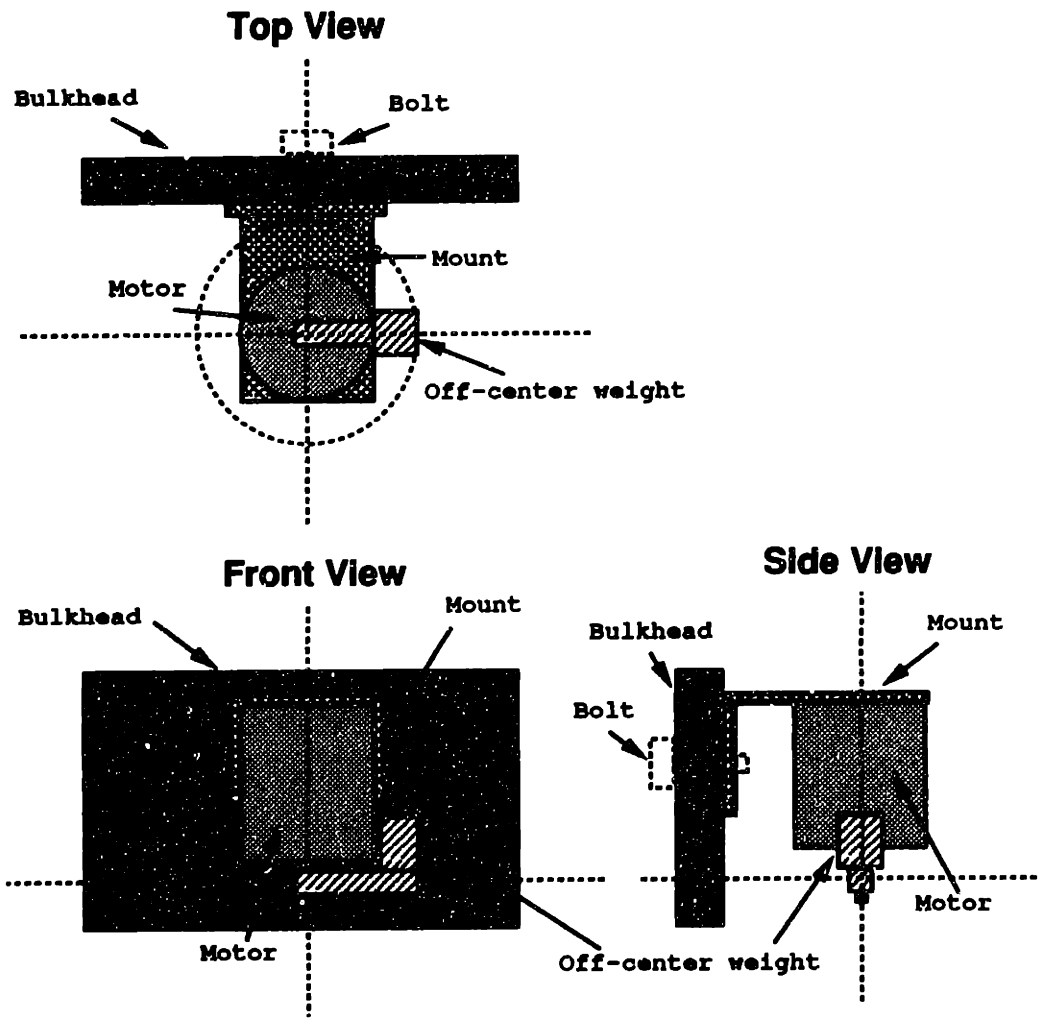

Figure 6-6: "Thor", the Shaker

motor with an off-center weight mounted on its shaft, and was mounted on the bulkhead behind the keel trunk, with its shaft vertical. The device as mounted on the model, is shown in figure 6-6. A single bolt was used to mount the device in place, so that it could easily be rotated when the model was heeled, in order to maintain the vertical position of the shaft.

The motor's shaft was designed to be vertical because if the off-center weight did not rotate in the horizontal plane, an oscillatory force component would be produced in the vertical direction, causing the model to heave. This was undesirable because such heaving motions were not significantly present in the normal runs without the shaker installed. Since the objective of this experiment was to examine the effect of the *carriage* vibrations, it was desired to simulate them as closely as possible.

In order to produce noise which resembles that of the carriage vibrations, several data were examined over the whole range of the tank run sequence. Appendix A shows strip charts (the signals at the force sensors in the time and frequency domains), of several runs at various speeds, heel angles and yaw angles.It was thus observed that the dominant frequency of the carriage vibrations was approximately 4 Hz and the noise amplitude as recorded on the force sensors, was roughly 40 lbs.

It was therefore decided that a sinusoidal disturbance of 40 lbs amplitude and 4 Hz frequency was to be produced by the shaker. The product of the mass and its off-center distance may be easily calculated in order to produce such a disturbance.

In one direction (forward, for example), the motion of the off-center weight may be written as :

$$x(t) = d\ sin(2\pi ft) \tag{6.2}$$

where d is the off-center distance of the mass, f is the frequency of rotation (4 Hz, as determined above), and t is time.

Differentiating twice, the acceleration of the mass in the forward direction is found.

$$\frac{d^2x(t)}{dt^2} = -4\pi^2 f^2 d\ sin(2\pi ft) \tag{6.3}$$

Having obtained the acceleration, it is a matter of multiplying it by the off-center

mass, m, in order to obtain the disturbance force. Knowing that the amplitude of this force should be 40 lbs, a required value for the product md may be found.

$$|F| = 4\pi^2 f^2 m\ d \Longrightarrow md = \frac{40\ lb_f\ 32.19 \frac{ft\ lb_m}{s^2 lb_f}}{4\ 3.1416^2\ 4^2\ Hz^2} \approx 2\ lb_m\ ft \tag{6.4}$$

In order to obtain a compact device so that it may be easily installed in the model, the distance, d, was made just large enough for the mass to clear the motor itself (see figure 6-6). A mass of 4 lbs at a distance of 6 inches from the shaft was therefore chosen to produce the required force at the required frequency.

6.2.2 Experimental results

After installing the device on one of the models as indicated above, a full test was performed with the shaker in operation. A few strip charts are provided in appendix B for comparison with the ones obtained without the shaker in use. As it can be seen, the amplitude of the noise has been approximately doubled with the shaker in use.

Figure 6-7 shows the upright resistance coefficients for the model with and without the shaker in operation. As it can be observed, the only real differences between the two cases occur at very low speeds and, to a lesser extent, at speed-length ratios close to 1.1.

The runs with the shaker operating had less resistance at the low speed end, but the measurements are not very reliable at such low speeds anyway. Apart from leading to a different form factor estimation, this should not affect the performance prediction, as those speeds are well under the expected sailing range. Considering the fact that in the past, some serious towing tank data analysis was done without even considering the form factor, it can be assumed that the error in its estimation due to the low speed differences in resistance should not seriously affect the velocity prediction.

Any difference around speed-length ratio of 1.1, however, may considerably affect the performance prediction, as this is precisely the speed at which the vessels are expected to sail. In this case, the whole difference in that region is caused by a single

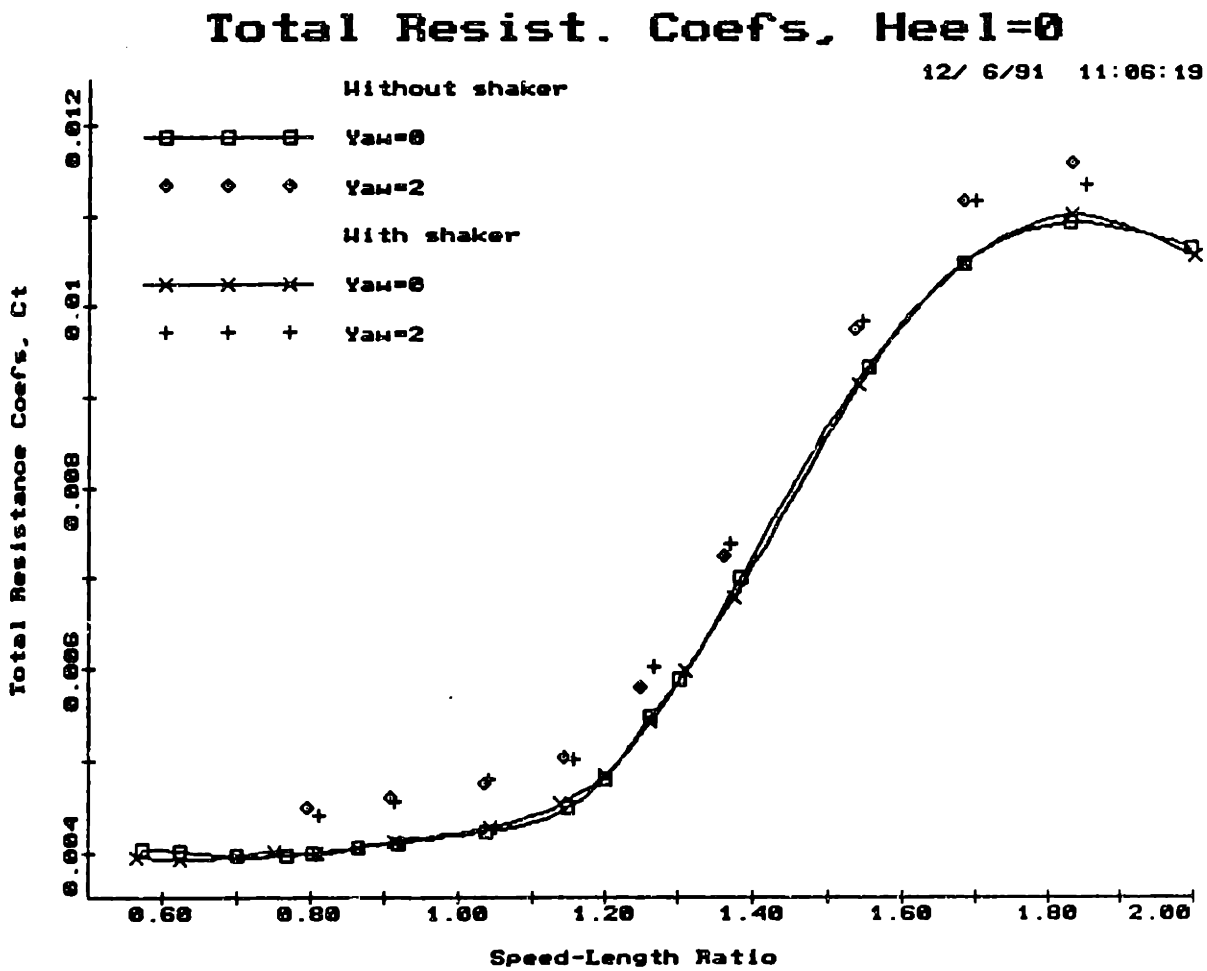

Figure 6-7: Comparison of total model upright resistances with and without the shaker in operation

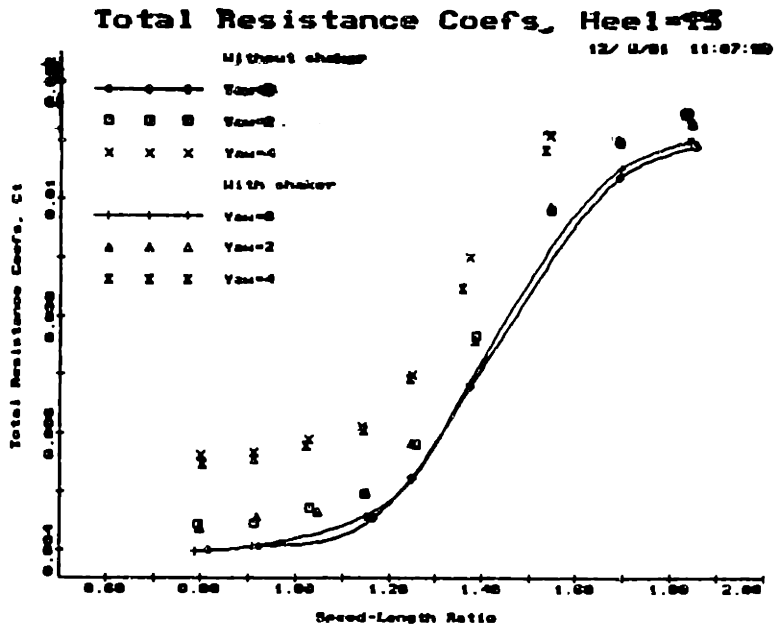

Figure 6-8: Comparison of resistances at 15 degrees heel with and without the shaker in operation

data point at speed-length ratio of 1.15. This may be due to tank measurement errors, but even if it is not, the resistance difference is only of the order of 2.5%. Although this is not good accuracy for data repeatability, it must be remembered that in this experiment, the "shaking" added is much more than the difference in "shaking" between normal retests of the model. Hence it is concluded that the effect of carriage vibrations on the measured *upright* resistance repeatability is negligible.

Figures 6-8, 6-9 and 6-10, show the total resistance coefficients for nominal heel angles of 15, 22 and 28 degrees respectively. In order to easily determine the difference between resistance due to heel for the two cases, a cubic spline was fitted through the data points with no yaw.

As it can be seen, with the shaker in operation the model has more resistance at heel with no yaw. When, however, the model is yawed (especially at 4 degrees yaw), it presents less resistance with the shaker working. The fact that the upright resistance was virtually identical for the two cases implies that the shaker caused the model to have more resistance due to heel but less resistance due to yaw.

Figures 6-11, 6-12 and 6-13 show the sideforce coefficients for nominal heel angles of 15, 22 and 28 degrees respectively. From these plots it may be observed that the

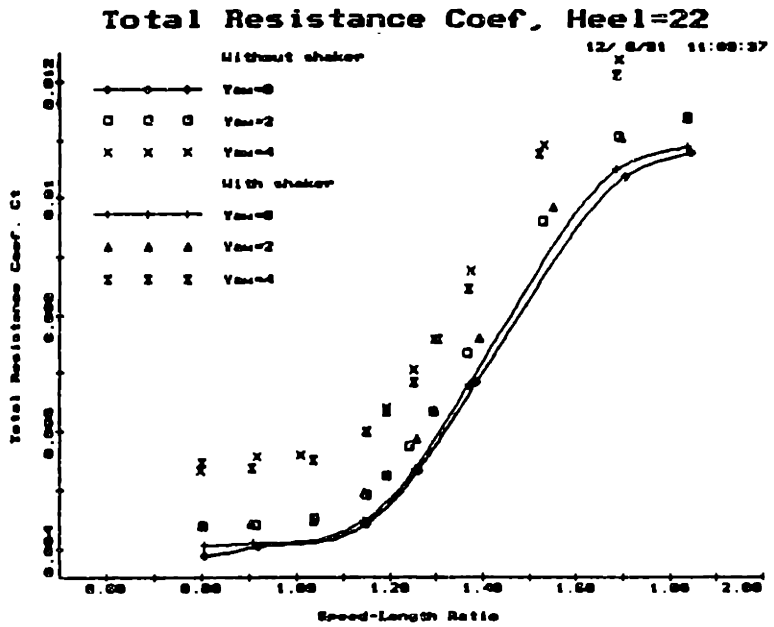

Figure 6-9: Comparison of resistances at 22 degrees heel with and without the shaker in operation

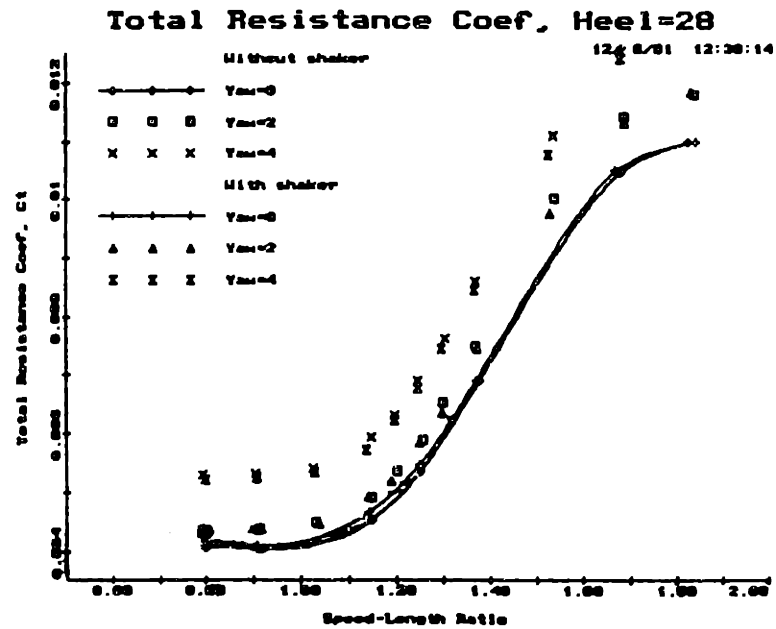

Figure 6-10: Comparison of resistances at 28 degrees heel with and without the shaker in operation

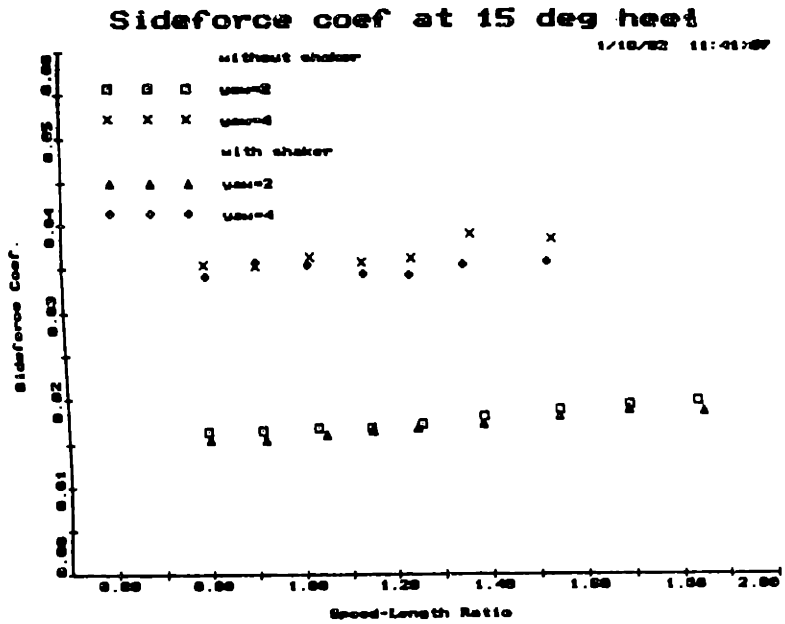

Figure 6-11: Comparison of sideforce coefs at 15 degrees heel with and without the shaker in operation

sideforce was consistently lower for the test with the shaker.

One possible explanation of the above results, may be that the shaker was not accurately set for the no-yaw cases, but when the model was yawed the slight increase in heel made the plane of motion more nearly horizontal. Vertical motion was thus produced only in the heel/no yaw runs, hence increasing the resistance mainly in those runs. Note that the effect of vertical vibrations is not known, but this theory assumes that they somehow increase the model resistance, in order to agree with the observed facts.

The decrease in sideforce may be partially explained by the reduced drag due to yaw. Even if the rudder or tab angles were not identical for the two tests, the drag due to yaw should be roughly proportional to the sideforce squared. For the shaker test, however, the decrease in sideforce is considerably more than the above estimate based on the induced drag reduction. So the reason for this extra sideforce decrease remains unknown.

Hence, this theory concludes that the shaking in a horizontal plane has virtually no effect on resistance, and that the "go-no go" effect is either not eliminated by shaking, or has no significant effect on drag measurement. The resistance data agrees

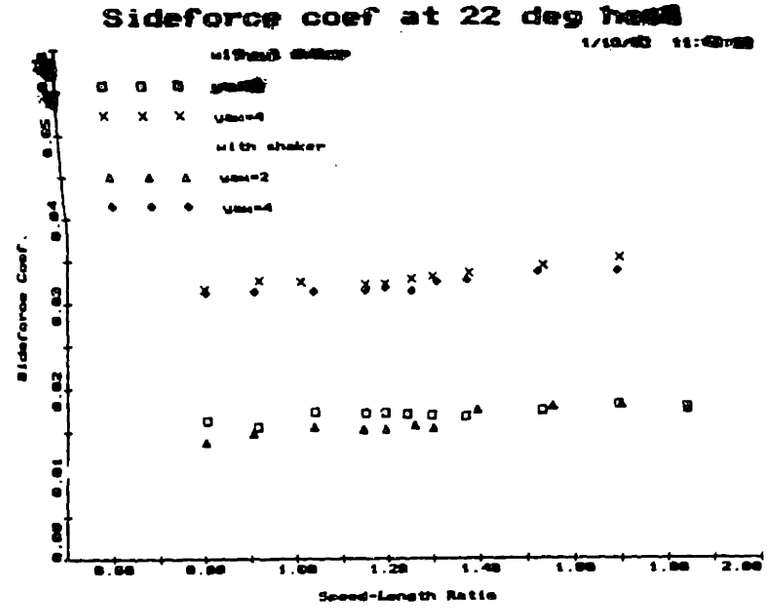

Figure 6-12: Comparison of sideforce coefs at 22 degrees heel with and without the shaker in operation

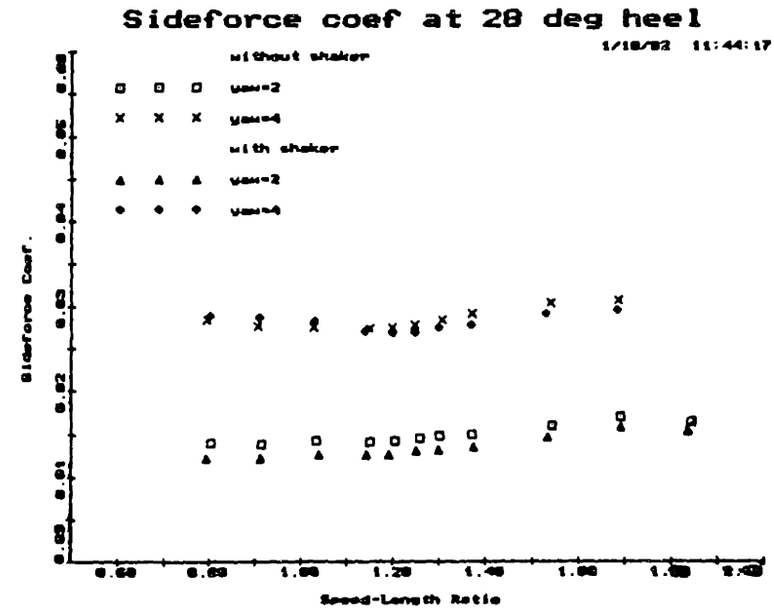

Figure 6-13: Comparison of sideforce coefs at 28 degrees heel with and without the shaker in operation

quite well with this theory, but does not fully explain the sideforce decrease. Since in many retests of the same model the drags agreed but there were serious sideforce differences, this theory may provide a clue to the solution.

One possibility is that the extra noise produced errors associated with non-linear behavior in the sideforce measurement sensors. Hence, for retests with carriage vibrations greater than normal, the sideforce measurements would change. Since the amount of carriage vibrations varies according to the state of the tires, for example, the inconsistencies between retests may be partly due to vibrations.

The next step was to run the VPP and find the velocity prediction for the test with the shaker. Table 6.1 shows a comparison between the performance prediction with and without the shaker. As it can be seen, the results are extremely close for reaches and when sailing to leeward. All the differences are when beating to windward, but even then the results are within one minute around the course at the low wind speeds and within 10 seconds at the high wind speeds. Hence, the difference in performance is almost entirely due to the extra sideforce decrease and drag due to heel increase of the test with the shaker.

6.2.3 Conclusions

As seen in the previous section, although the amplitude of the model vibrations were doubled, the difference in performance prediction only changed by 0.1 – 0.5%. Since normally the difference in carriage motions between retests are expected to be of a much smaller order, it is concluded that the vibrations do not have a detrimental effect on the tank testing repeatability.

A side effect of the shaking action was observed to be a decrease in the sideforce measurements. The exact source of this effect was not known, but is was suspected to be due to stiction elimination, or sensor non-linearities. Further investigation is necessary to examine the exact source of this sideforce decrease with shaking.

In any case, this sideforce decrease was the major contributor to the difference in performance prediction between the two tests. Given that inconsistencies between sideforce measurements had been the source of difference between many other retests,

Test	Wind Speed (knots)	Race Times (minutes)				
		Windward	Leeward	135 Reach	100 Reach	Total
Normal	7.00	92.65	70.21	29.97	15.54	208.38
Shaker		93.46	70.16	29.99	15.55	209.16
Normal	8.00	85.61	62.12	26.46	14.88	189.07
Shaker		86.44	62.20	26.52	14.91	190.07
Normal	9.00	81.10	55.89	23.93	14.35	175.27
Shaker		81.66	56.13	24.02	14.36	176.18
Normal	10.00	78.07	51.56	22.36	13.91	165.90
Shaker		78.41	51.79	22.35	13.89	166.43
Normal	11.00	76.03	47.81	21.11	13.51	158.46
Shaker		76.17	47.96	21.13	13.49	158.74
Normal	12.00	74.64	45.12	20.16	13.13	153.05
Shaker		74.66	45.09	20.13	13.12	152.99
Normal	13.00	73.59	42.98	19.34	12.78	148.68
Shaker		73.51	42.96	19.30	12.77	148.55
Normal	14.00	72.74	41.24	18.59	12.44	145.02
Shaker		72.60	41.18	18.57	12.44	144.80
Normal	16.00	71.37	38.39	17.21	11.83	138.80
Shaker		71.15	38.32	17.21	11.84	138.51
Normal	18.00	70.19	35.72	15.85	11.28	133.04
Shaker		70.01	35.70	15.87	11.30	132.88

Table 6.1: Comparison of Performance Prediction with and without the shaker

it is believed that this experiment has helped locate the problem.

6.3 Other Possible Errors

It was initially thought that much of the inconsistency of the results of various retests of the same model was due to water temperature differences. Thus, a water temperature sensitivity analysis was performed, by examining the performance prediction of several models tested at various temperatures. Then, the velocity prediction for each model was plotted against tank water temperature, in an attempt to determine a trend.

This analysis showed that there was no obvious effect of temperature on the results. There was, however, a definite decline in performance prediction with the number of retests performed on any particular model. In other words, for some reason, the more a model was retested, the slower it was predicted to be.

This effect could be due to some loss of "stiffness" of the model after being in the water for several tests, and subjected to the stresses associated with towing it down the tank.

Actually, on average, there was a slight decrease of performance with rising temperature, but it was thought that this was also associated with "model aging" explained above. The fact that the water temperature rose as testing progressed (due to the season of the year) made it *seem* like there was some sort of temperature dependence, while in reality the major differences occurred due to the deterioration of the models with testing.

All the possible sources of bad data repeatability make it evident that in order to compare the performance of a number of vessels, it is advisable that tank testing is done under identical conditions and within a short time span.

Chapter 7

CONCLUDING COMMENTS AND RECOMMENDATIONS

This chapter summarizes the conclusions that have been drawn from within this thesis.

First of all, it is evident that in order to compare the performance of two vessels, it is not enough to simply compare the resistances of their models. The different scale-up of frictional and residuary resistances, the significant effect of sideforce on windward performance, the importance of data points within the expected sailing conditions, all contribute to the significance of using a Velocity Prediction Program to evaluate the performance of sailing vessels.

In order have good data repeatability, it is best to perform tests under as similar conditions as possible, and within a short time span. This implies that it is bad practice to mix data points from different retests of the same model.

Water temperature differences, model deterioration, carriage vibrations, affect the results to some degree, although the temperature was found to have a negligible effect. Carriage vibrations did not directly affect the results, but somehow induced sideforce measurement errors, thus providing a clue to one source of bad data repeatability. Stimulator drag errors also have a relatively small effect.

It was found that towing tank tests of models with different appendages could give misleading results. It is therefore preferable to confirm the performance of such

appendages by means of wind tunnel tests.

Some recommended approaches for the data analysis include the consideration of the bare hull (without appendages) for form factor and frictional resistance purposes, and the modeling of the resistance due to heel and yaw as a parametric function of speed-length ratio, sideforce coefficient and heel angle.

Appendix A

STRIP CHARTS OF RUNS WITHOUT SHAKER

This appendix contains a series of typical "strip charts" taken at the following nominal conditions:

Model Scale Speed (feet/sec)	Heel Angle (degrees)	Yaw Angle (degrees)
6.25	0.0	0.0
13.00	0.0	0.0
9.00	22.0	0.0
8.25	0.0	2.0
11.00	22.0	4.0

Each set (page) of strip charts consists of six signal records. From top to bottom, these correspond to the readings of the two roll gauges, the aft and fore drag gauges, and the aft and fore lift gauges.

The time histories of the above signals are shown on the left-hand part of the charts. The values displayed on the left of these are the mean value and the root-mean-square of the voltage signal, the signal-to-noise-ratio (where the signal in this case is the difference between average voltage levels of the run and the zero recording), and the average force in pounds.

The scale of the above charts is shown in the bottom left-hand corner of each page, and should be interpreted as the distance between two *major* "tics" on the vertical axis.

On the right-hand side of the strip charts are the Fourier transforms of the signals. The scale is shown in the bottom right-hand corner of the page. The two numbers in that location are the height and width of the "boxes" allocated to each signal, in Volts and Hz respectively.

The numbers at the bottom of each page, between the two scale values, are (from right to left and top to bottom) :

Initial (stationary) heel angle, Heel angle for the duration of the run, Yaw angle, Rudder angle, Tab angle, Model speed in feet/sec, Total drag in pounds, Total lift in pounds, Roll, Yaw moment, Duration of run, Drag coefficient, lift coefficient, Coefficient of Heel moment and coefficient of Yaw moment.

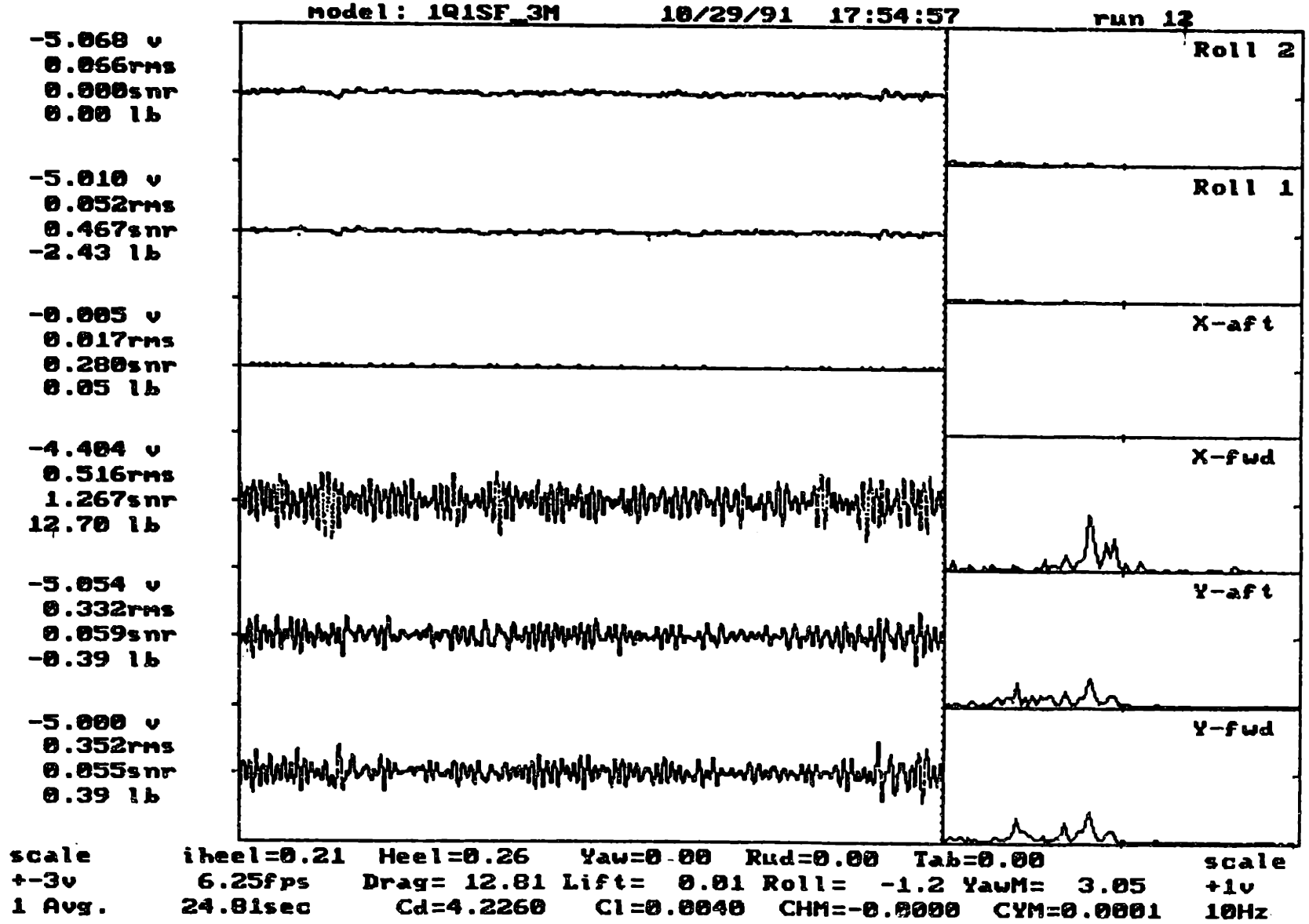
model: 191SF_3M 10/29/91 17:54:57 run 12
-5.068 v
0.066rms
0.000snr
0.00 lb
Roll 2
-5.010 v
0.052rms
0.467snr
-2.43 lb
Roll 1
-0.005 v
0.017rms
0.280snr
0.05 lb
X-aft
-4.404 v
0.516rms
1.267snr
12.70 lb
X-fwd
-5.054 v
0.332rms
0.059snr
-0.39 lb
Y-aft
-5.000 v
0.352rms
0.055snr
0.39 lb
Y-fwd
scale
+-3v
1 Avg.
iheel=0.21 Heel=0.26 Yaw=0.00 Rud=0.00 Tab=0.00
6.25fps Drag= 12.81 Lift= 0.01 Roll= -1.2 YawM= 3.05
24.81sec Cd=4.2260 Cl=0.0040 CHM=-0.0000 CYM=0.0001
scale
+1v
10Hz

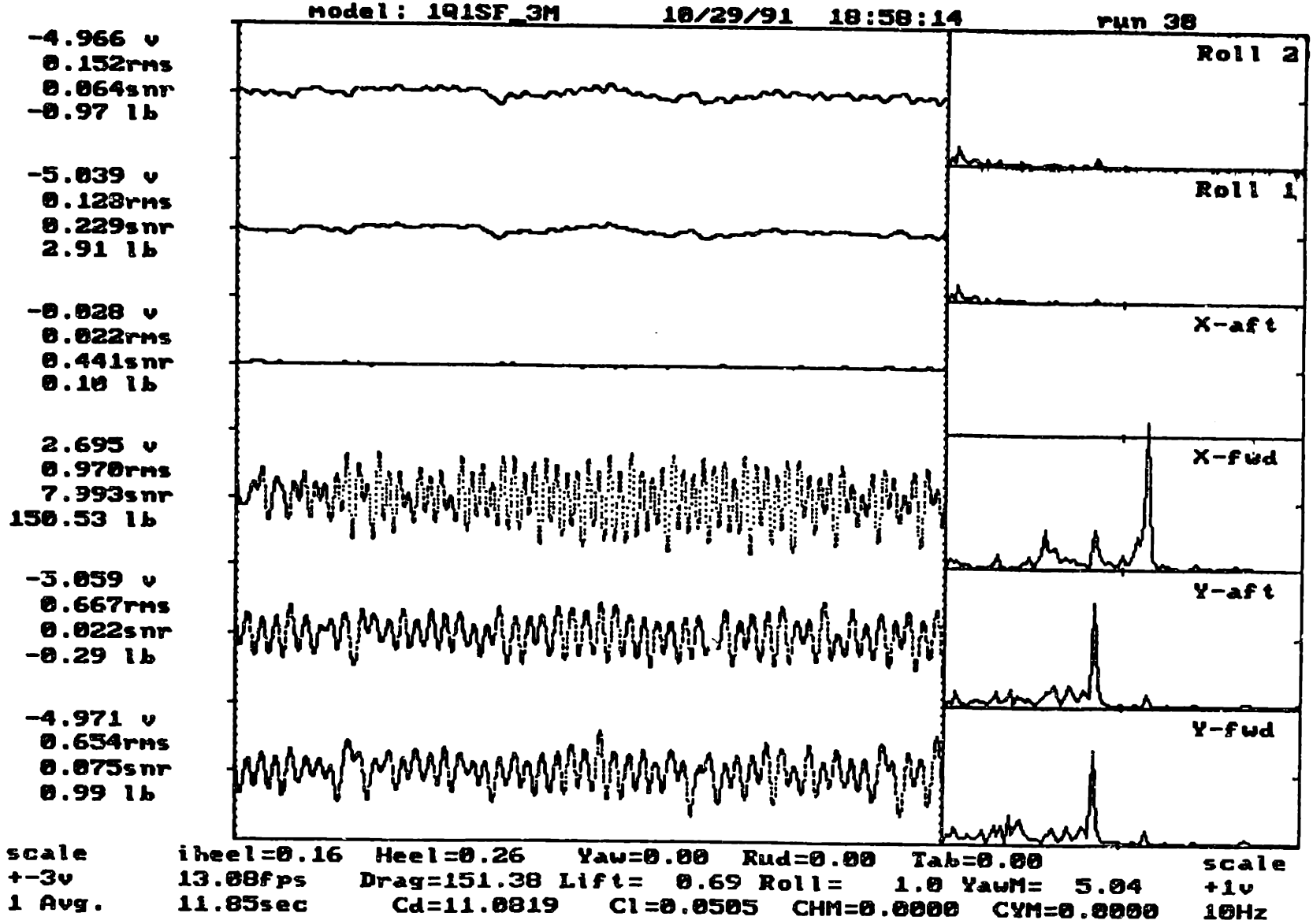
model: 191SF_3M 10/29/91 18:58:14 run 38
-4.966 v
0.152rms
0.064snr
-0.97 lb
Roll 2
-5.039 v
0.128rms
0.229snr
2.91 lb
Roll 1
-0.028 v
0.022rms
0.441snr
0.10 lb
X-aft
2.695 v
0.970rms
7.993snr
150.53 lb
X-fwd
-3.059 v
0.667rms
0.022snr
-0.29 lb
Y-aft
-4.971 v
0.654rms
0.075snr
0.99 lb
Y-fwd
scale
+-3v
1 Avg.
iheel=0.16 Heel=0.26 Yaw=0.00 Rud=0.00 Tab=0.00
13.08fps Drag=151.38 Lift= 0.69 Roll= 1.0 YawM= 5.04
11.85sec Cd=11.0819 Cl=0.0505 CHM=0.0000 CYM=0.0000
scale
+1v
10Hz

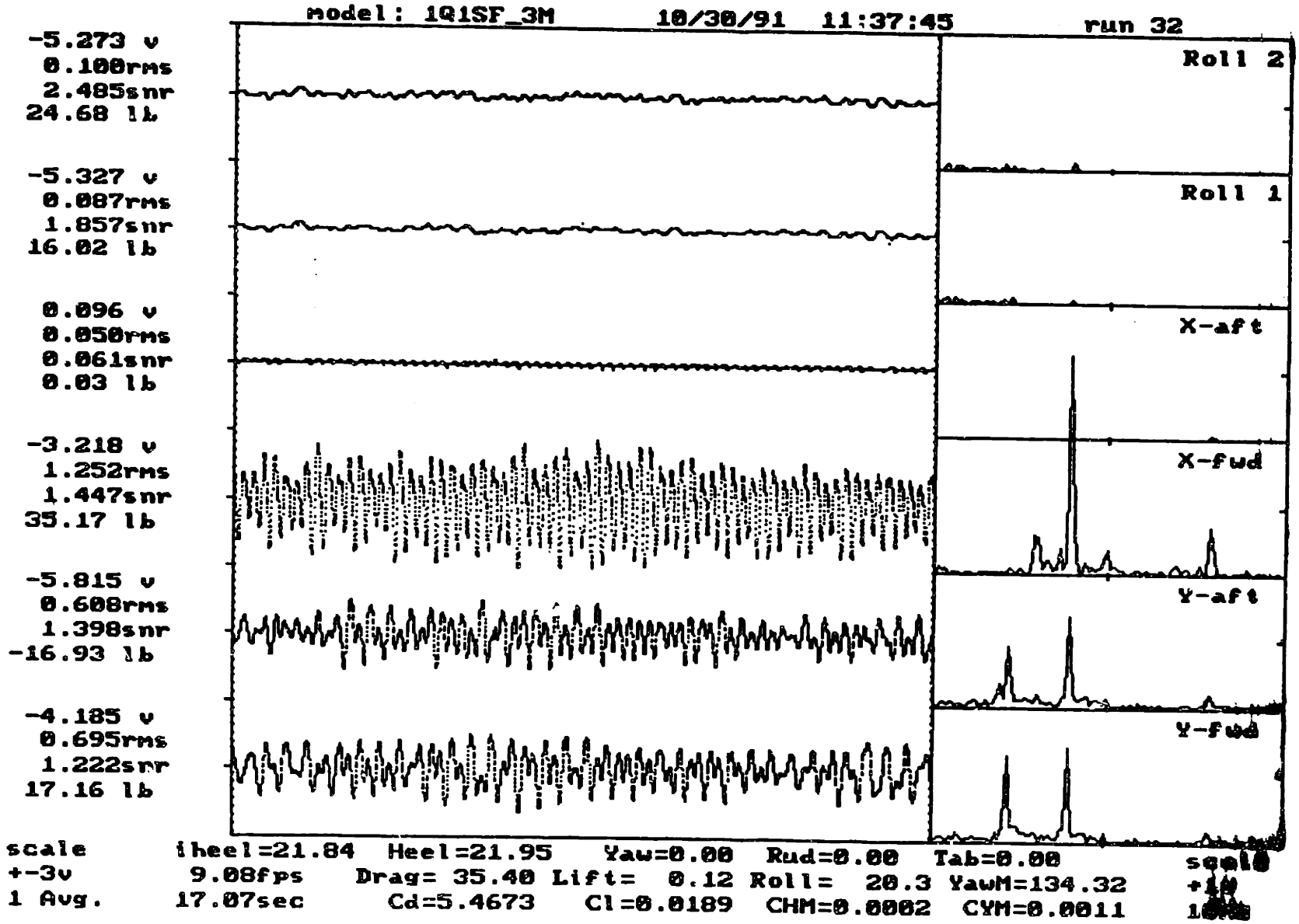
model: 1Q1SF_3M 10/30/91 11:37:45 run 32
-5.273 v
0.100rms
2.485snr
24.68 lb
Roll 2
-5.327 v
0.087rms
1.857snr
16.02 lb
Roll 1
0.096 v
0.050rms
0.061snr
0.03 lb
X-aft
-3.218 v
1.252rms
1.447snr
35.17 lb
X-fwd
-5.815 v
0.608rms
1.398snr
-16.93 lb
Y-aft
-4.185 v
0.695rms
1.222snr
17.16 lb
Y-fwd
scale
+-3v
1 Avg.
iheel=21.84 Heel=21.95 Yaw=0.00 Rud=0.00 Tab=0.00
9.08fps Drag= 35.40 Lift= 0.12 Roll= 20.3 YawM=134.32
17.07sec Cd=5.4673 Cl=0.0189 CHM=0.0002 CYM=0.0011

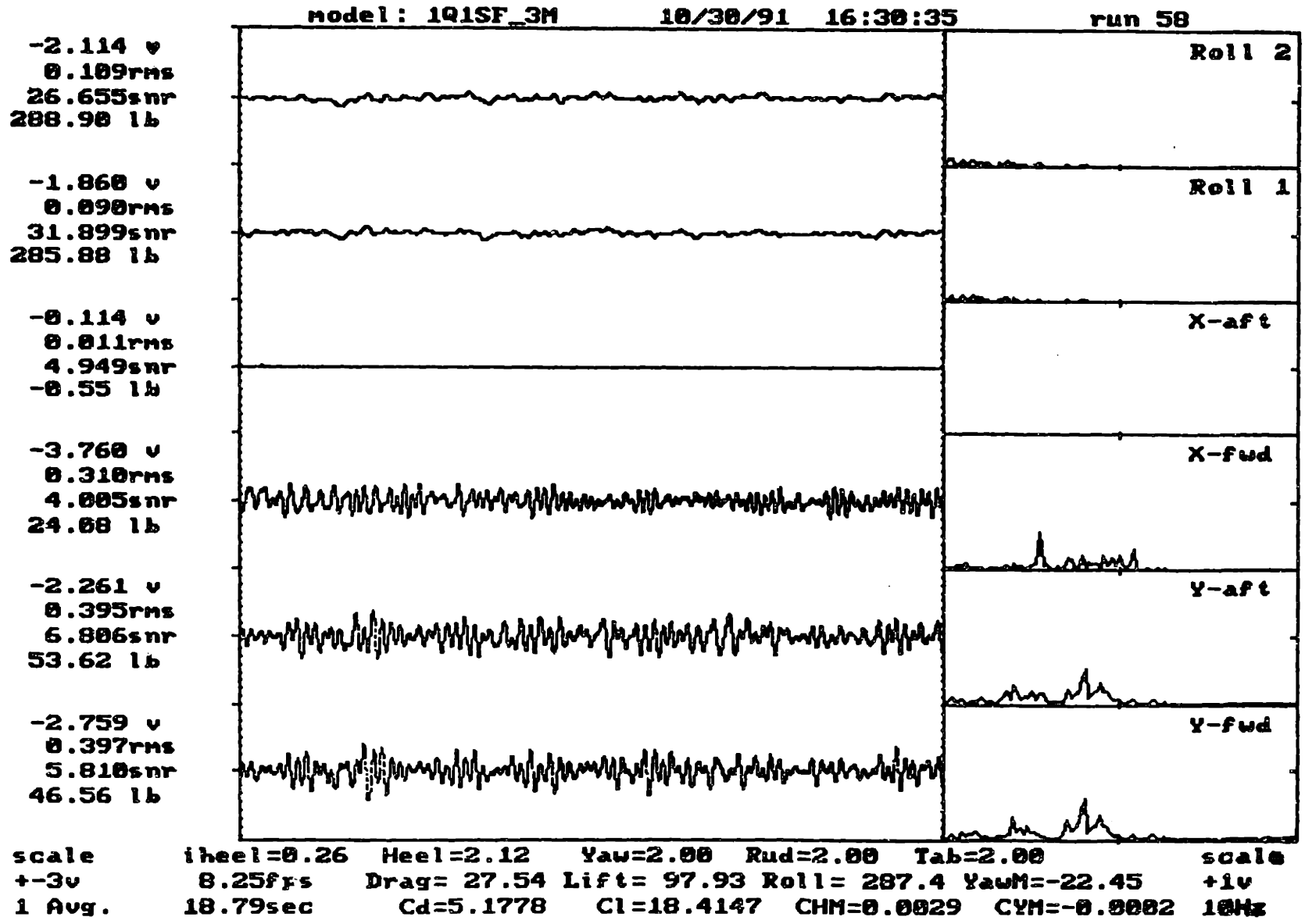
model: 1Q1SF_3M 10/30/91 16:30:35 run 58
-2.114 v
0.109rms
26.655snr
288.90 lb
Roll 2
-1.868 v
0.090rms
31.899snr
285.88 lb
Roll 1
-0.114 v
0.011rms
4.949snr
-0.55 lb
X-aft
-3.760 v
0.310rms
4.005snr
24.08 lb
X-fwd
-2.261 v
0.395rms
6.806snr
53.62 lb
Y-aft
-2.759 v
0.397rms
5.810snr
46.56 lb
Y-fwd
scale iheel=0.26 Heel=2.12 Yaw=2.00 Rud=2.00 Tab=2.00 scale
+-3v 8.25fps Drag= 27.54 Lift= 97.93 Roll= 287.4 YawM=-22.45 +1v
1 Avg. 18.79sec Cd=5.1778 Cl=18.4147 CHM=0.0029 CYM=-0.0002 10Hz

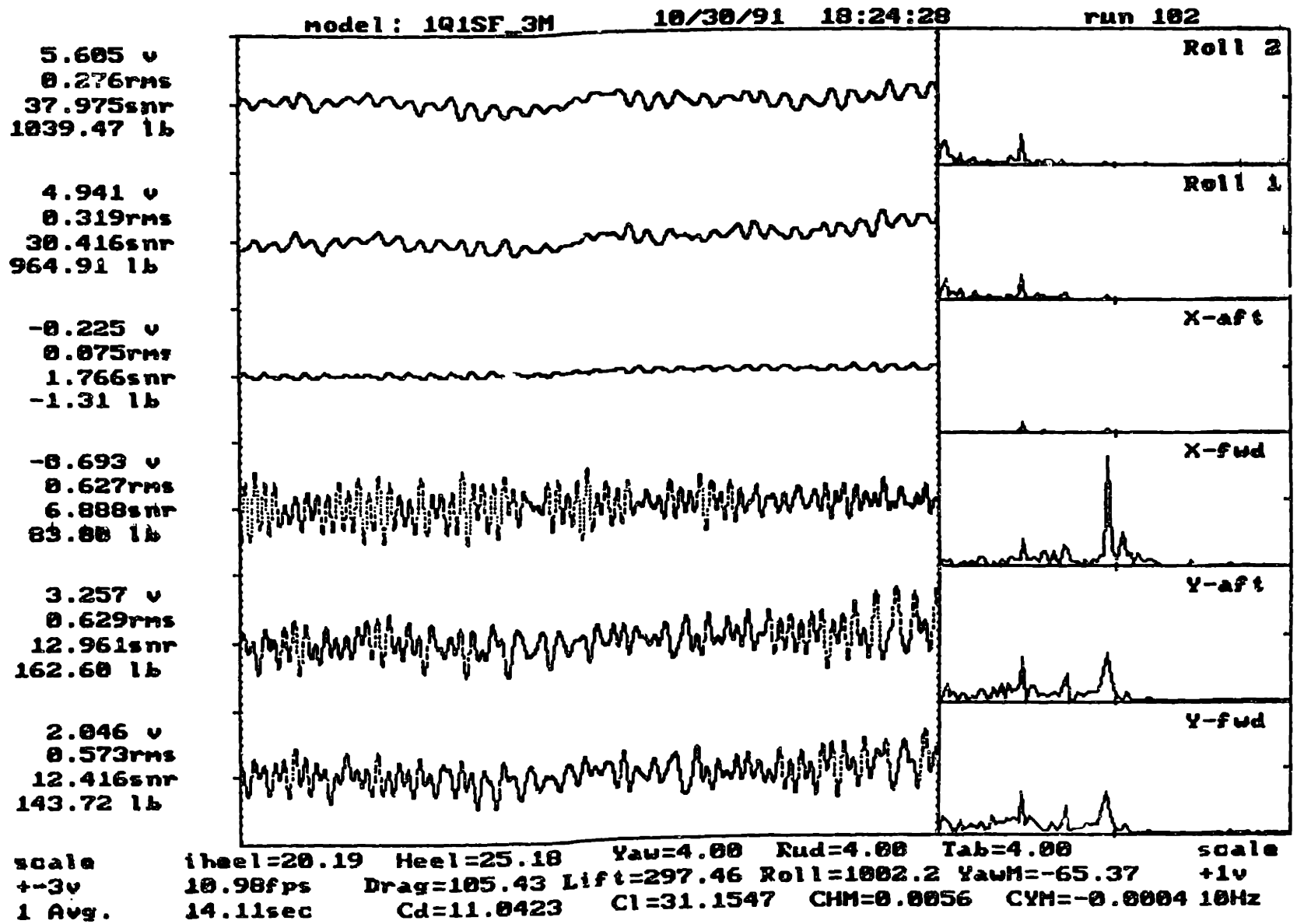
model: 1Q1SF_3M 10/30/91 18:24:28 run 102
5.605 v
0.276rms
37.975snr
1039.47 lb
Roll 2
4.941 v
0.319rms
30.416snr
964.91 lb
Roll 1
-0.225 v
0.075rms
1.766snr
-1.31 lb
X-aft
-0.693 v
0.627rms
6.888snr
83.88 lb
X-fwd
3.257 v
0.629rms
12.961snr
162.60 lb
Y-aft
2.046 v
0.573rms
12.416snr
143.72 lb
Y-fwd
scale
+-3v
1 Avg.
iheel=20.19 Heel=25.18 Yaw=4.00 Rud=4.00 Tab=4.00
10.98fps Drag=105.43 Lift=297.46 Roll=1002.2 YawM=-65.37
14.11sec Cd=11.0423 Cl=31.1547 CHM=0.0056 CYM=-0.0004
scale
+1v
10Hz

Appendix B

STRIP CHARTS OF RUNS WITH SHAKER

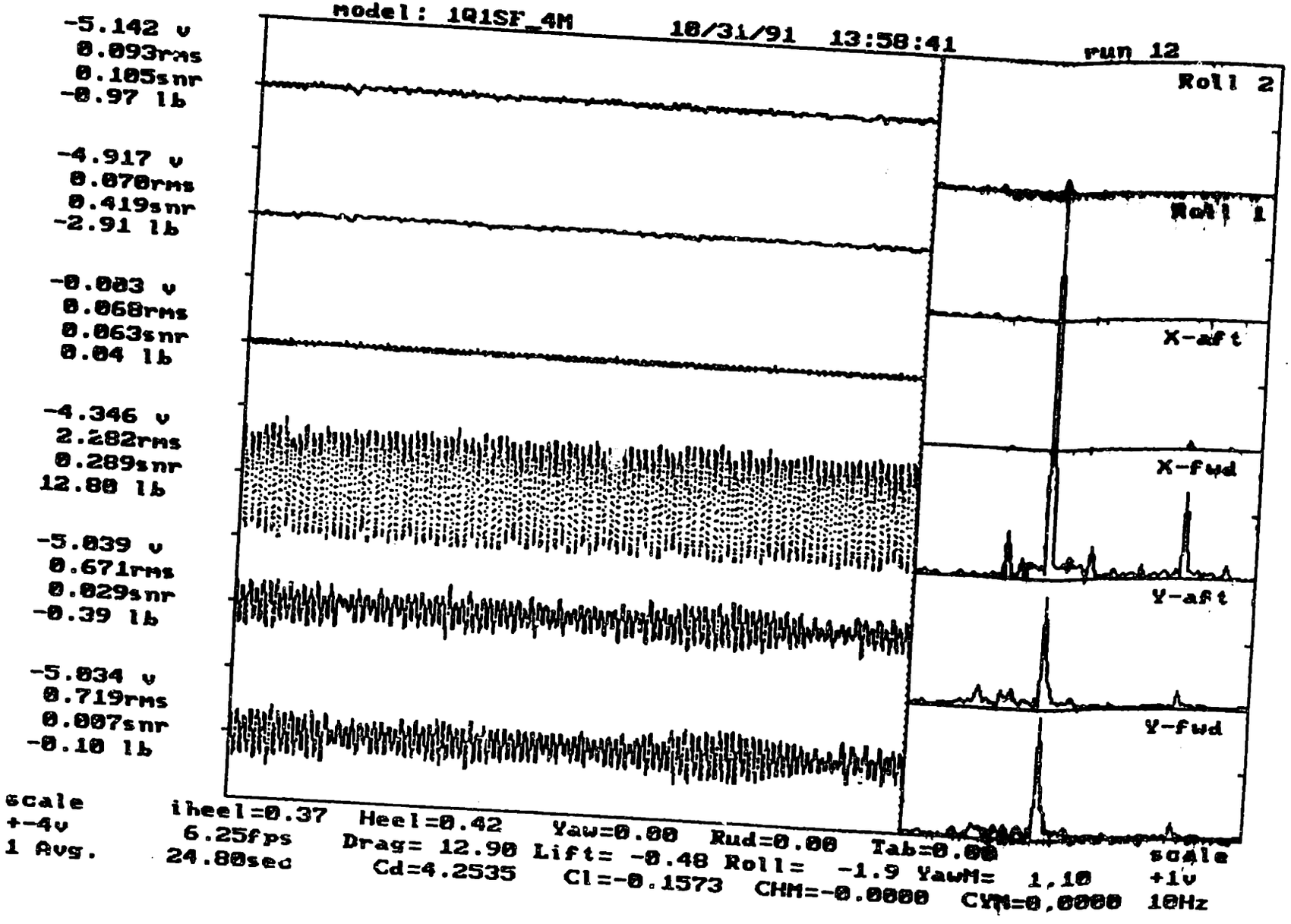
model: 101SF_4M
10/31/91 13:58:41
run 12
-5.142 v
0.093rms
0.105snr
-0.97 lb
-4.917 v
0.070rms
0.419snr
-2.91 lb
-0.003 v
0.068rms
0.063snr
0.04 lb
-4.346 v
2.282rms
0.289snr
12.80 lb
-5.039 v
0.671rms
0.029snr
-0.39 lb
-5.034 v
0.719rms
0.007snr
-0.10 lb
Roll 2
Roll 1
X-aft
X-fwd
Y-aft
Y-fwd
scale
+-4v
1 Avg.
iheel=0.37 Heel=0.42 Yaw=0.00 Rud=0.00 Tab=0.00
6.25fps Drag= 12.90 Lift= -0.48 Roll= -1.9 YawM= 1.10
24.80sec Cd=4.2535 Cl=-0.1573 CHM=-0.0000 CYM=0.0000
scale
+1v
10Hz

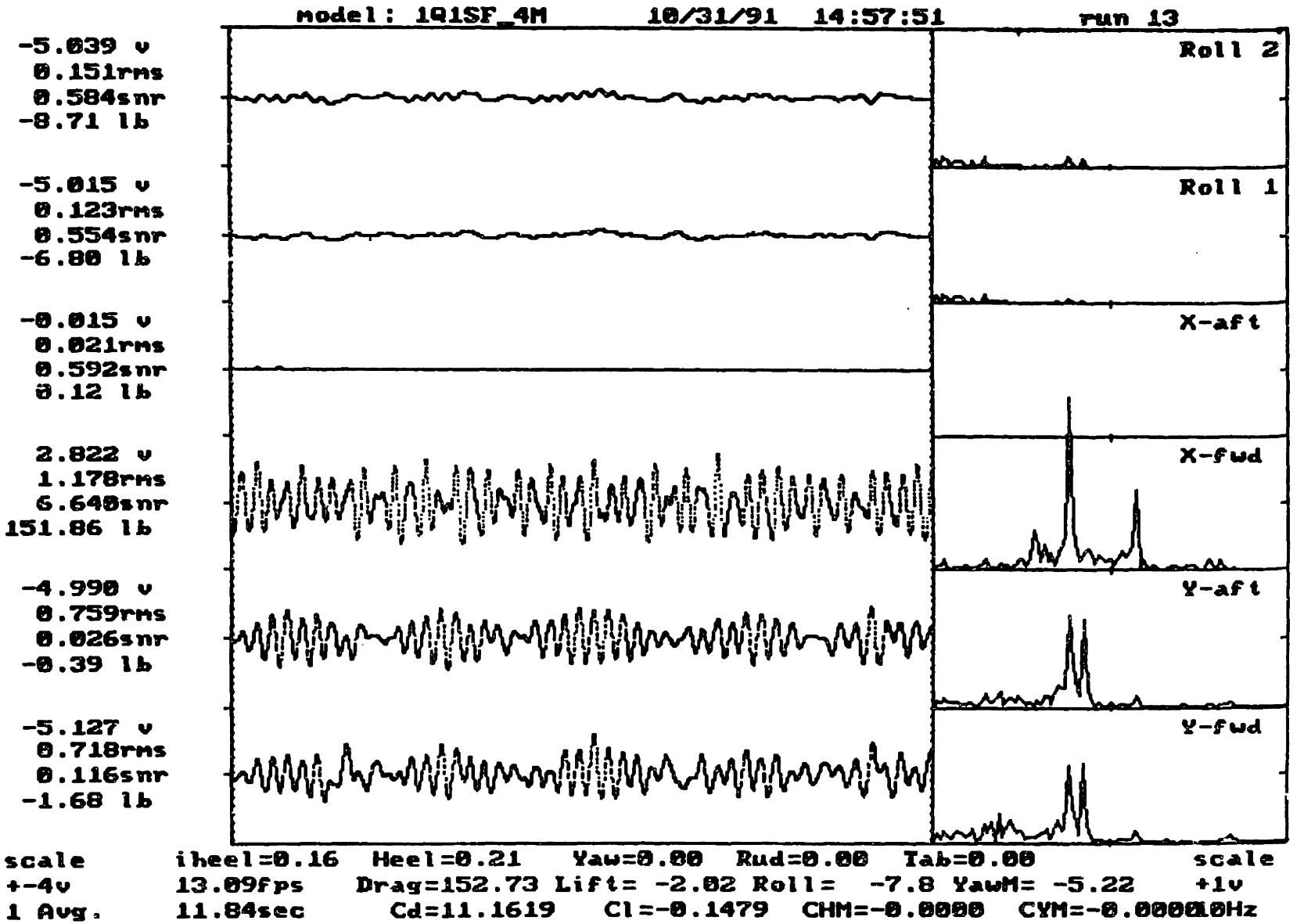
model: 191SF_4M 10/31/91 14:57:51 run 13
-5.039 v
0.151rms
0.584snr
-8.71 lb
Roll 2
-5.015 v
0.123rms
0.554snr
-6.80 lb
Roll 1
-0.015 v
0.021rms
0.592snr
0.12 lb
X-aft
2.822 v
1.178rms
6.640snr
151.86 lb
X-fwd
-4.990 v
0.759rms
0.026snr
-0.39 lb
Y-aft
-5.127 v
0.718rms
0.116snr
-1.68 lb
Y-fwd
scale
+-4v
1 Avg.
iheel=0.16 Heel=0.21 Yaw=0.00 Rud=0.00 Tab=0.00
13.09fps Drag=152.73 Lift= -2.02 Roll= -7.8 YawM= -5.22
11.84sec Cd=11.1619 Cl=-0.1479 CHM=-0.0000 CYM=-0.000010Hz
scale
+1v

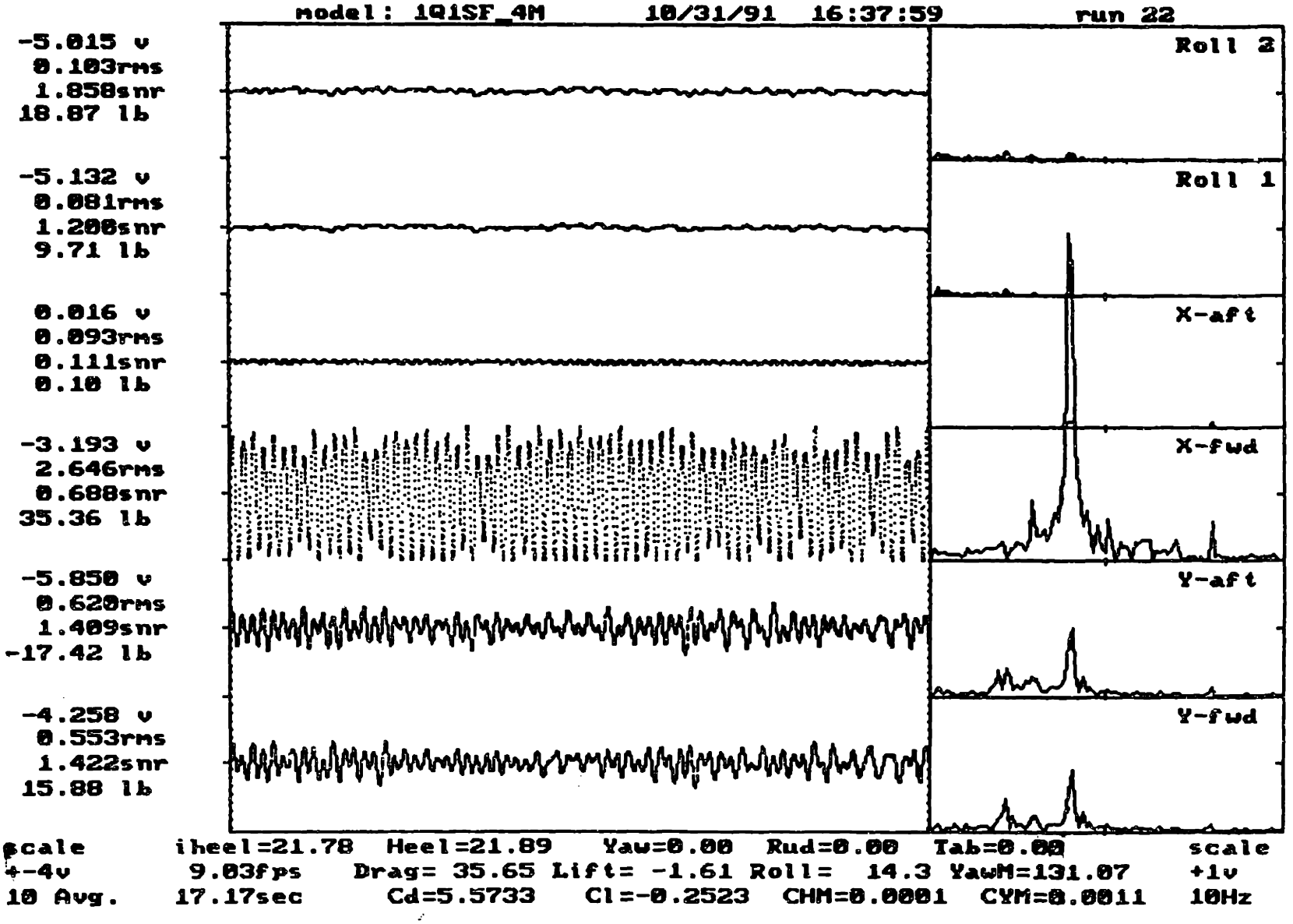
model: 1Q1SF_4M 10/31/91 16:37:59 run 22
-5.015 v
0.103rms
1.858snr
18.87 lb
Roll 2
-5.132 v
0.081rms
1.208snr
9.71 lb
Roll 1
0.016 v
0.093rms
0.111snr
0.10 lb
X-aft
-3.193 v
2.646rms
0.688snr
35.36 lb
X-fwd
-5.850 v
0.620rms
1.409snr
-17.42 lb
Y-aft
-4.258 v
0.553rms
1.422snr
15.88 lb
Y-fwd
scale
+-4v
10 Avg.
iheel=21.78 Heel=21.89 Yaw=0.00 Rud=0.00 Tab=0.00
9.03fps Drag= 35.65 Lift= -1.61 Roll= 14.3 YawM=131.07
17.17sec Cd=5.5733 Cl=-0.2523 CHM=0.0001 CYM=0.0011
scale
+1v
10Hz

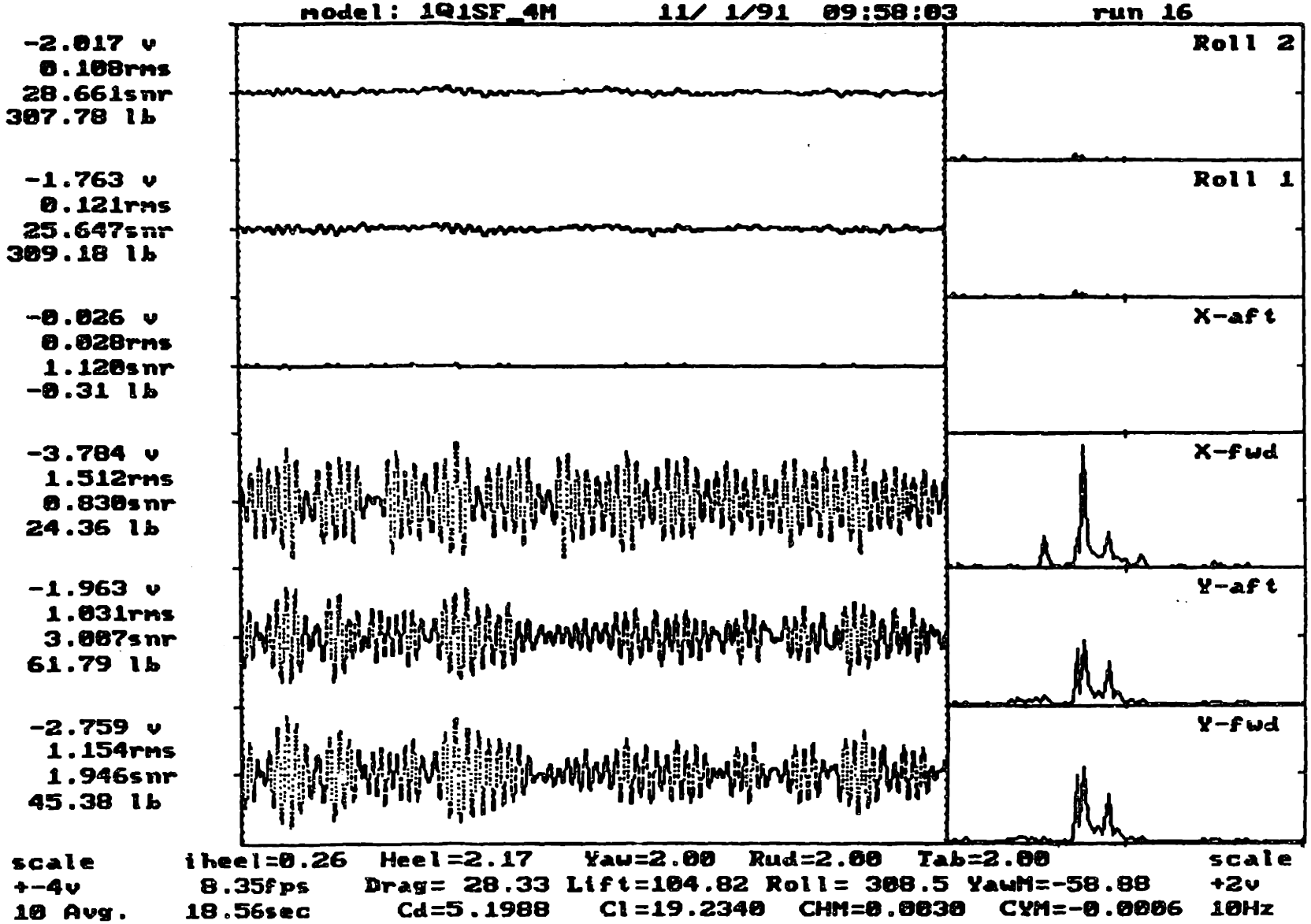
model: 1Q1SF_4M 11/ 1/91 09:58:03 run 16
-2.017 v
0.108rms
28.661snr
307.78 lb
Roll 2
-1.763 v
0.121rms
25.647snr
309.18 lb
Roll 1
-0.026 v
0.028rms
1.120snr
-0.31 lb
X-aft
-3.784 v
1.512rms
0.830snr
24.36 lb
X-fwd
-1.963 v
1.031rms
3.007snr
61.79 lb
Y-aft
-2.759 v
1.154rms
1.946snr
45.38 lb
Y-fwd
scale
+-4v
10 Avg.
iheel=0.26 Heel=2.17 Yaw=2.00 Rud=2.00 Tab=2.00
8.35fps Drag= 28.33 Lift=104.82 Roll= 308.5 YawM=-58.88
18.56sec Cd=5.1988 Cl=19.2340 CHM=0.0030 CYM=-0.0006
scale
+2v
10Hz

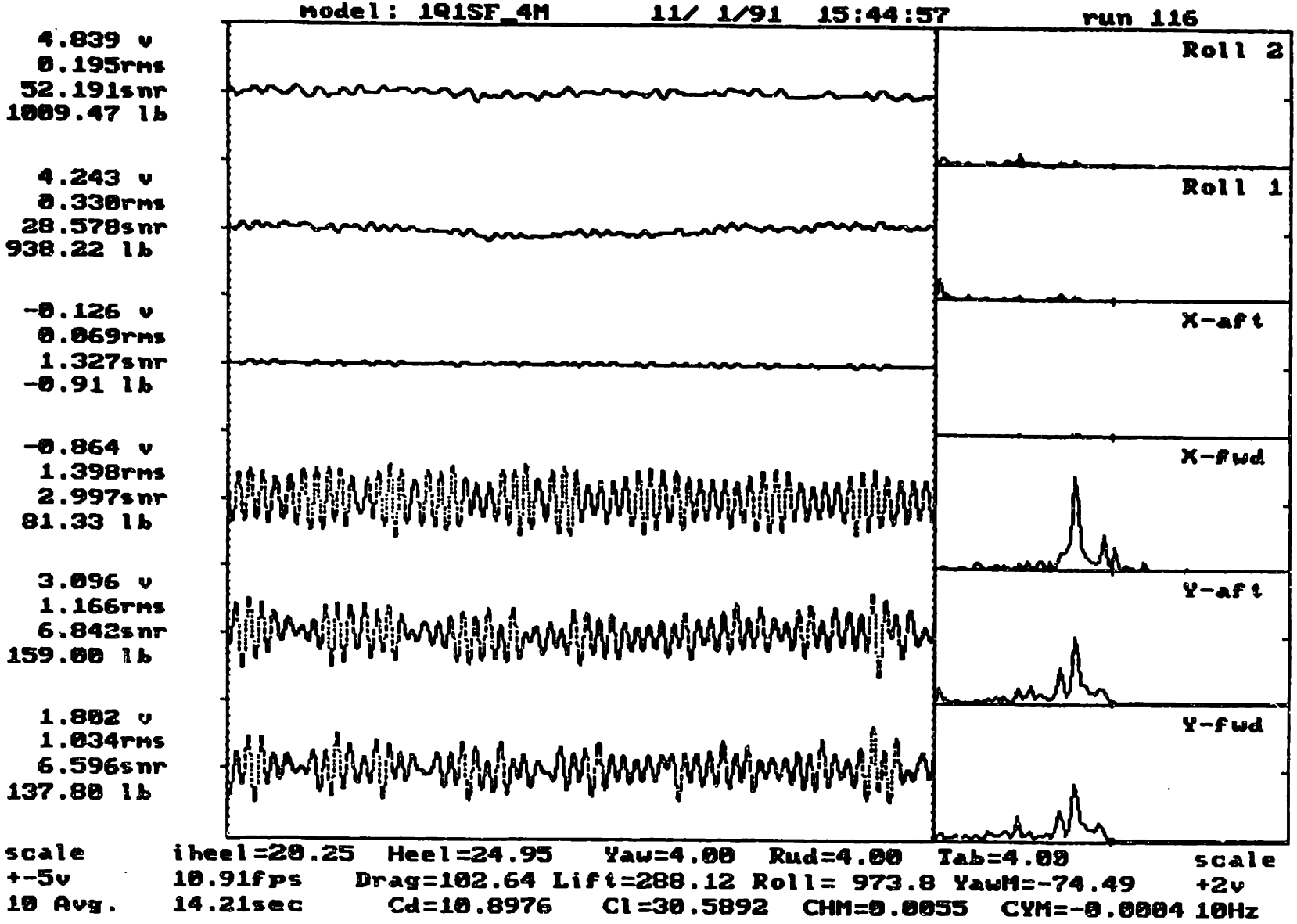
model: 191SF_4M
11/ 1/91 15:44:57
run 116
4.839 v
0.195rms
52.191snr
1009.47 lb
Roll 2
4.243 v
0.330rms
28.578snr
938.22 lb
Roll 1
-0.126 v
0.069rms
1.327snr
-0.91 lb
X-aft
-0.864 v
1.398rms
2.997snr
81.33 lb
X-fwd
3.096 v
1.166rms
6.842snr
159.00 lb
Y-aft
1.802 v
1.034rms
6.596snr
137.80 lb
Y-fwd
scale
+-5v
10 Avg.
iheel=20.25 Heel=24.95 Yaw=4.00 Rud=4.00 Tab=4.00
10.91fps Drag=102.64 Lift=288.12 Roll= 973.8 YawM=-74.49
14.21sec Cd=10.8976 Cl=30.5892 CHM=0.0055 CYM=-0.0004
scale
+2v
10Hz

Appendix C

STUD DRAG CALCULATION FOR HEEL/YAW

What follows is series of plots of the stimulator drag coefficient, C_{stim}, as defined in chapter 5, for runs with heel/yaw, versus speed-length ratio.

The values of the drag coefficient indicated on the vertical axis should be multiplied by 10^{-6}.

The stimulator drag coefficient (per stimulator) is estimated from a pair of tests performed with a different number of studs. Shown in each plot is also the nominal value of 1.11×10^{-6}.

The nominal values of heel and yaw for each plot are indicated at the top of the page.

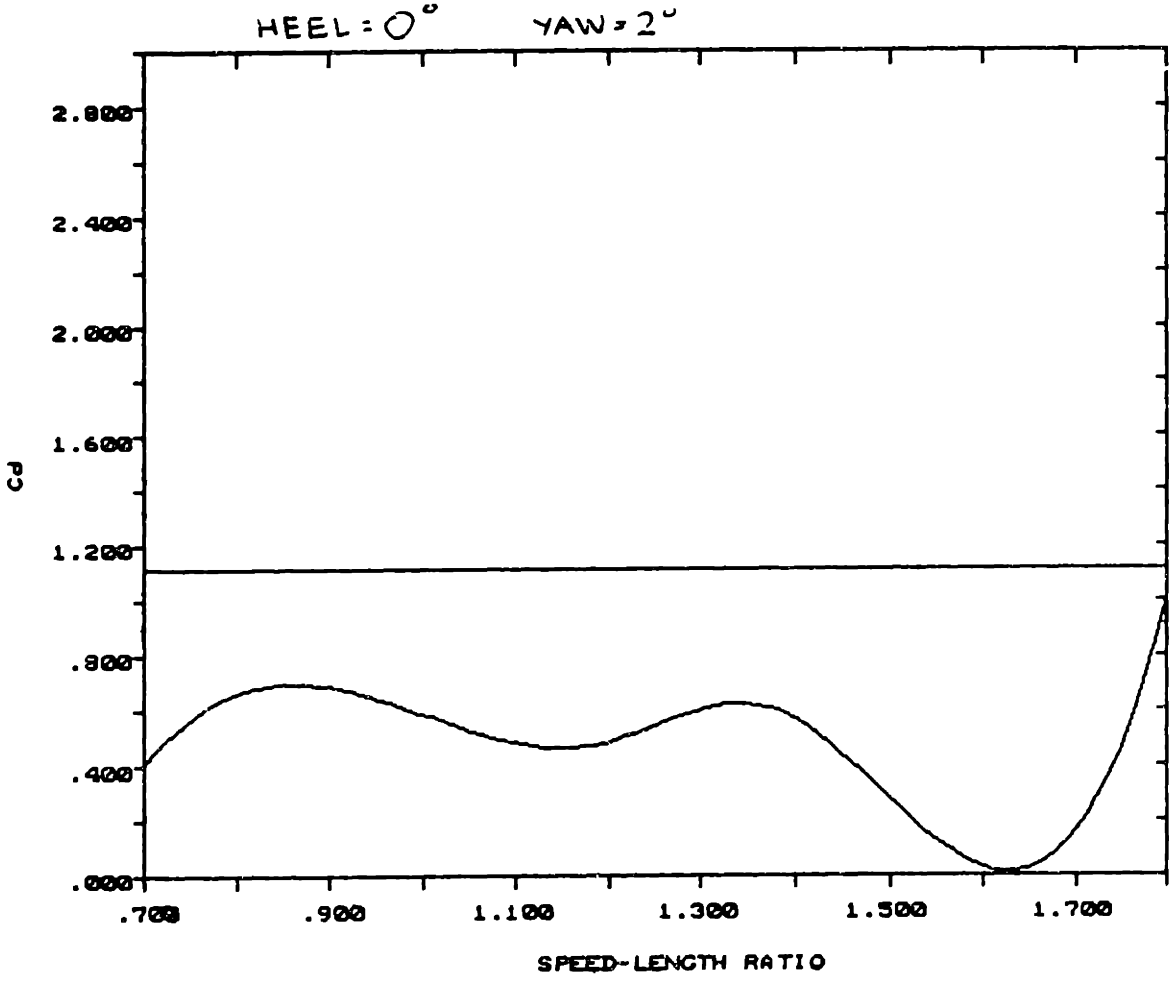
HEEL = 0°
YAW = 2°
2.800
2.400
2.000
1.600
1.200
.800
.400
.000
CD
.700
.900
1.100
1.300
1.500
1.700
SPEED-LENGTH RATIO

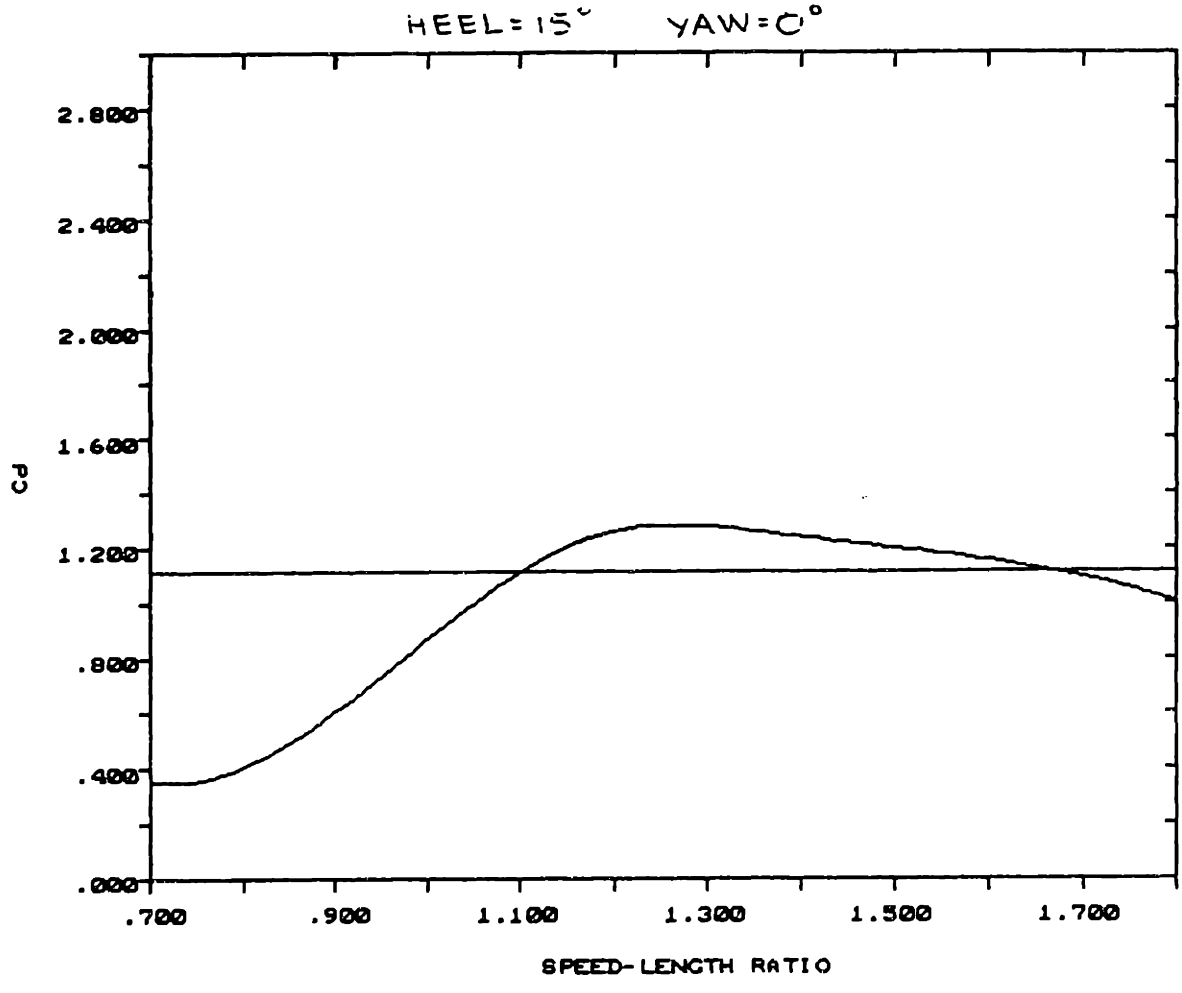
HEEL=15° YAW=0°
2.800
2.400
2.000
1.600
1.200
.800
.400
.000
CD
.700
.900
1.100
1.300
1.500
1.700
SPEED-LENGTH RATIO

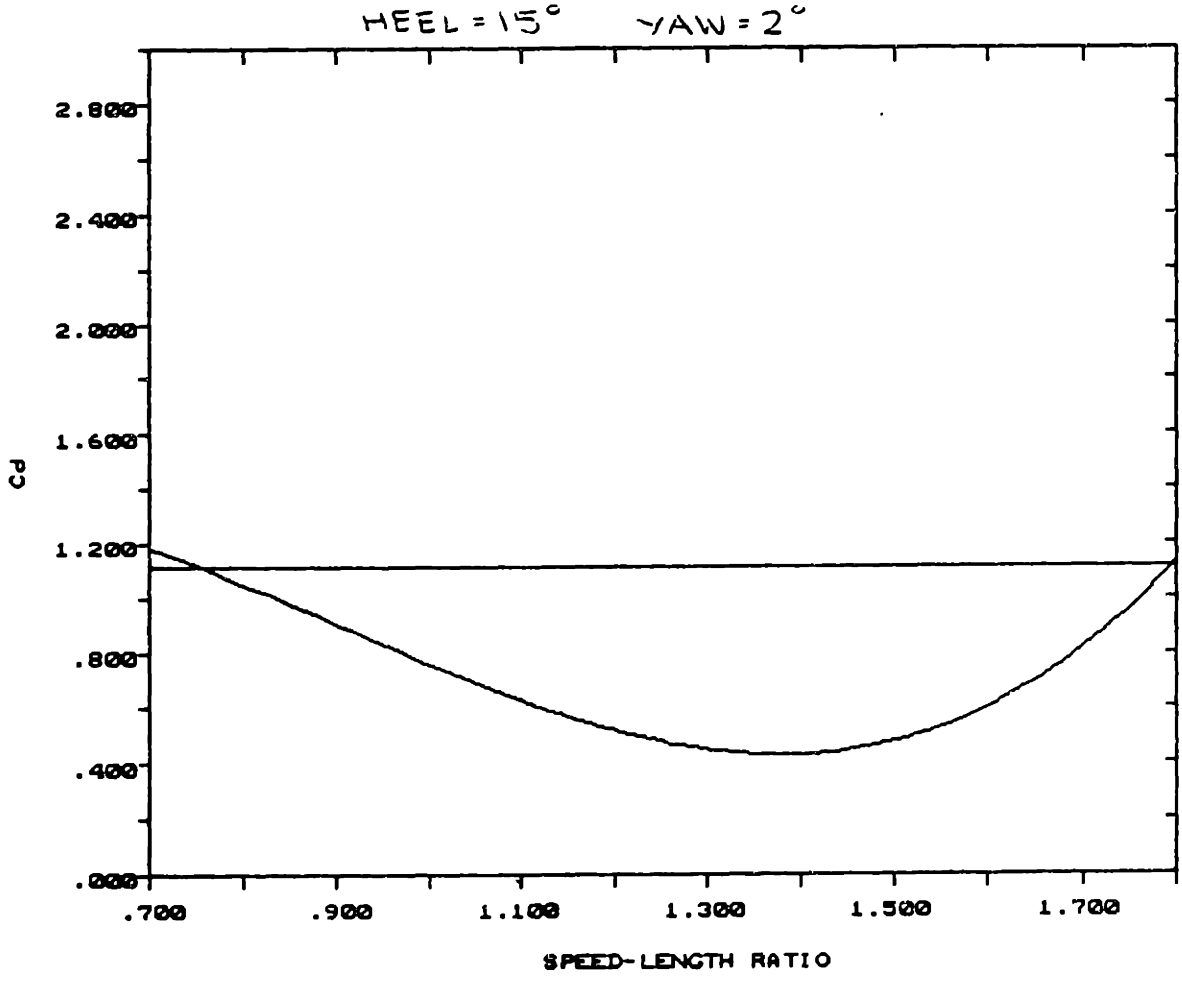
HEEL = 15°
YAW = 2°
2.800
2.400
2.000
1.600
1.200
.800
.400
.000
Cd
.700
.900
1.100
1.300
1.500
1.700
SPEED-LENGTH RATIO

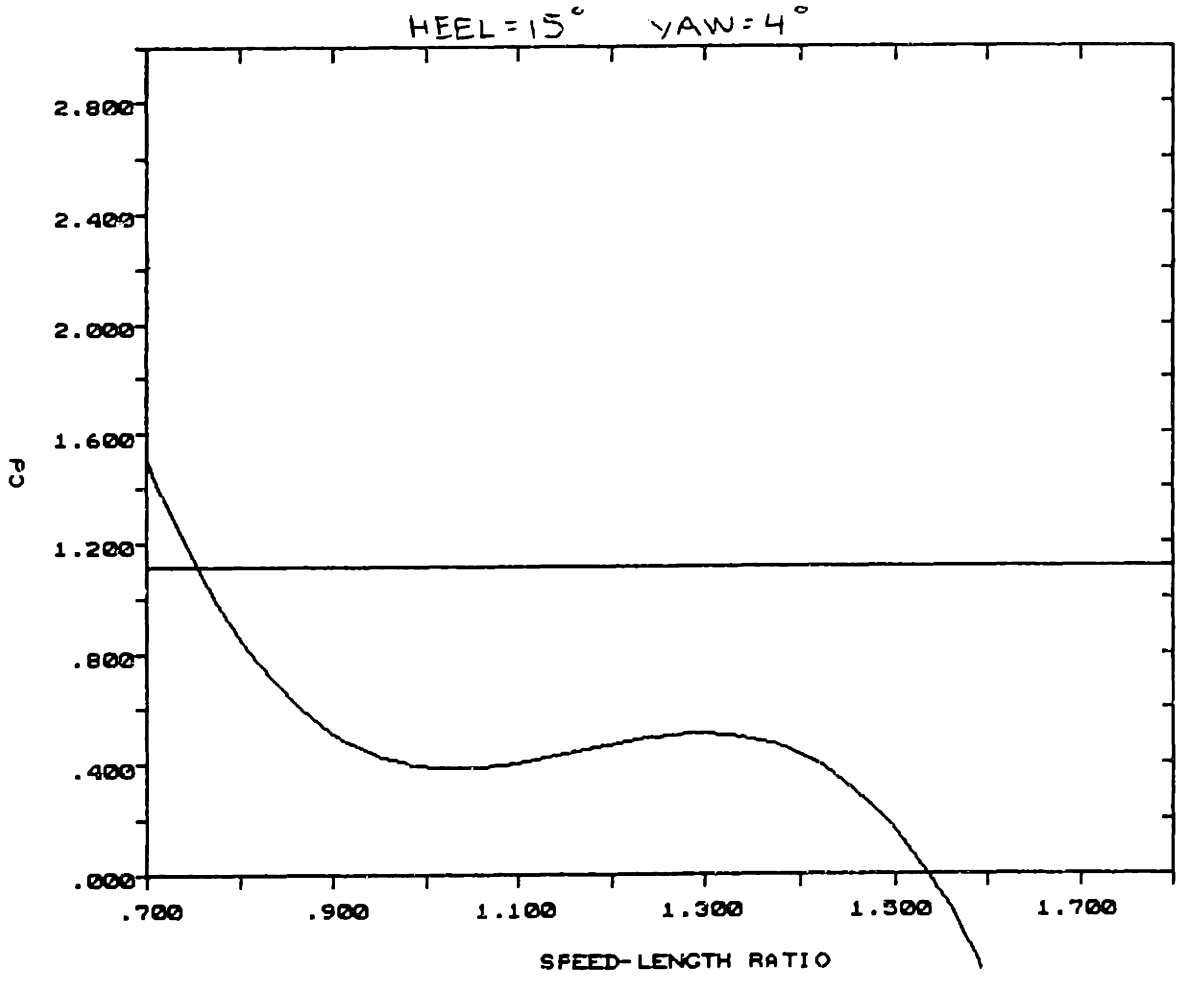
HEEL = 15° YAW = 4°
2.800
2.400
2.000
1.600
1.200
.800
.400
.000
Cd
.700
.900
1.100
1.300
1.500
1.700
SPEED-LENGTH RATIO

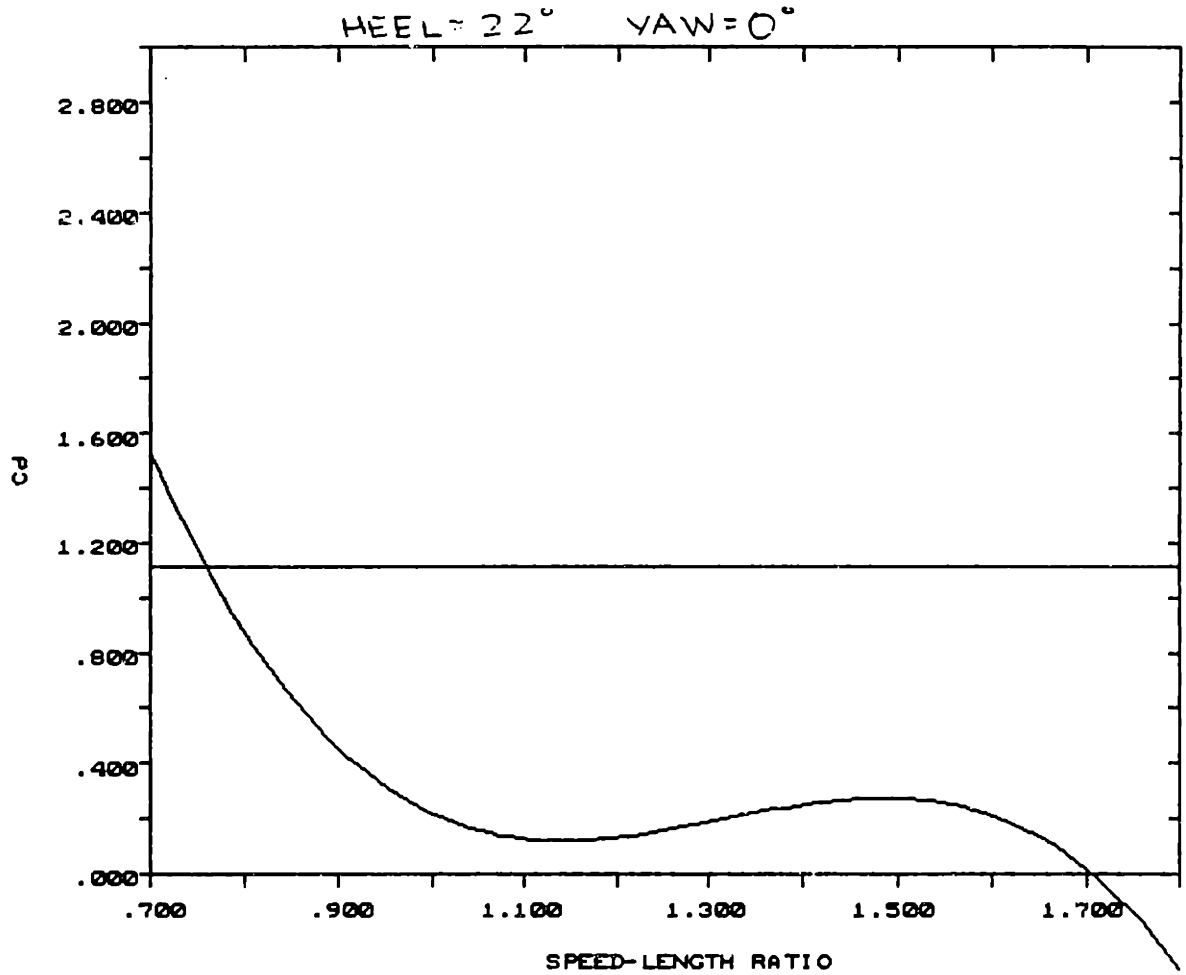
HEEL=22° YAW=0°
2.800
2.400
2.000
1.600
1.200
.800
.400
.000
Cd
.700
.900
1.100
1.300
1.500
1.700
SPEED-LENGTH RATIO

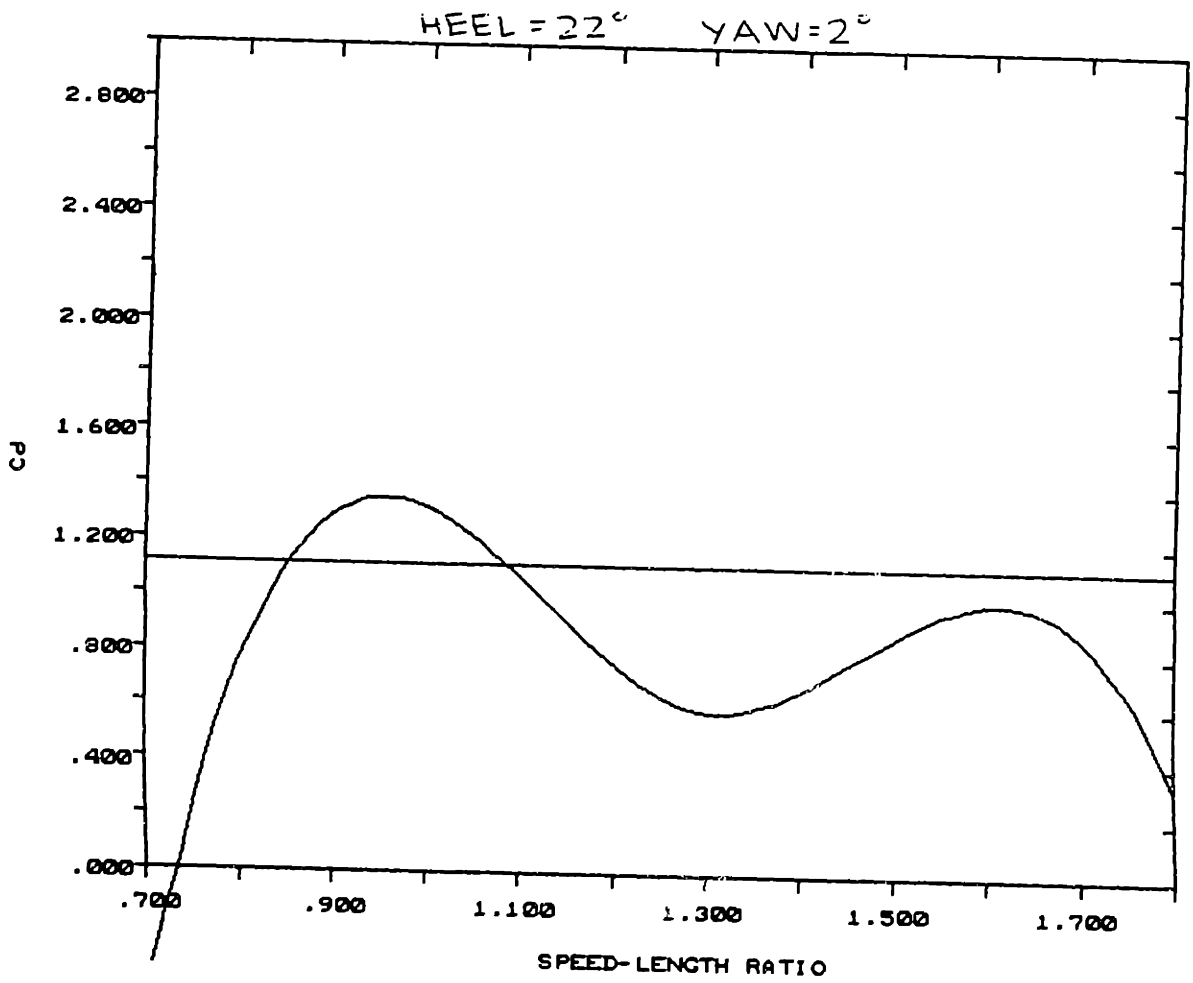
HEEL = 22° YAW = 2°
2.800
2.400
2.000
1.600
1.200
.800
.400
.000
Cp
.700
.900
1.100
1.300
1.500
1.700
SPEED-LENGTH RATIO

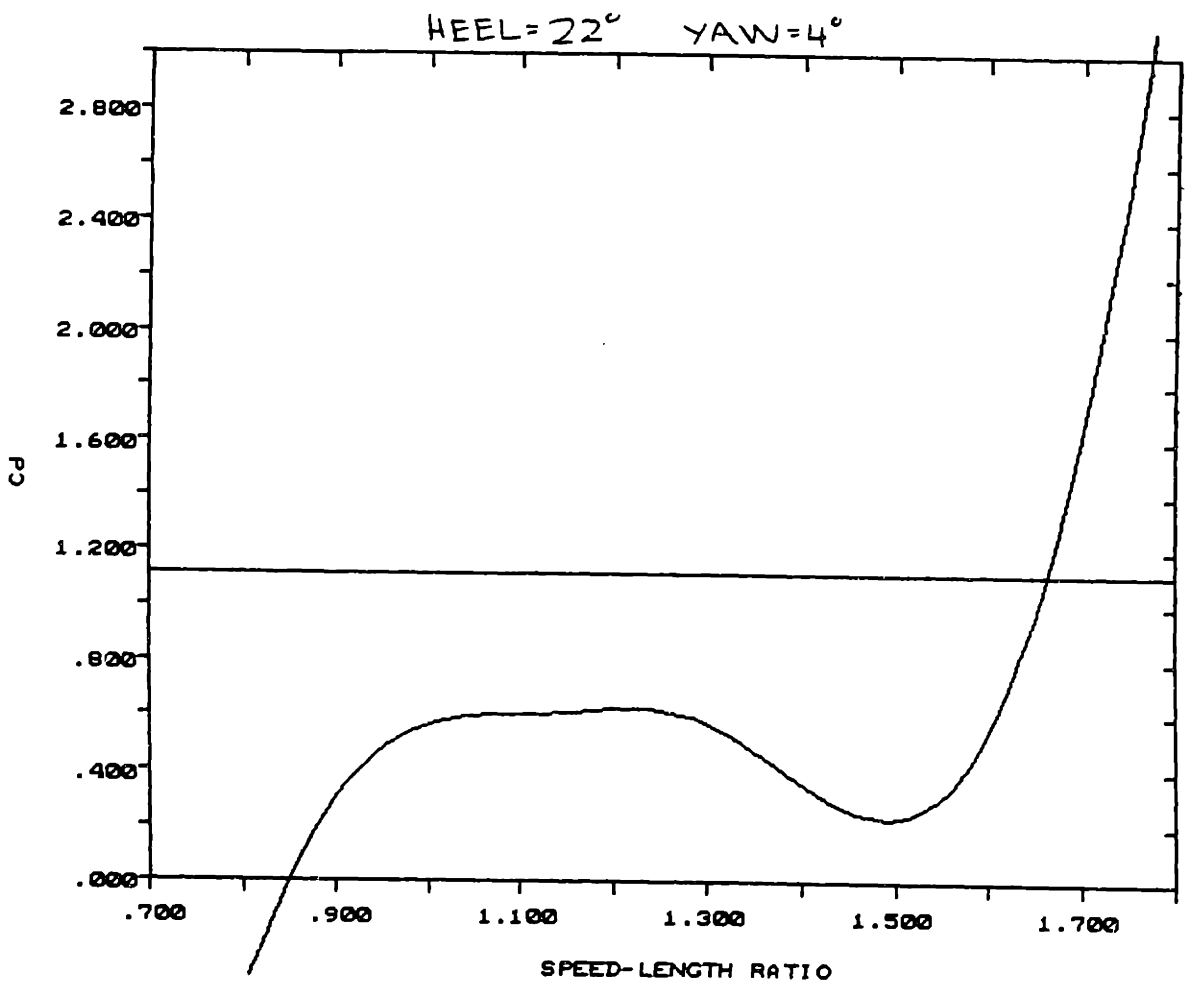
HEEL=22° YAW=4°
2.800
2.400
2.000
1.600
1.200
.800
.400
.000
Cd
.700
.900
1.100
1.300
1.500
1.700
SPEED-LENGTH RATIO

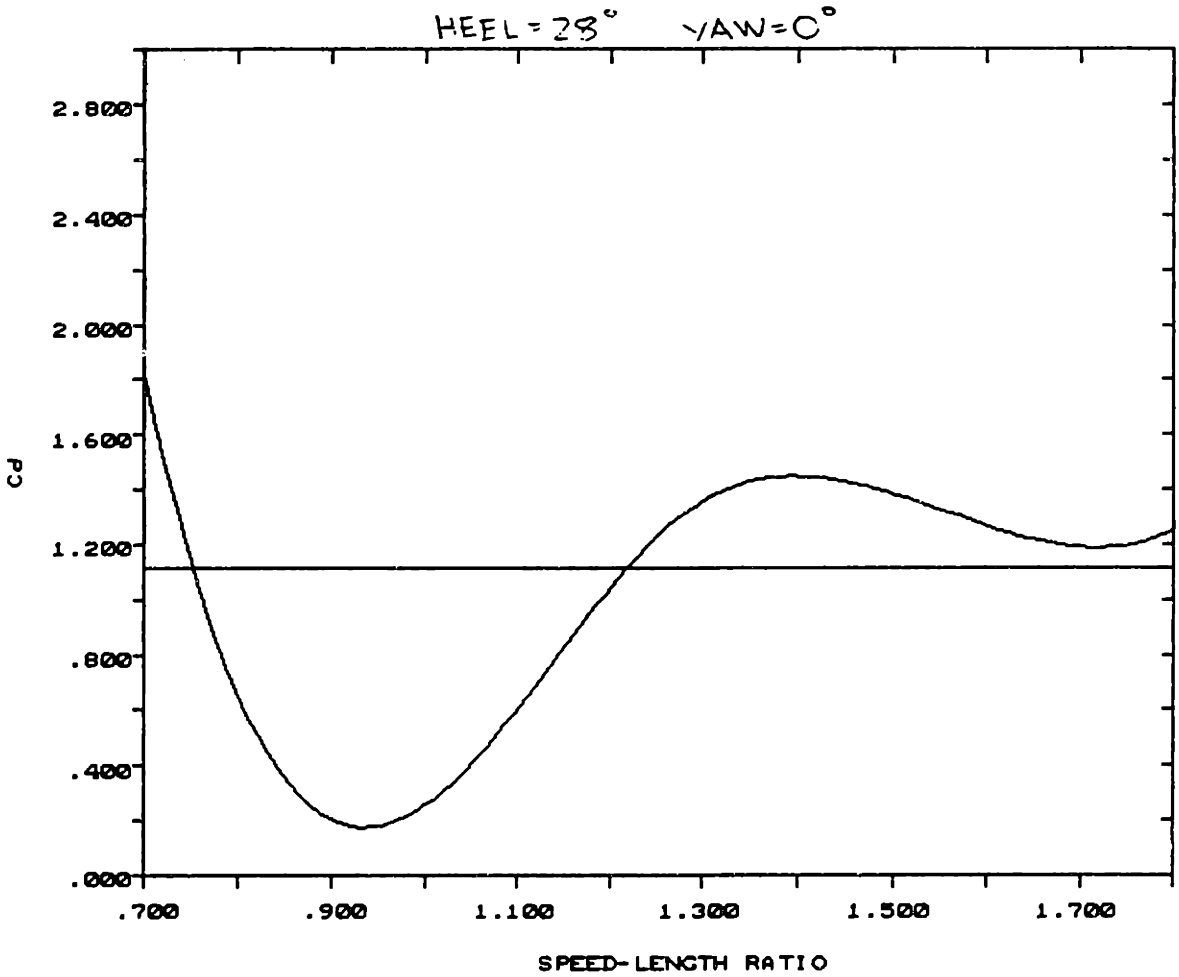
HEEL = 28°
YAW = 0°
2.800
2.400
2.000
1.600
1.200
.800
.400
.000
Cd
.700
.900
1.100
1.300
1.500
1.700
SPEED-LENGTH RATIO

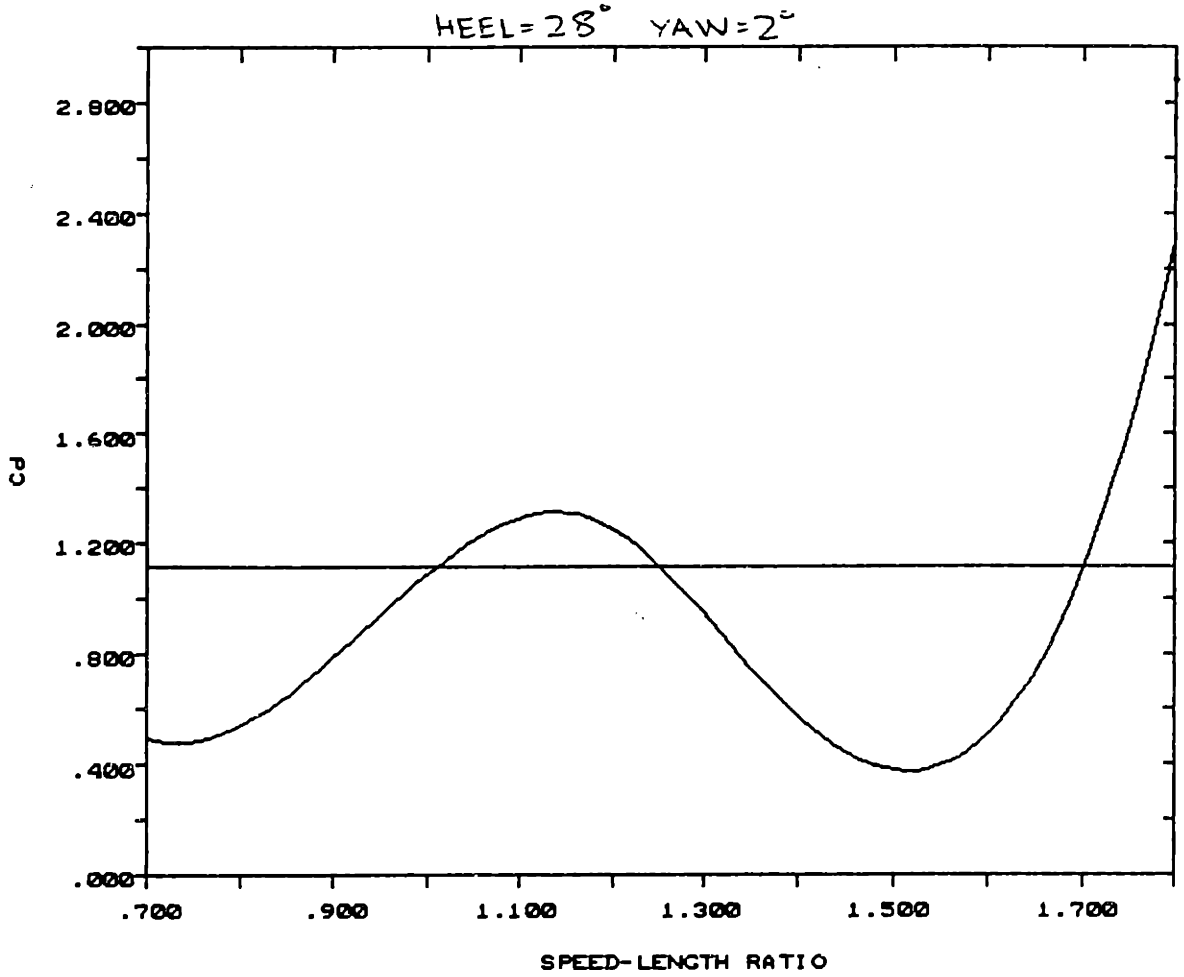
HEEL=28° YAW=2°
2.800
2.400
2.000
1.600
1.200
.800
.400
.000
Cd
.700
.900
1.100
1.300
1.500
1.700
SPEED-LENGTH RATIO

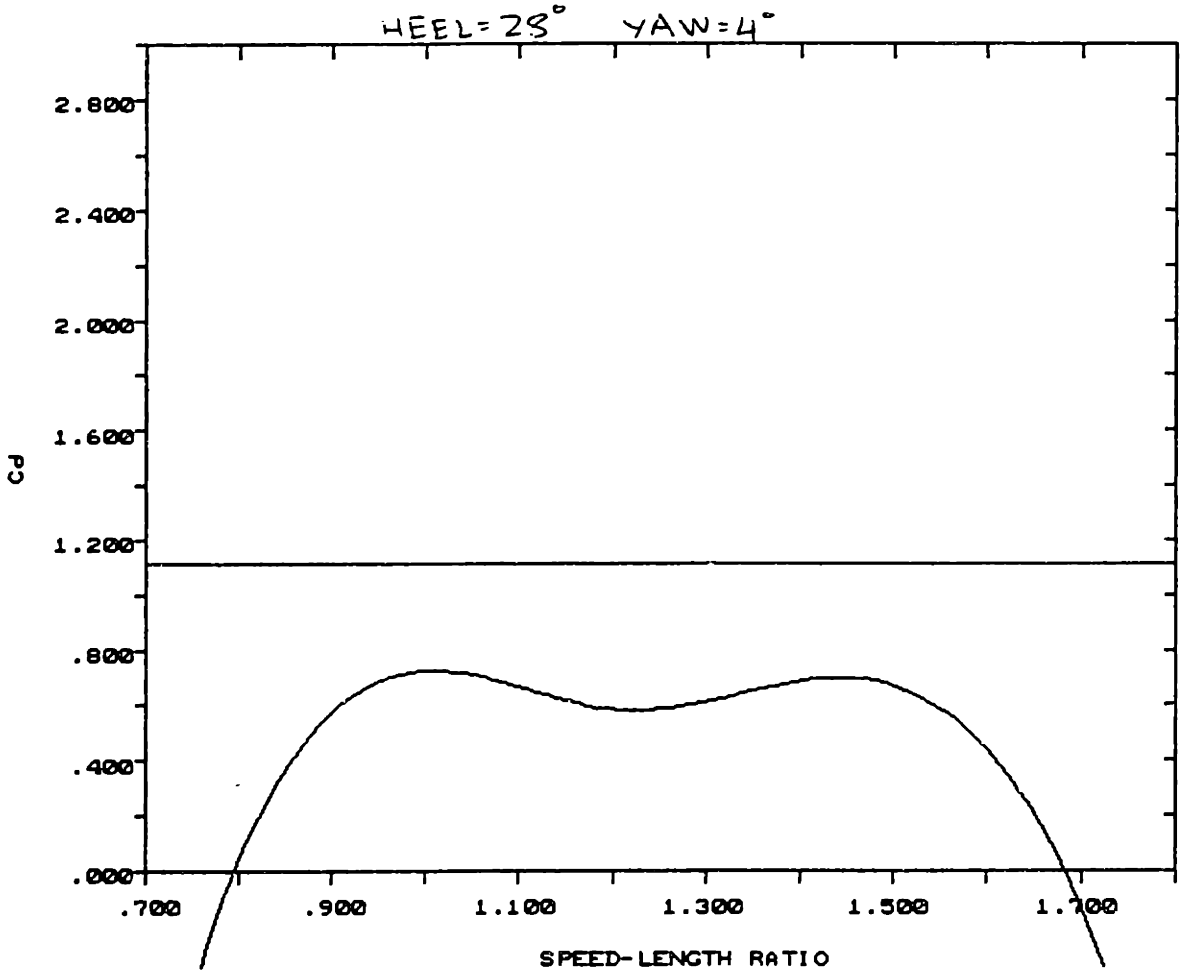
HEEL=28° YAW=4°
2.800
2.400
2.000
1.600
1.200
.800
.400
.000
CD
.700
.900
1.100
1.300
1.500
1.700
SPEED-LENGTH RATIO

Bibliography

[1] A. Cross. Report of performance committee, appendix 4 : Form factor. *ITTC Vol 3*, 1975.

[2] Thomas R. Dyer. Boundary layer transition and separation on yacht models. *MIT S.M. Thesis*, 1962.

[3] Justin E. Kerwin. A velocity prediction program for ocean racing yachts revised to june 1978. *Irving Pratt Project No 78-11*, 1978.

[4] C. W. Prohaska. A simple method for the evaluation of the form factor and the low speed wave resistance. *Proceedings, 11th ITTC*, 1966.

[5] SNAME. *Principles of Naval Architecture, Vol II.* The Society of Naval Architects and Marine Engineers, Jersey City, 1988.